NASA Contractor Report 177928

NASA-CR-177928
19860016859

Six Degree-of-Freedom "LIVE" Isolation System Tests

Part I: Interim Report

Dennis R. Halwes and Colby O. Nicks

Bell Helicopter Textron

Fort Worth, TX 76101

Contract Nas1-16969

April 1986

National Aeronautics and
Space Administration

Langley Research Center
Hampton, Virginia 23665

TABLE OF CONTENTS

PART I: INTERIM REPORT

This Page Intentionally Left Blank

LIST OF FIGURES

PART I: INTERIM REPORT

LIST OF FIGURES (CONTINUED)

LIST OF FIGURES (CONCLUDED)

This Page Intentionally Left Blank

LIST OF TABLES

PART I: INTERIM REPORT

1. INTRODUCTION

This interim report is submitted in partial fulfillment of the Total Main Rotor Isolation system program conducted under contract NAS1-16969 for NASA-Langley/AVSCOM. The objective of this contract is to develop a main rotor vibration isolation system that will achieve total isolation at minimum weight with no degradation in vehicle stability, handling qualities, alignment tolerance, or reliability and maintainability. In accordance with the program contract, "total main rotor isolation" is defined as 90% (or greater) isolation of the helicopter fuselage from forces and moments input at the rotor hub.

The developmental program for the isolation system consists of four phases. The first phase included component and system analysis, and detailed design. Results were reported to the Government in an oral review presented at BHTI. The results of individual component vibration tests (phase two) were submitted on October 21, 1983, in an informal letter report to Dr. F. D. Bartlett of AVSCOM (Structures Lab - LaRC). The third phase of the program consisted of bench vibration tests of the assembled isolation system to evaluate the overall system performance for hub excitations in all six degrees of freedom. Phase four will include testing of the isolation system installed on the helicopter, with a series of shake tests, ground runs, and flight tests being performed to evaluate complete system performance.

This report concerns the system bench vibration test phase (phase three) of the Total Main Rotor Isolation System program. In addition to static and dynamic test results from the system bench tests, the information presented in the oral review and the letter report is included as background material.

BACKGROUND

During the 1970's several antiresonant isolation concepts were developed to isolate the fuselage from the helicopters' main rotor oscillatory forces. These include the Kaman DAVI[1], Boeing Vertol IRIS[2], and Bell Nodal Beam[3]. All of these concepts use a spring and a mechanically amplified mass to develop isolation at the main rotor excitation frequency. An example of this type of

anti-resonant isolator concept is the Bell Nodal Beam installation on the 206L light helicopter. Key design features of the 206L Nodal Beam are: steel flexure located to operate as both spring and tuning weight, elastomeric bearings to reduce damping, and incorporation of a Focused Pylon to isolate pitch and roll.

Although the Nodal Beam provides excellent isolation performance (over 90% isolation to vertical and roll excitations at the blade passage frequency), it has several inherent drawbacks. Typically, weight penalties are substantial, ranging from 1.8 to 2.5% of design gross weight. Other shortcomings include nonlinearities due to changes in spring rate with large amplitudes of motion, excessive damping, mechanical complexity, the space required for moving weights and arms, and cost. As a result of these factors, an alternate method of achieving the same isolation performance was developed.

LIVE Isolation[4]

In 1972, research was begun at BHT using a hydraulic fluid in cylinders with different areas to amplify the motion of a tungsten piston which acted as a tuning weight. This concept progressed to a very compact system using a high density, low viscosity liquid (mercury) as both the "hydraulic fluid" and the tuning weight.

The action of this Liquid Inertia Vibration Eliminator (LIVE) unit is shown schematically in cross section in Figure 1a and 1b. An inner cylinder is bonded to an outer cylinder with a layer of rubber as in a coaxial bushing rubber spring. Cavities, top and bottom, are enclosed, creating reservoirs for the "hydraulic fluid." The inner cylinder is attached to the transmission, and the outer cylinder is attached to the fuselage. The hole or "tuning port" through the inner cylinder connects the upper and lower reservoirs.

To understand the action of the LIVE system, it is useful to compare it to the mechanically amplified inertia isolator, Figure 2, since their actions and reactions are analogous. In the LIVE system, the area ratio of the outer cylinder to the tuning port is analogous to the length ratio of arms on the mechanical spring, and the inertial effect of high density liquid in the

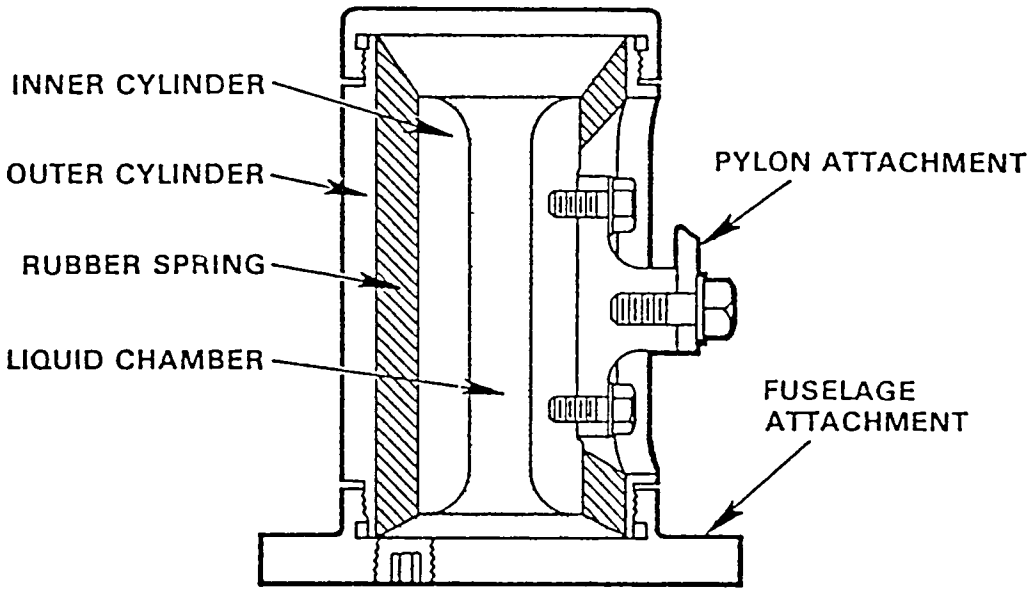

Figure 1a. Design of LIVE Isolator

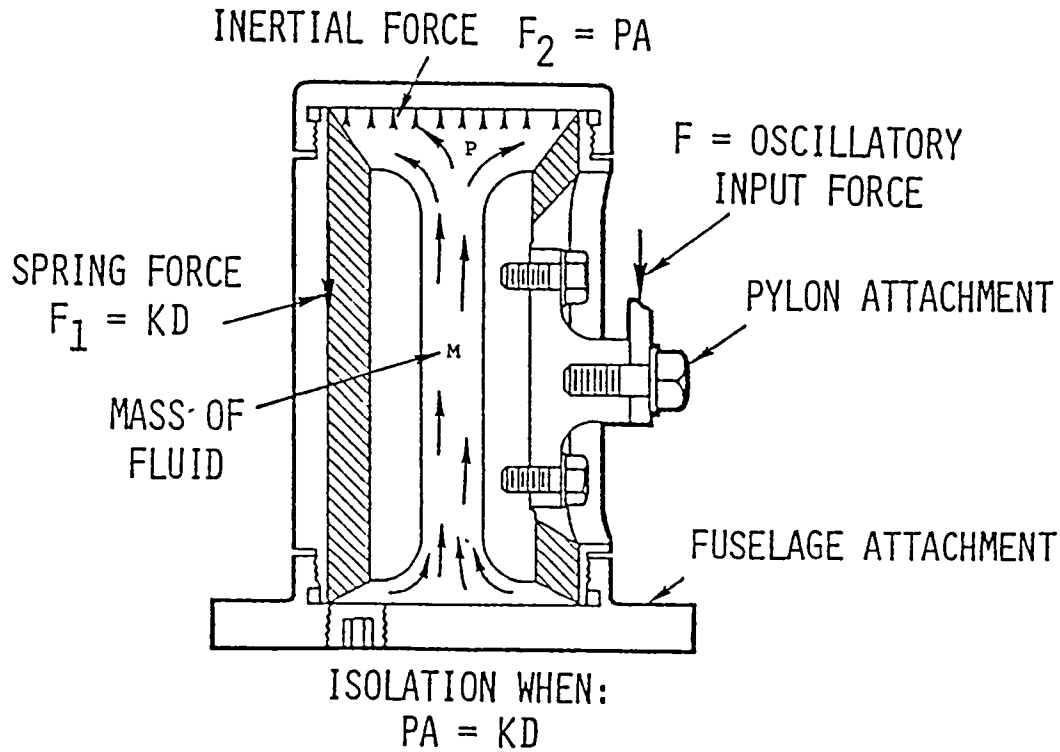

Figure 1b. Principle of LIVE Isolator.

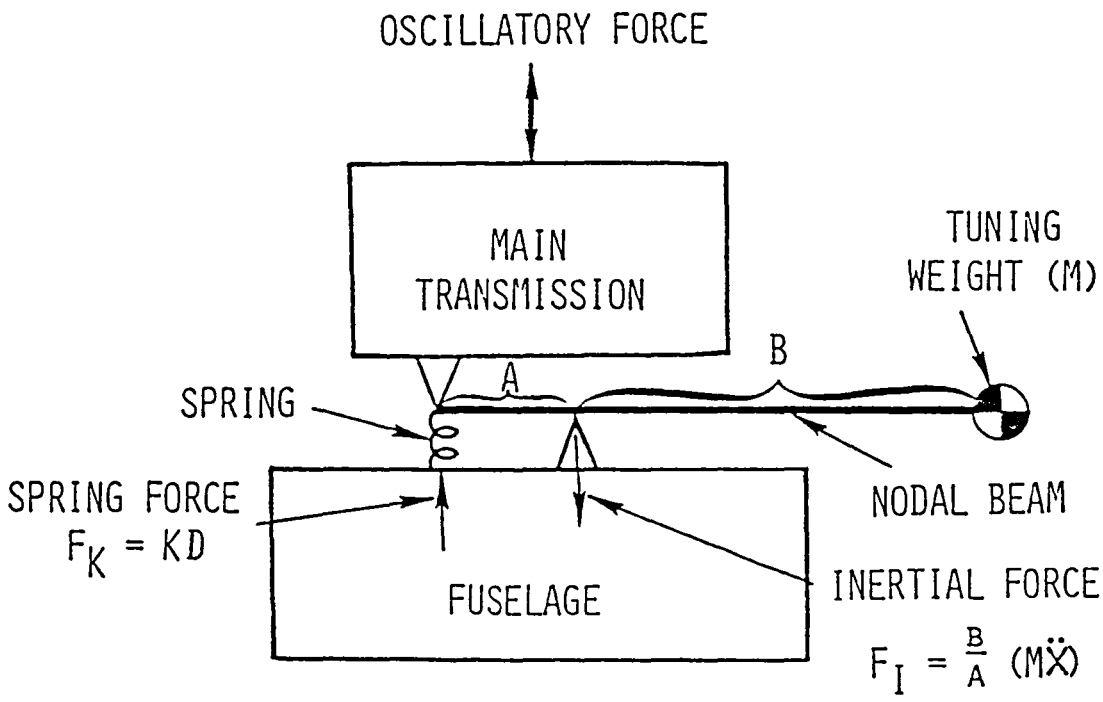

ISOLATION WHEN:
$M\ddot{X} = KD$

Figure 2. Principle of Nodalization.

tuning port is analogous to the inertial effect of the tuning weight on the arm. Therefore, if the spring rate of the elastomeric spring, the weight of the liquid in the tuning port, and the area ratio of the LIVE system are equal to their counterparts on the nodal beam, then the LIVE system will isolate the same frequency with the same efficiency as the nodal beam system. This action can be seen in Figure 1b where an oscillatory force is applied to the transmission atachment lug. This applied oscillatory force creates an oscillatory reaction force in the outer cylinder due to the strain in the rubber spring (F_1 = KD). At the same time, the liquid is pumped through the tuning port creating oscillatory accelerations of the liquid mass.

These accelerations create oscillatory pressures in the upper and lower reservoirs out of phase with the force created by the rubber spring. The size of the tuning port is chosen such that the force on the outer cylinder due to the pressure in the reservoir (F_2 = PA) cancels the force due to the rubber spring, and the outer housing is nodalized at the excitation frequency. Figure 3 shows the static and dynamic motions the isolator goes through as different flight conditions are encountered.

Analysis of LIVE System Motions

To further understand the dynamics involved in the LIVE system, an analysis of the equations of motion is summarized here. Two assumptions are made about the system to simplify the analysis: (1) zero damping and (2) harmonic motion. For this analysis, refer to Figure 4a for a simplified schematic of the LIVE system. Let the pylon mass be attached to the inner cylinder, and the fuselage be attached to the outer cylinder. There are four unknowns to solve for: x_1, x_2, x_3 and P.

Notice that the mass of the liquid in the reservoir must have the same vertical motion as m_3. Due to the principles of hydraulics there is a constraint equation that causes the motion of any one body to be proportional to the difference in the motion of the other two bodies. This can be seen by fixing m_3 (the fuselage) and forcing a displacement on m_1 (the pylon) and observing the motion of m_2 (the tuning weight). The equation of this motion is:

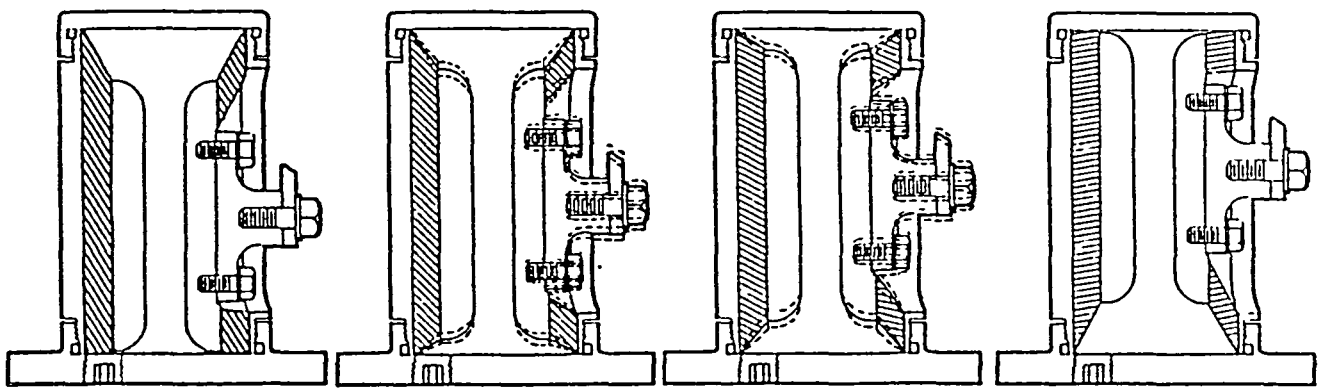

Figure 3. Flight Motions of LIVE.

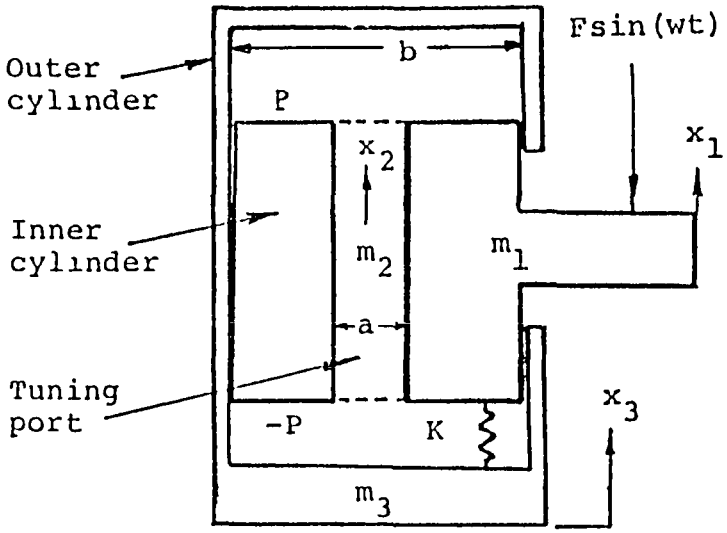

Figure 4a. LIVE Schematic.

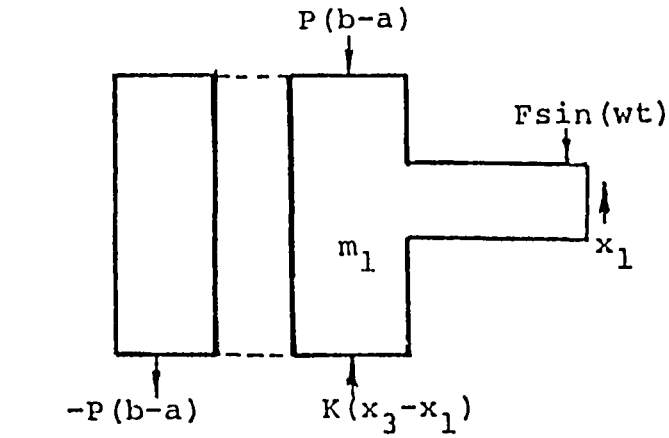

$$-m_1\ddot{x}_1=Fsin(wt)+2P(b-a)-K(x_3-x_1)$$

Figure 4b. Free body of m_1

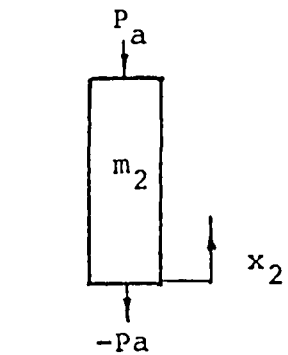

$$-m_2\ddot{x}_2 = 2Pa$$

Figure 4c. Free body of m_2

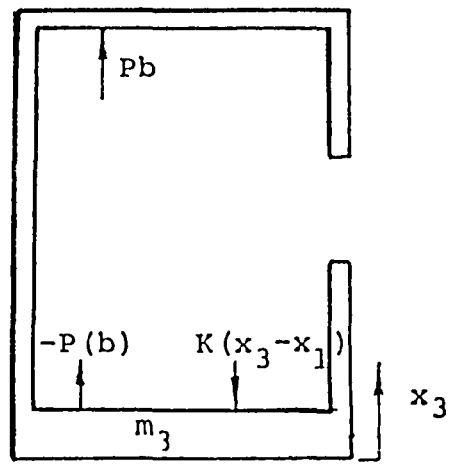

$$-m_3\ddot{x}_3 = K(x_3-x_1) - 2Pb$$

Figure 4d. Free body of m_3

Figure 4. LIVE Analysis Free Body Diagrams and Equations of Motion.

$$x_1 = \frac{bx_3 - ax_2}{(b-a)} \qquad \text{Constraint equation (1)}$$

By observing the dynamic loads applied to the free body diagram of m_1 in Figure 4b, a force balance yields:

$$-m_1\ddot{x}_1 = F\sin(wt) + 2P(b-a) - K(x_3-x_1) \tag{2}$$

Similarly a force balance of m_2 in Figure 4c yields:

$$-m_2\ddot{x}_2 = 2Pa \tag{3}$$

and a force balance of m_3 in Figure 4d yields:

$$-m_3\ddot{x}_3 = K(x_3-x_1) - 2Pb \tag{4}$$

These four equations then give us the necessary information to solve for the four unknowns. This yields:

$$P = -\omega^2 m_2 x_2/2a; \quad x_1 = \frac{bx_3 - ax_2}{(b-a)}$$

$$x_2 = \frac{F\sin(wt)\ (a(b-a)m_3\omega^2+Ka^2)}{\omega^2a^2(m_1+m_2+m_3)K-\omega^4(m_1m_2b_2+m_1m_3a^2+m_2m_3(b-a)^2)} \tag{5}$$

$$x_2 = \frac{F\sin(wt)\ (b(b-a)\omega^2m_2-Ka^2)}{\omega^2a^2(m_1+m_2+m_3)K-\omega^4(m_1m_2b^2+m_1m_3a^2+m_2m_3(b-a)^2)} \tag{6}$$

To solve for the isolation frequency set $x_3 = 0$, then:

$$\frac{b}{a}m_2\omega^2 - \frac{Ka}{b-a} = 0 \quad \text{or} \quad f_i = \frac{1}{2\pi}\left(\frac{Ka^2}{m_2b(b-a)}\right)^{1/2} \tag{7}$$

to determine the tuning mass required for a given area ratio and spring rate:

$$m_2 = \frac{Ka^2}{(2\pi f_1)^2\ b(b-a)}$$

the resonant frequency is:

$$f_n = \frac{1}{2\pi}\left\{\frac{Ka^2(m_1+m_2+m_3)}{m_1m_2b^2 + m_2m_3(b-a)^2 + m_1m_3a^2}\right\}^{1/2} \qquad (8)$$

BHT's experience shows the LIVE system has these advantages over the mechanical inertia isolators:

1. Reduced complexity

2. Bearingless

3. Motion safety stops inherent to the concept

4. Smaller envelope for installation (no external masses moving through large amplitudes)

5. Linear response at high g's

6. Much lower weight and cost

7. Very low reliability and maintainability requirements

2. DESIGN AND ANALYSIS

The total main rotor isolation system was designed with the objective of isolating all six degrees-of-freedom (D.O.F.) of pylon motion from the helicopter fuselage. The six D.O.F. system was designed to utilize Liquid Inertia Vibration Eliminator (LIVE) isolators which have been successfully employed in other helicopter vibration reduction programs at BHT. A Bell Model 206LM was selected as the baseline helicopter, and the analysis and hardware design was undertaken with this as the subject ship. The 206LM is a 1914 kg (4000 lb) class, turbine-powered helicopter modified with a four-bladed soft-inplane flexbeam rotor system and skid gear designed to avoid ground resonance. The isolation system selected for the baseline helicopter during the analysis phase was the six LIVE system, using the LIVE unit in a pinned-pinned link configuration.

The mechanics of a classical pinned-pinned link is such that only axial loads can be transmitted; no moments can be input through the spherical bearings at its ends. If the LIVE unit in the link is tuned to isolate the blade passage frequency, then no oscillatory loads at the blade passage frequency in any direction will be transmitted through the link. By using six pinned-pinned isolator links attaching the pylon to the fuselage (in any configuration that is statically stable in all six degrees of freedom) and no other attachments, then every attachment will isolate the blade passage frequency and no oscillatory loads will be transmitted to any degree of freedom.

A representative LIVE isolator for the six D.O.F. application is shown in the cross-section view of Figure 5. The inner member is attached to the pylon, and the outer member is attached to the fuselage. The two members are bonded to the elastomer that fills the annulus between them. This elastomer (working in shear) acts as a spring which reacts to the static and dynamic loads placed on the isolator. Pressurized liquid mercury fills the center port in the inner member and both cavities at the ends of the isolator. No air space remains in the isolator.

PINNED-PINNED LIVE LINK

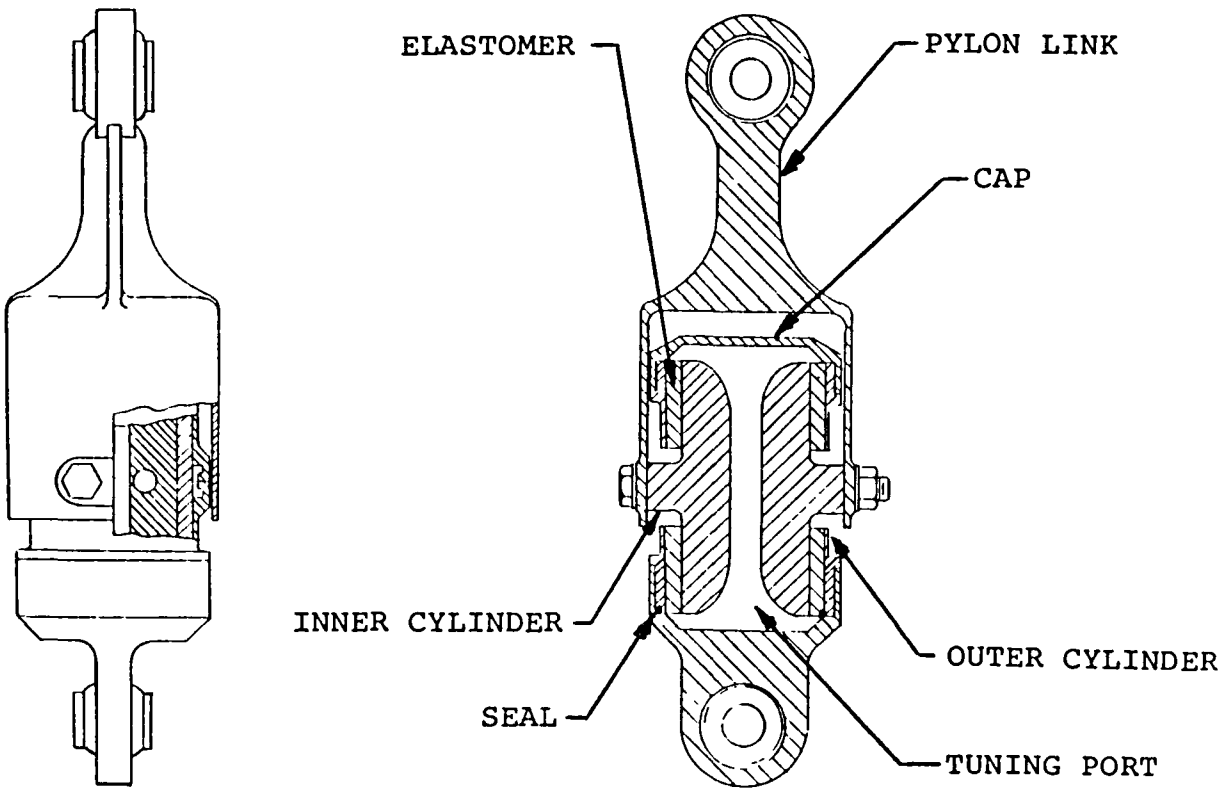

Figure 5. Cut-Away View of LIVE Link.

In operation, the liquid mercury oscillates within the LIVE unit, and isolation is achieved when the force due to pressure created by the motion of the mercury cancels the spring force due to the displacement of the rubber. By altering the spring rate and port diameter, the LIVE unit can be tuned to isolate the desired blade-passage frequency.

The six D.O.F. isolation system and 206LM helicopter was analyzed using a NASTRAN computer model. The NASTRAN model has a rigid fuselage and the fully flexible pylon from the 206LM. Figure 6 shows the undeformed system model. Figures 7a - 7e illustrate the pylon mode shapes at various frequencies. The placement of pylon modes is of interest in order to avoid coincidence with various excitation frequencies of the baseline helicopter.

The NASTRAN analysis was also implemented to calculate response curves for the six D.O.F. system. These curves are included in Figures 8 - 13 and show the calculated baseline helicopter c.g. response to hub inputs corresponding to the six degrees-of-freedom. These plots indicate that an idealized six D.O.F. system has the potential to provide better than 95% isolation to the fuselage.

The final configuration of the six D.O.F. system is shown in Figure 14. The isolator mounting hardware replaces the standard 206LM hardware with minimal changes to the helicopter and transmission assemblies. The isolators are manufactured by Lord Kinematics.

While the six D.O.F. system offers significant potential improvement in vibration isolation, it suffers an attendant weight penalty. Table 1 provides a weight comparison of a rigidly mounted, non-isolated mounting system and the six D.O.F. isolation system. The driveline weight calculations are included because more flexures are required to allow increased pylon motion with the isolated system. As the table indicates, a total weight difference of 69.6 lbs exists between the six D.O.F. isolation system and the non-isolated one. As a basis of comparison, the focal pylon-nodal beam isolation system used on the Bell 206L has a weight penalty of 128 lbs (3.2% gross weight), while isolating 3 degrees-of-freedom.

The weights listed for the six D.O.F. system correspond to fully adjustable, steel-bodied isolators. Reducing the degree of adjustability of the isolators would result in some weight reduction. Also, the replacement of steel components with parts made from aluminum and/or composite materials would result in a substantial weight savings, reducing the weight penalty of the six D.O.F. isolation system even further.

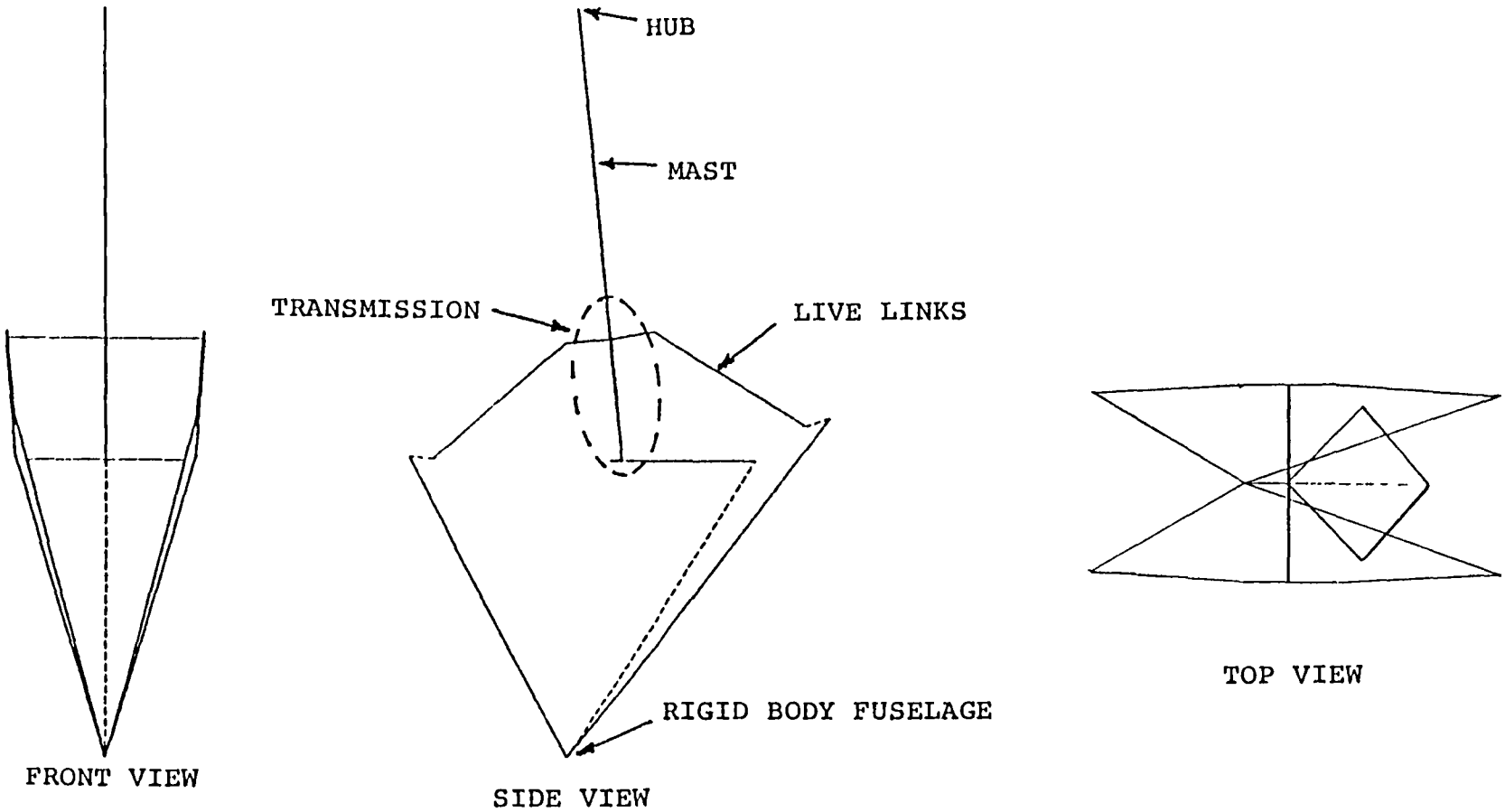

Figure 6. NASTRAN Model of Six LIVE Isolation System Installed on the 206LM (Undeformed).

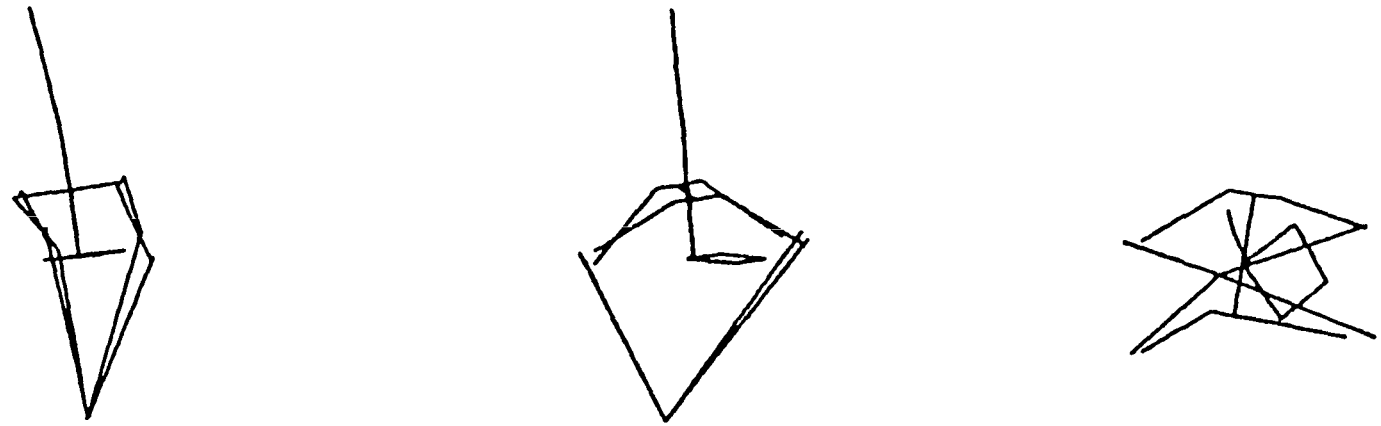

First Pylon Yaw Mode 2.58 Hz

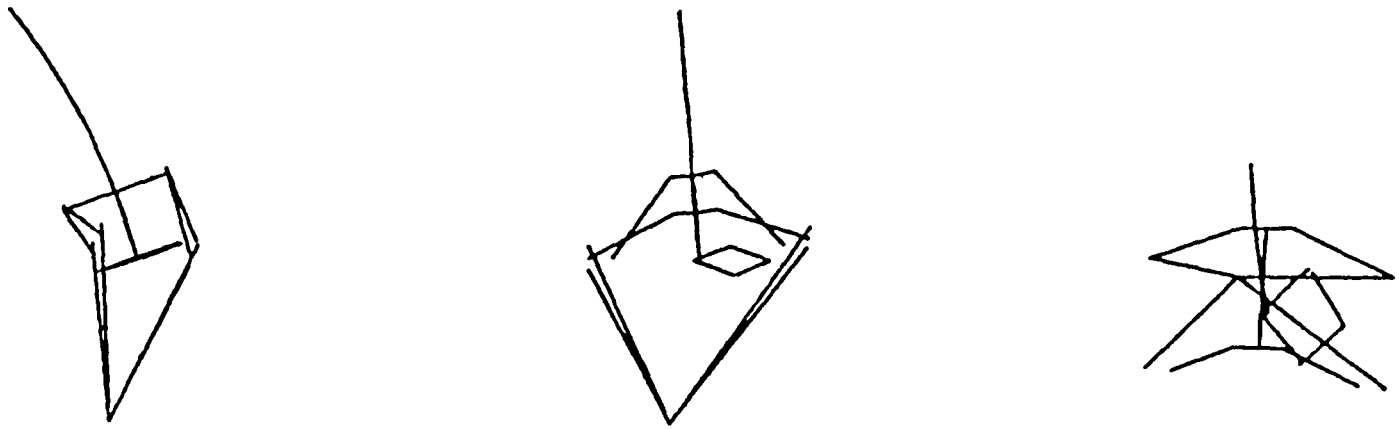

First Pylon Roll Mode - 2.91 Hz

Figure 7a. Baseline Helicopter NASTRAN Mode Shapes.

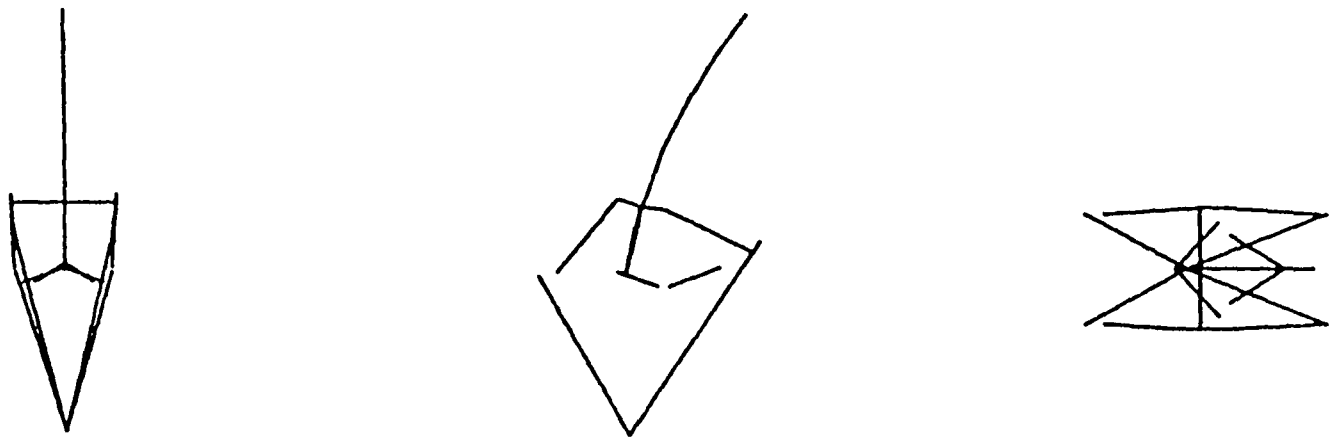

First Pylon Pitch Mode - 3.02 Hz

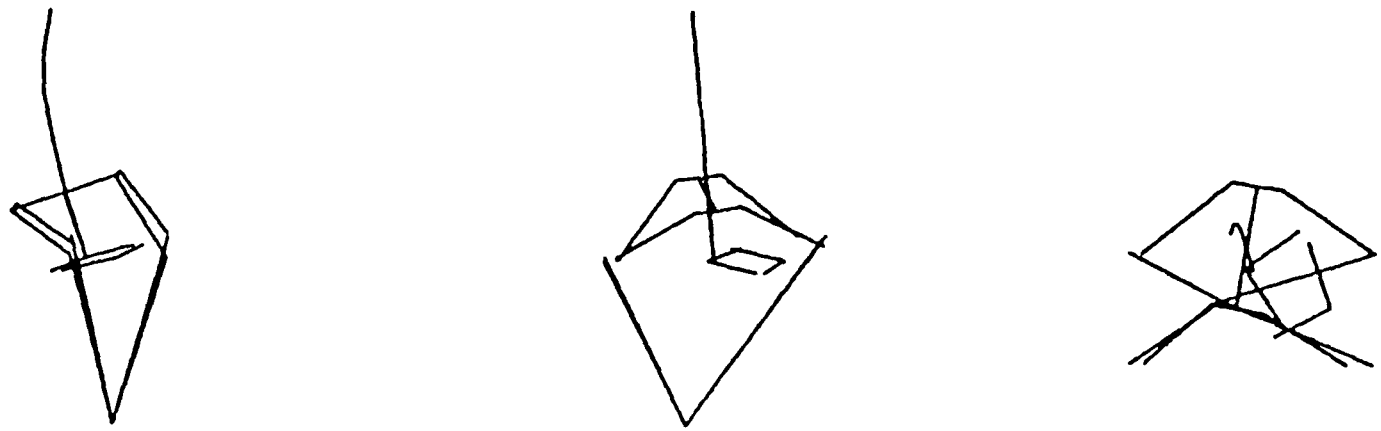

First Pylon Lateral Translation Mode - 8.42 Hz

Figure 7b. Baseline Helicopter NASTRAN Mode Shapes.

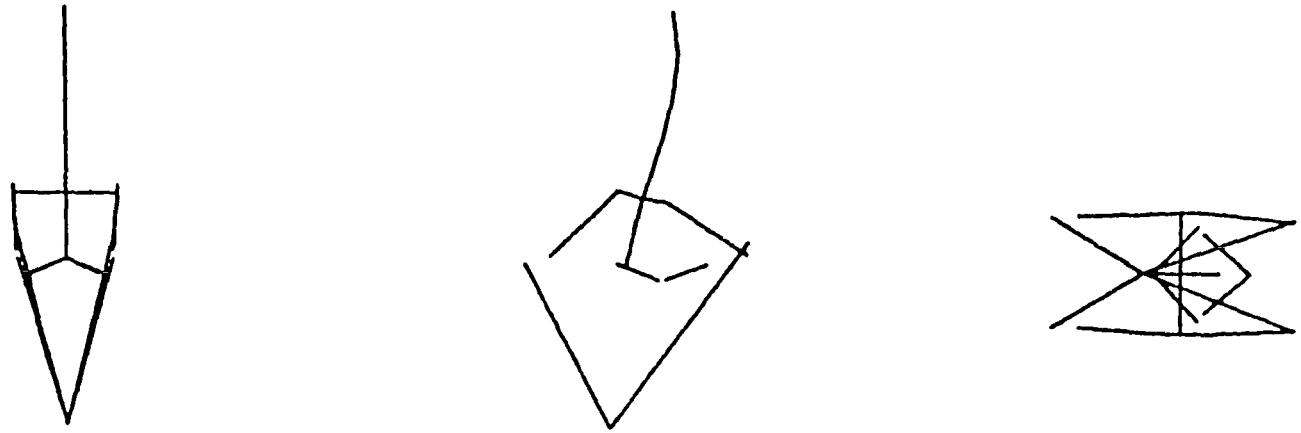

First Pylon Longitudinal Translation Mode - 12.53 Hz

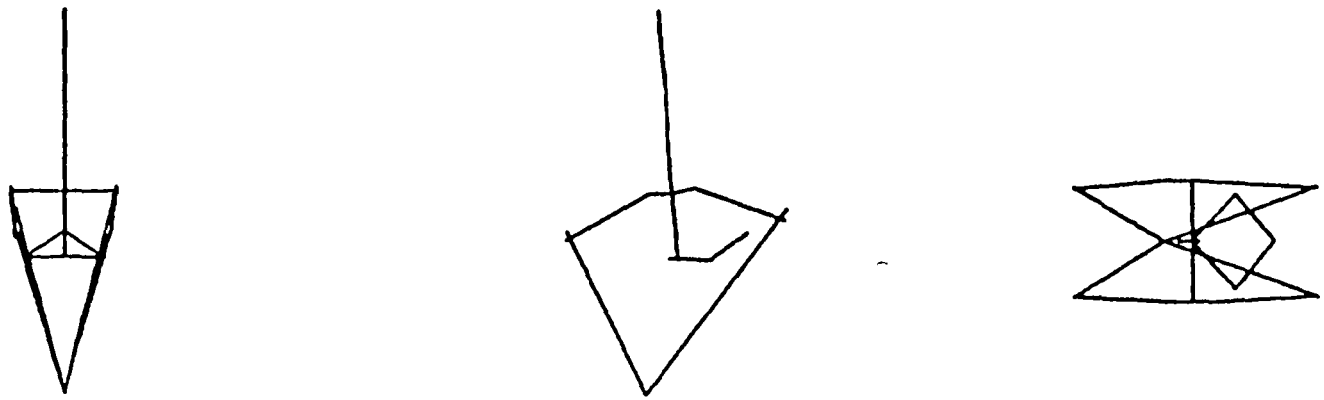

First Pylon Vertical Translation Mode - 14.14 Hz

Figure 7c. Baseline Helicopter NASTRAN Mode Shapes.

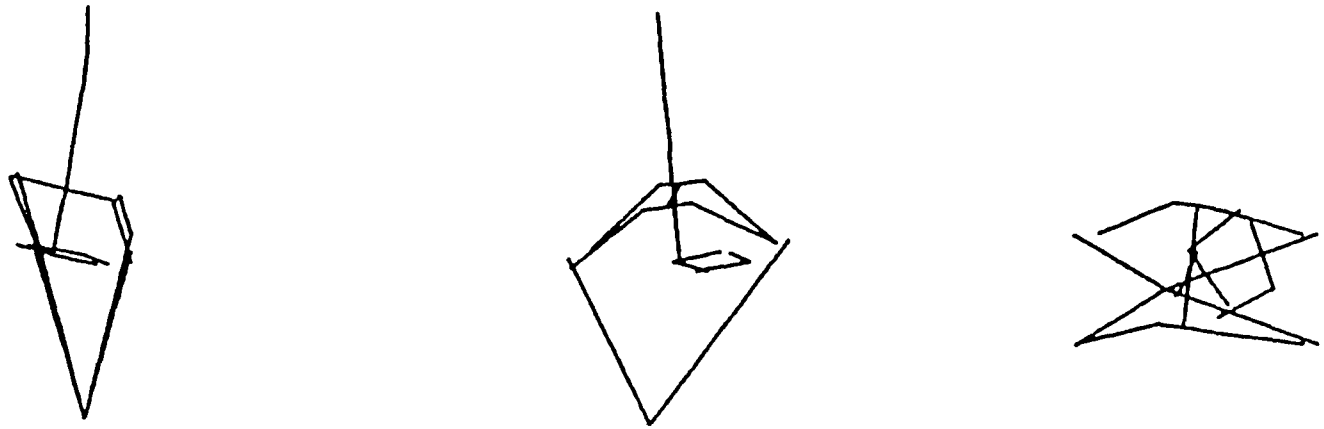

First LIVE Isolator Lateral Mode - 20.84 Hz

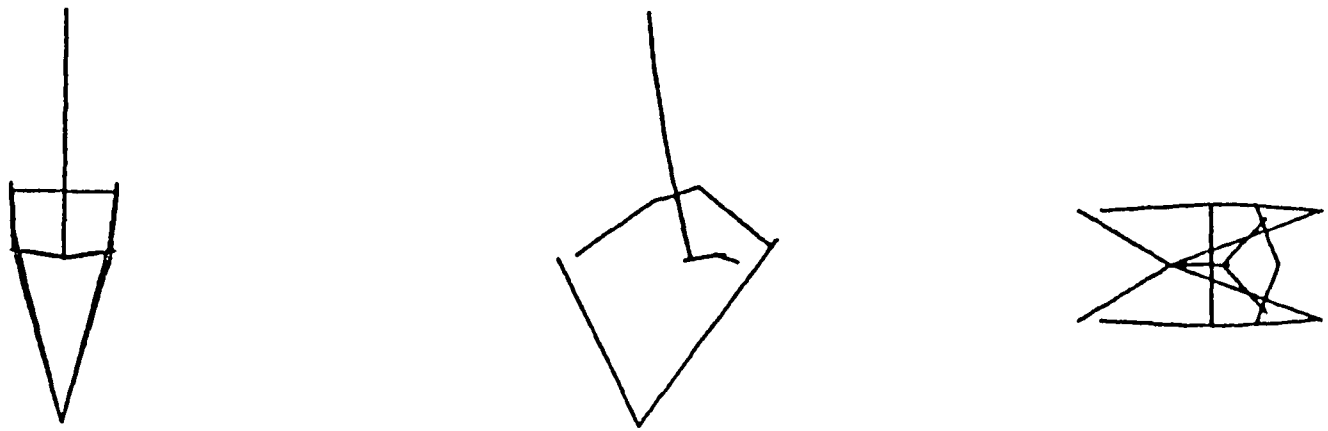

First LIVE Isolator Longitudinal Mode - 22.01 Hz

Figure 7d. Baseline Helicopter NASTRAN Mode Shapes.

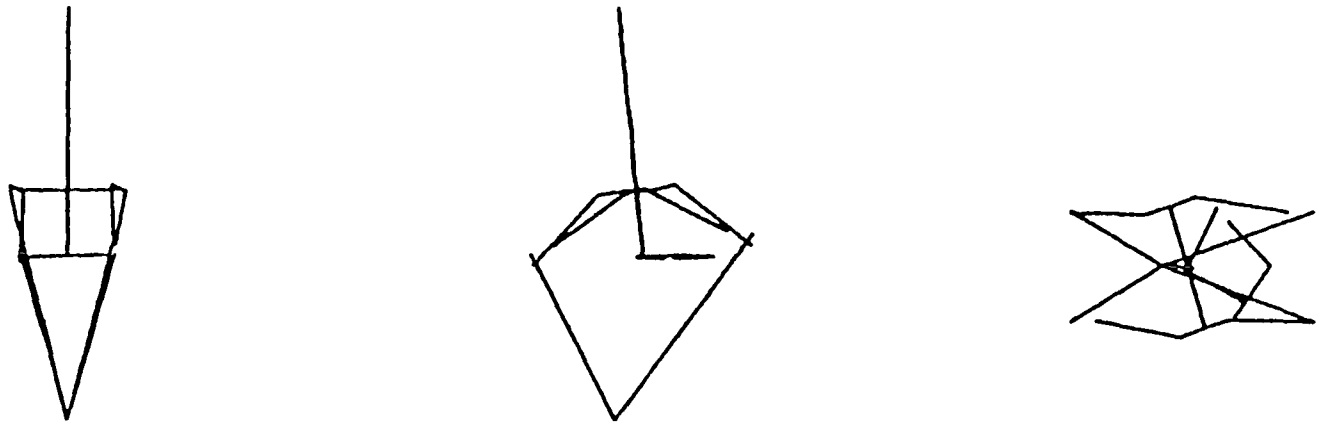

First LIVE Yaw Mode - 25.97 Hz

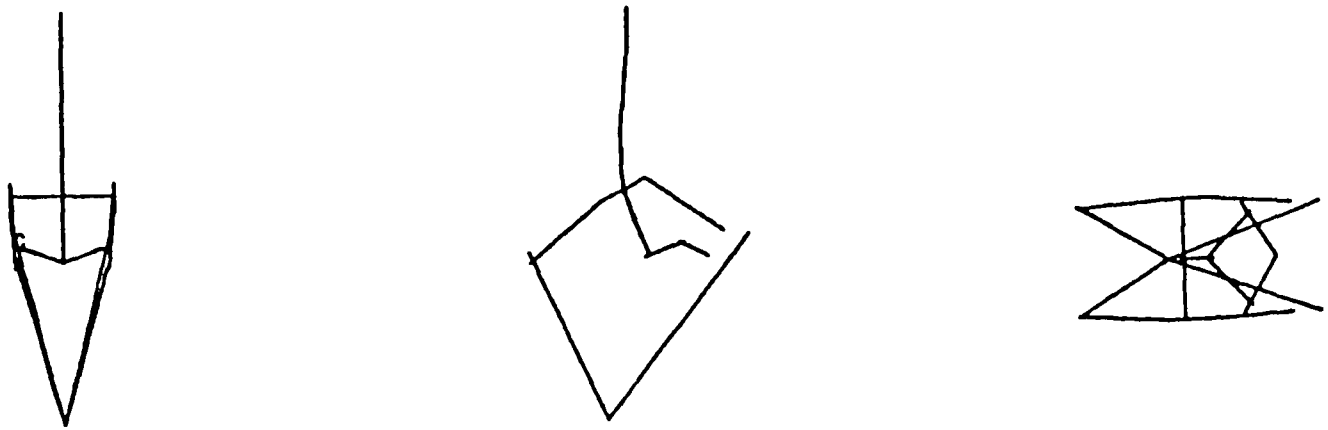

Longitudinal Mast Bending Mode - 36.66 Hz

Figure 7e. Baseline Helicopter NASTRAN Mode Shapes.

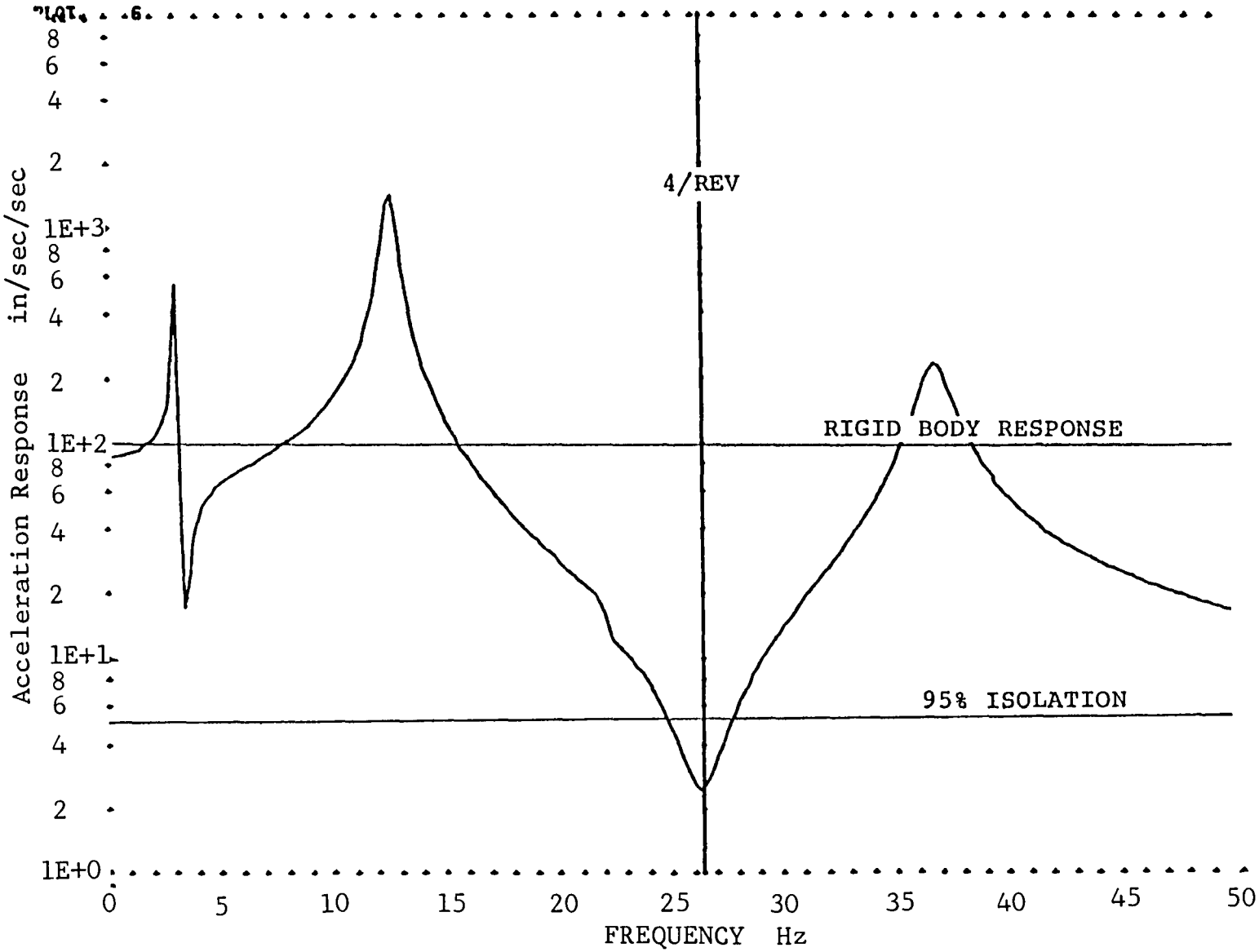

Figure 8. Baseline Helicopter C.G. Longitudinal Response to a 1000 Lb Longitudinal Hub Force.

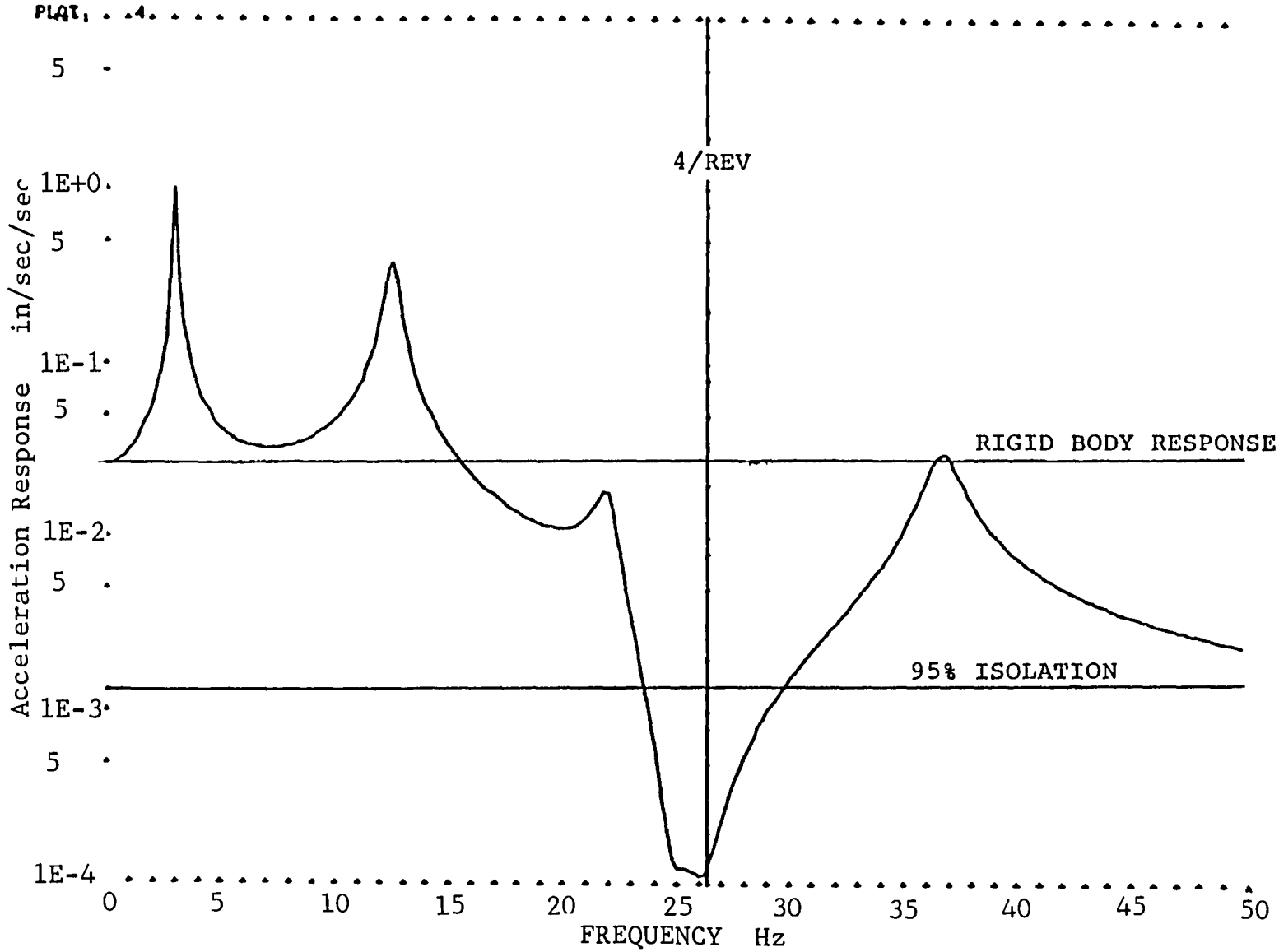

Figure 9. Baseline Helicopter C.G. Pitch Response to a 1000 In-Lb Pitch Hub Mmoent.

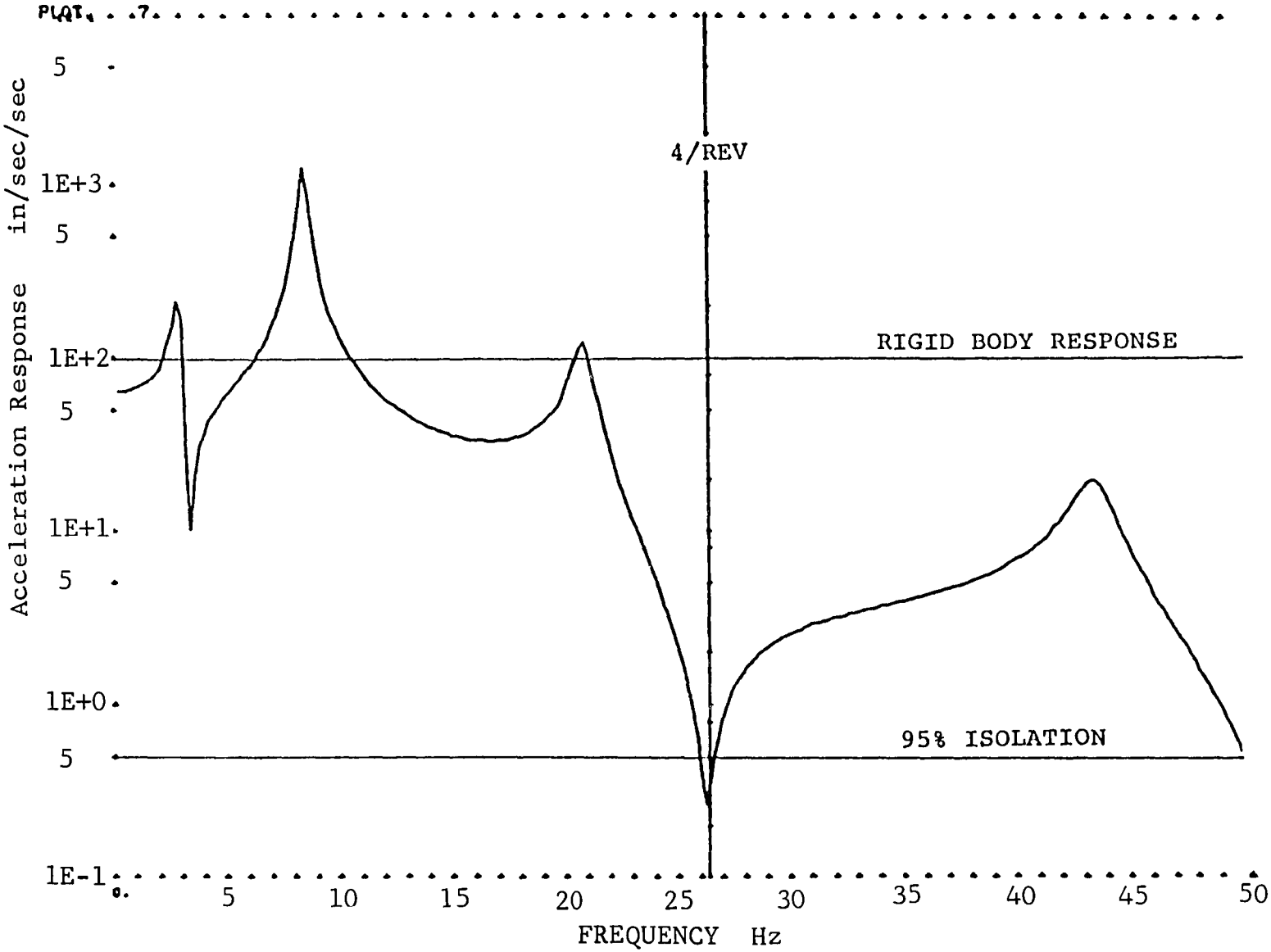

Figure 10. Baseline Helicopter C.G. Lateral Response to a 1000 Lb Lateral Hub Force.

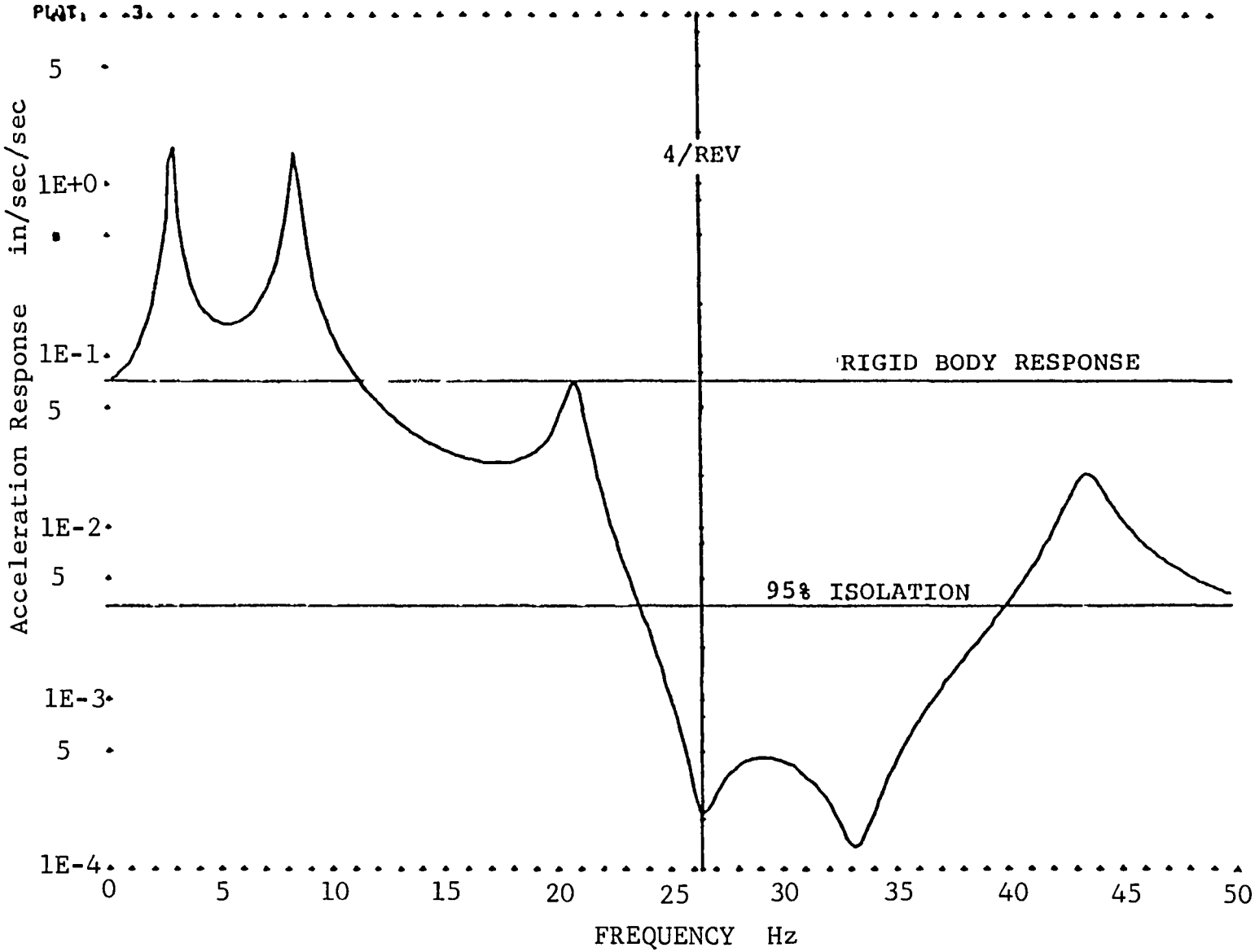

Figure 11. Baseline Helicopter C.G. Roll Response to a 1000 In-Lb Roll Hub Moment

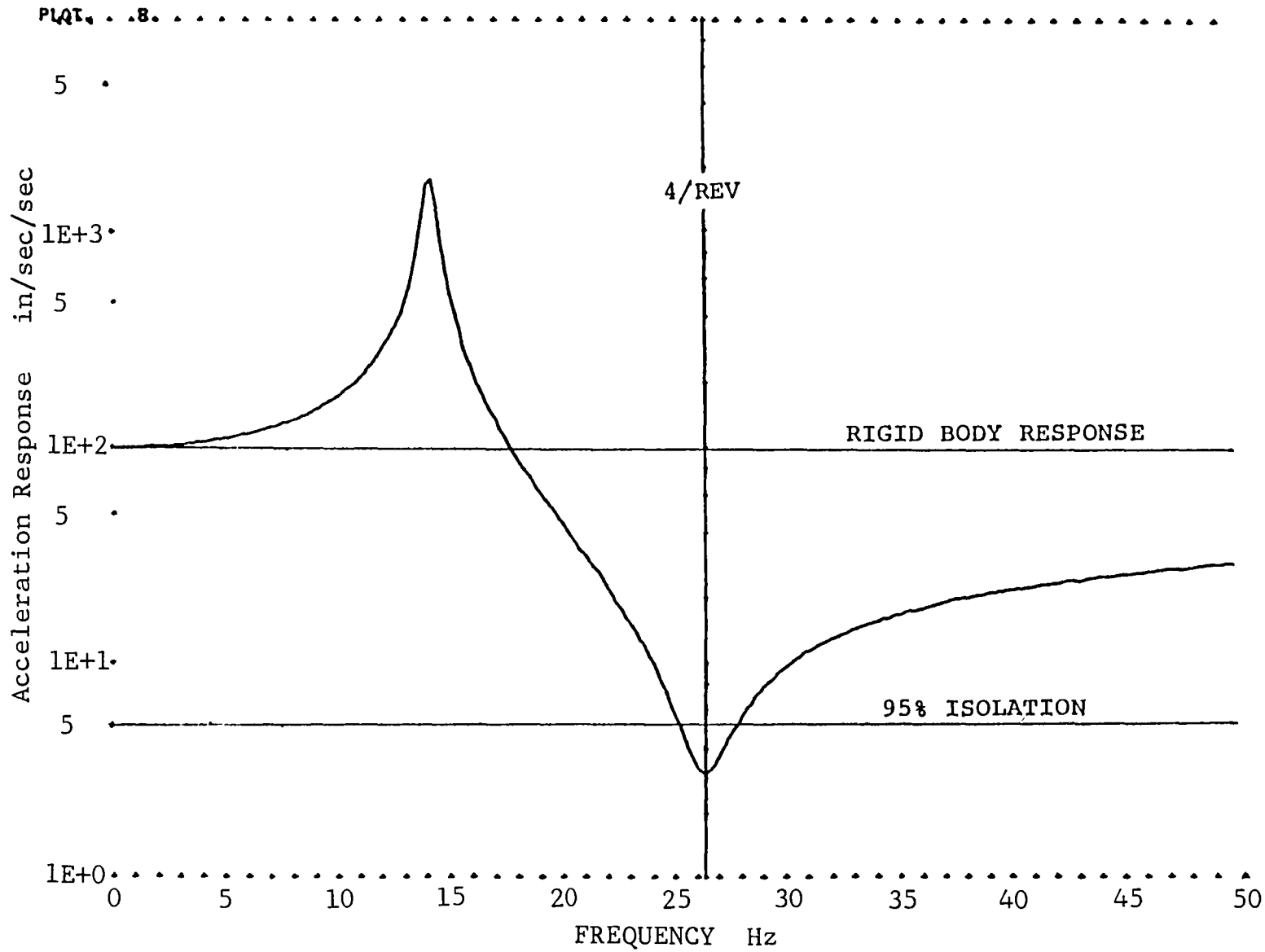

Figure 12. Baseline Helicopter C.G. Vertical Response to a 1000 lb Vertical Hub Force.

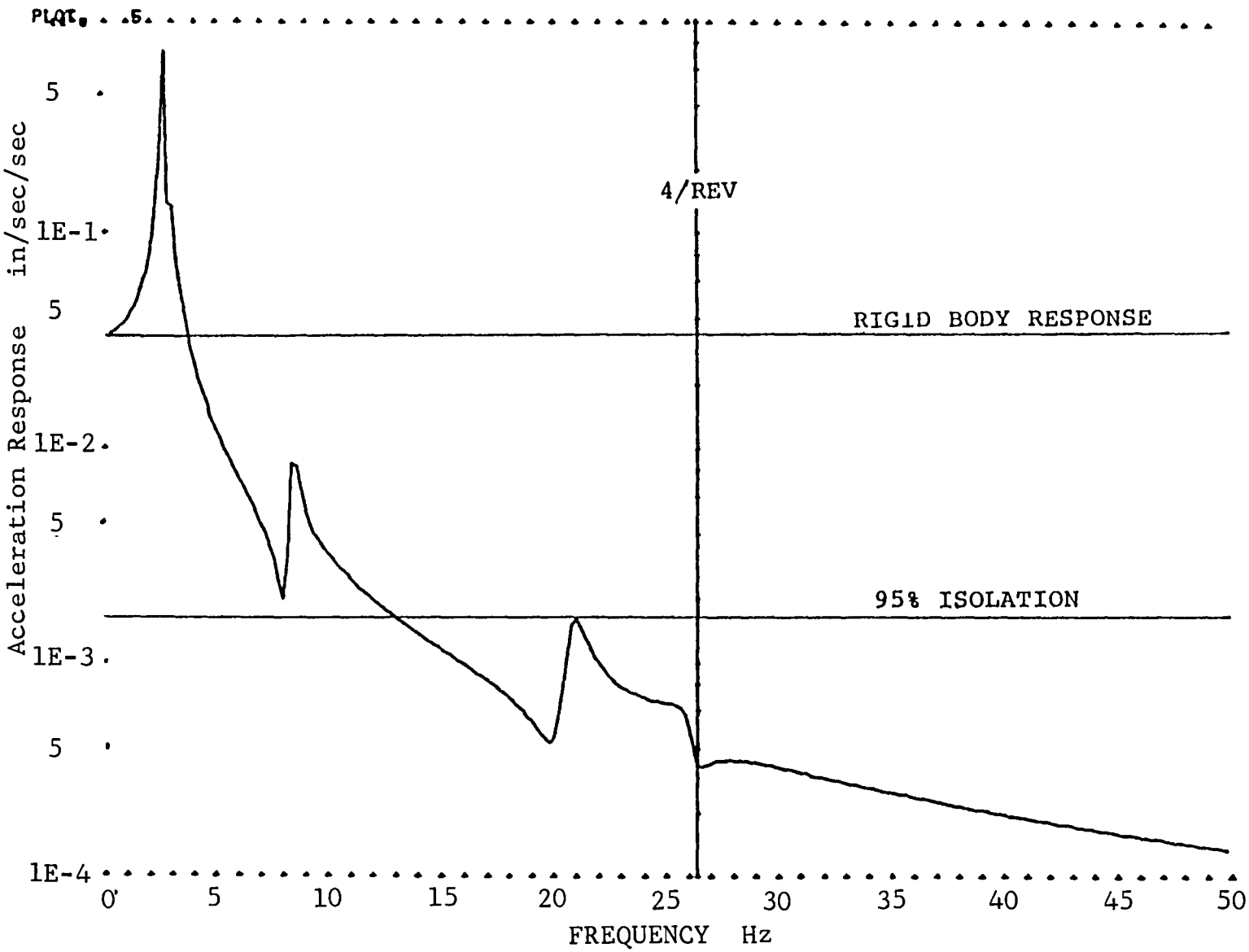

Figure 13. Baseline Helicopter C.G. Yaw Response to a 1000 in-lb Yaw Hub Moment.

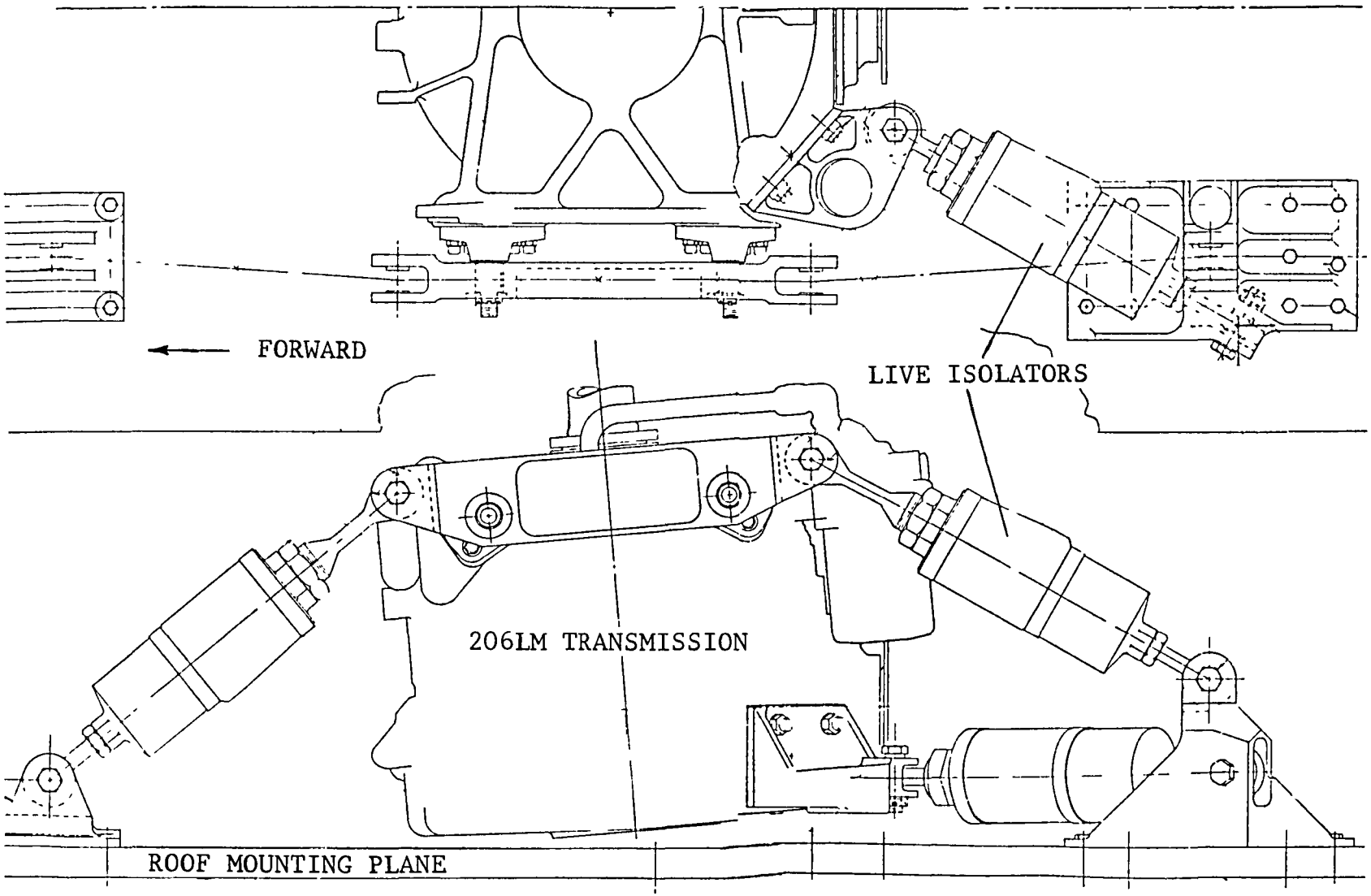

Figure 14. Installation of Six Degree-of-Freedom Isolation System on Helicopter.

TABLE 1. A COMPARISON OF WEIGHTS FOR NON-ISOLATED AND ISOLATED PYLON MOUNTING SYSTEMS

NON-ISOLATED (RIGID)		ISOLATED (6 D.O.F.)	
Rigid Link (6 req'd)	1.83 lb ea	Isolator (6 req'd)	12.34 lb ea
Conventional Clevis Mount w/Hardware (6 req'd)	1.75 lb ea	Conventional Clevis Mount w/Hardware (2 req'd)	1.75 lb ea
Driveshaft Flexure (2 req'd)	0.37 lb ea	Double Clevis Mount w/Hardware (2 req'd)	6.10 lb ea
*Additional Driveshaft Length (1.40 in. req'd)	0.17 lb	Driveshaft Flexure (6 req'd)	0.37 lb ea
(.35 in/flexure x 4 flexure x .424 in^2 x .283 lb/in^3)			
TOTAL SYSTEM WEIGHT:		TOTAL SYSTEM WEIGHT:	
6 x 1.83 lb/link	= 10.98 lb	6 x 12.34 lb/isol.	= 74.04 lb
6 x 1.75 lb/mount	= 10.50 lb	2 x 1.75 lb/mount	= 3.50 lb
2 x 0.37 lb/flexure	= 0.74 lb	2 x 6.10 lb/mount	= 12.20 lb
Add. Driveshaft Length	= 0.17 lb	6 x 0.37 lb/flexure	= 2.22 lb
	22.39 lb		91.96 lb

WEIGHT PENALTY = ISOLATED SYSTEM - NON-ISOLATED SYSTEM
= 91.96 - 22.39

WEIGHT PENALTY = 69.57 lb

*Due to the reduction in number of flexures required for the non-isolated system, additional driveshaft length must be added.

3. COMPONENT VIBRATION TESTS

Before testing the complete six D.O.F. isolation system, each individual isolator was tested and tuned. By adjusting the internal volume of mercury, and therefore changing the oscillating mass, all of the isolators were tuned to isolate approximately 26.3 Hz (4/rev) vibration.

The hardware involved in the isolator tuning process is shown in Figures 15 and 16. A 758-lb weight is suspended from the isolator, which was itself hung from an electromagnetic shaker. A 150-lb weight is attached above the isolator. The 150-lb weight simulates the portion of the pylon weight, and the 758-lb weight simulates the portion of the fuselage weight that must be supported by each of the four isolators on the 206LM baseline helicopter. (The other two isolators in the six D.O.F. system do not support any vertical load.) This combination of weights places the vertical natural frequency of a individual unit in this test approximately equal to the natural frequency of the installed system on the baseline helicopter.

Figure 17a is a measured response plot slowing the acceleration of the "fuselage" (isolated side) normalized by the "pylon" (non-isolated side) acceleration for isolator S/N LK0010. This plot was generated by sweeping the frequency of a 500-lb dynamic input force (approximately twice the maximum expected load per isolator) from 10 to 57 Hz. The figure shows a resonance at 12 Hz and an isolation valley at 26.3 Hz with a transmissibility of over 90% and no amplification at 8P (52.6 Hz). For the remainder of the tuning tests the frequency range investigated was from 10 to 30 Hz to cut test time in half and increase frequency resolution. Figures 17b, 17c, and 17d show a test of linearity with input forces at 200, 300, and 500 lb, respectively. These figures show that the isolation frequency and the transmissibility are effectively unchanged with force input, with a slight reduction in the isolation frequency with increasing force. The frequency reduction is a result of the dynamic spring rate of the elastomer decreasing slightly with increasing oscillatory motion. Figures 18 - 21 show the final tuning of all eight isolator units with a 500-lb force input. The isolation frequencies and the transmissibility ratios are summarized in Table 2.

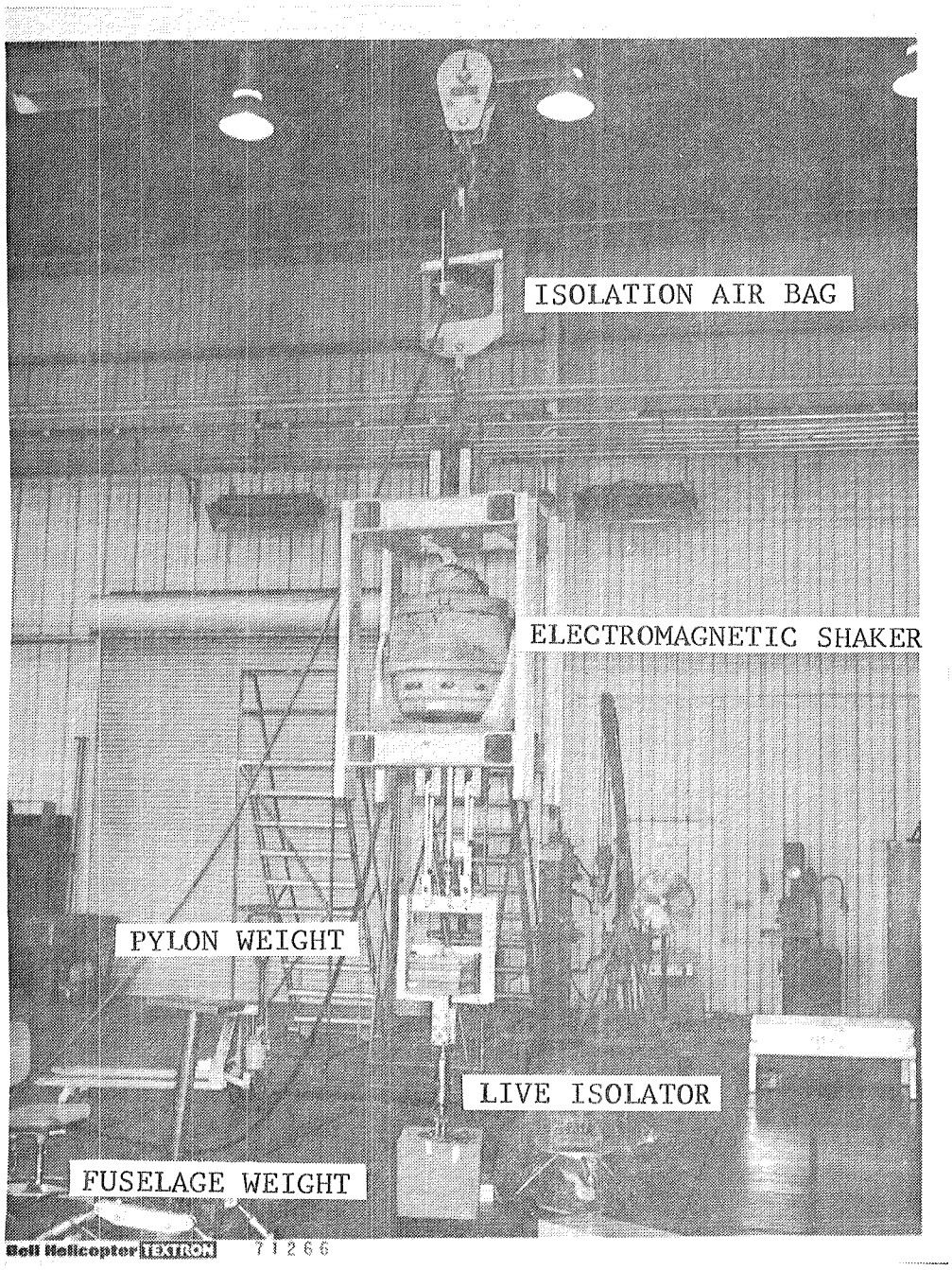

Figure 15. Test Apparatus Used for Tuning Isolators.

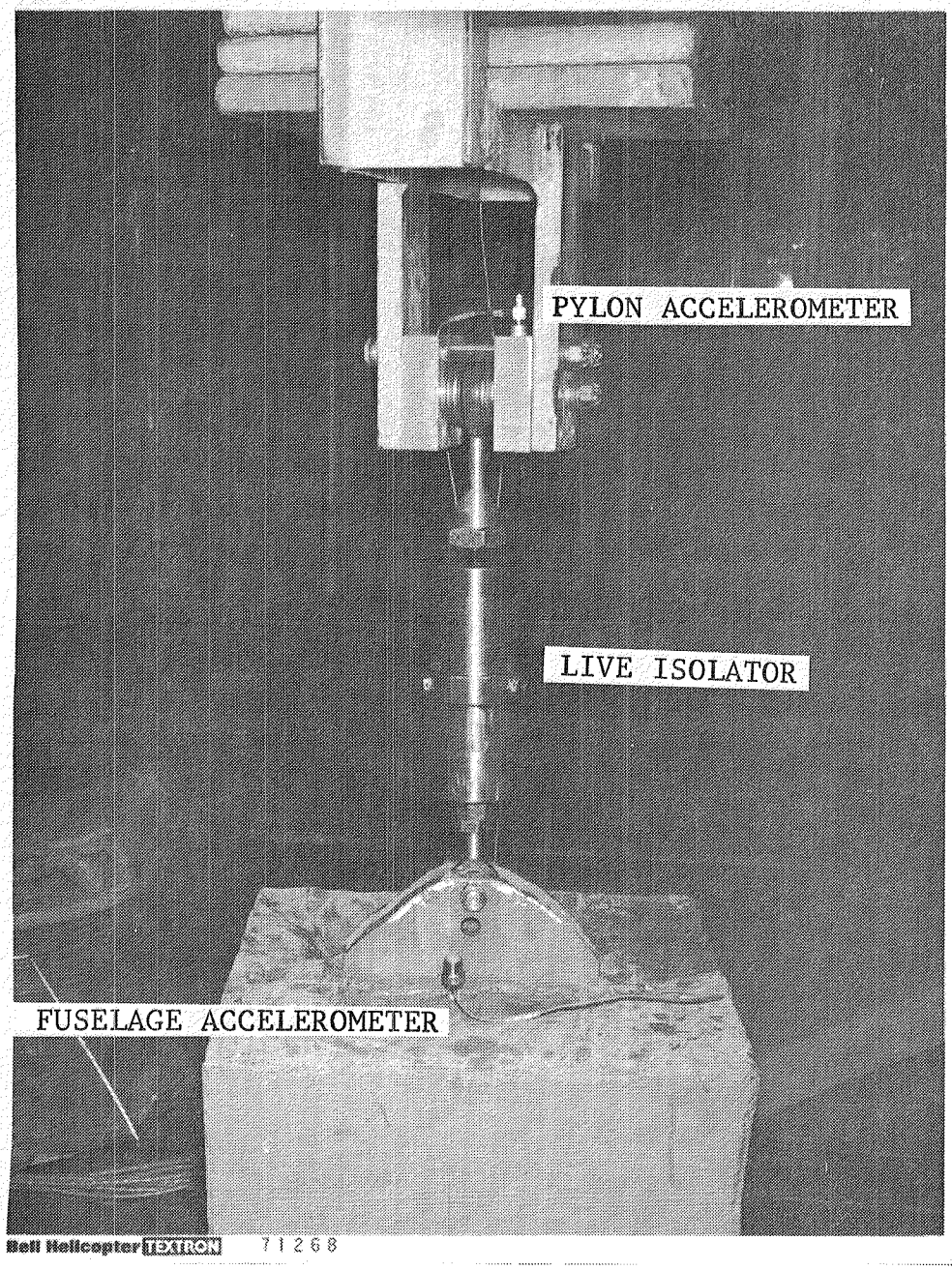

Figure 16. LIVE Isolator Installed in Test Apparatus.

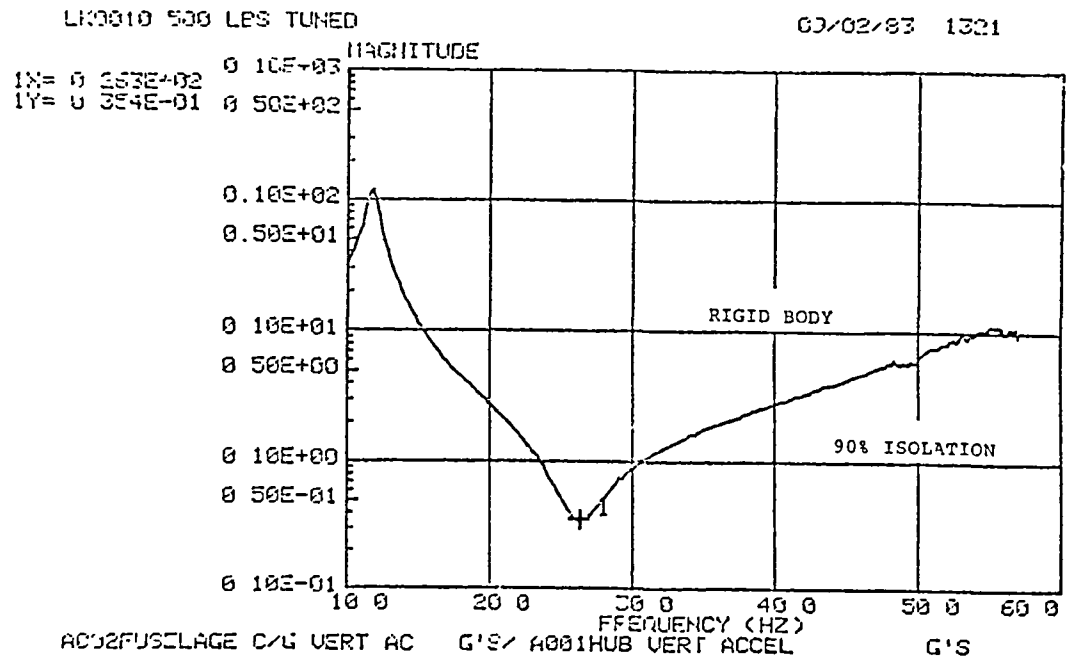

Figure 17a. Response of Isolator LK 0010--500 lb Force Input.

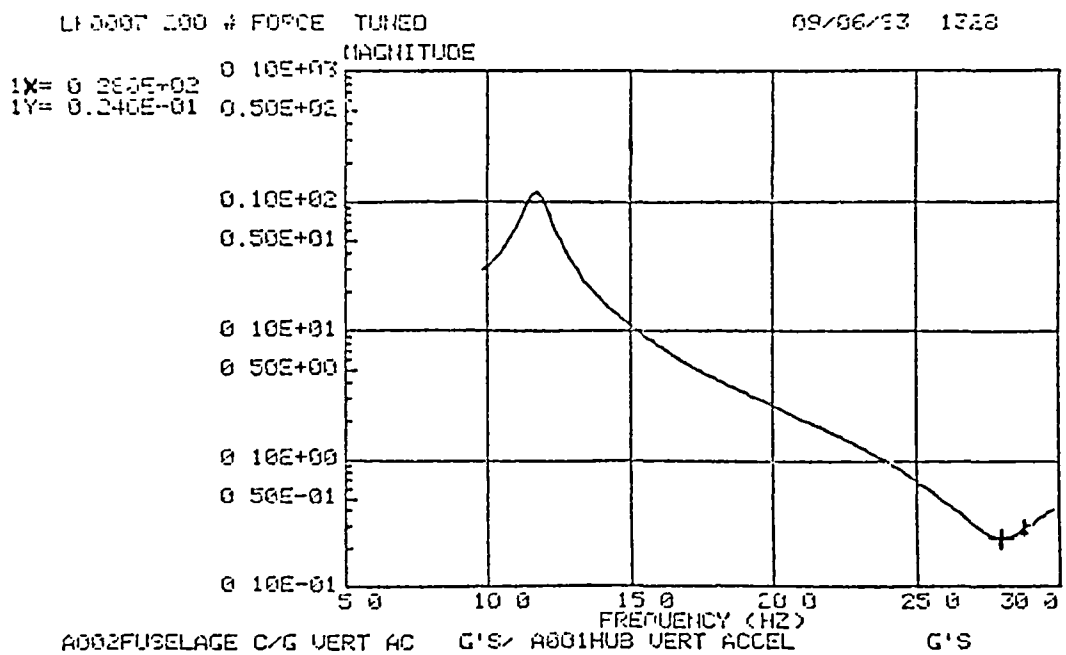

Figure 17b. Response of Isolator LK 0007--200 lb Force Input.

Figure 17. Responses of Individual LIVE Isolators.

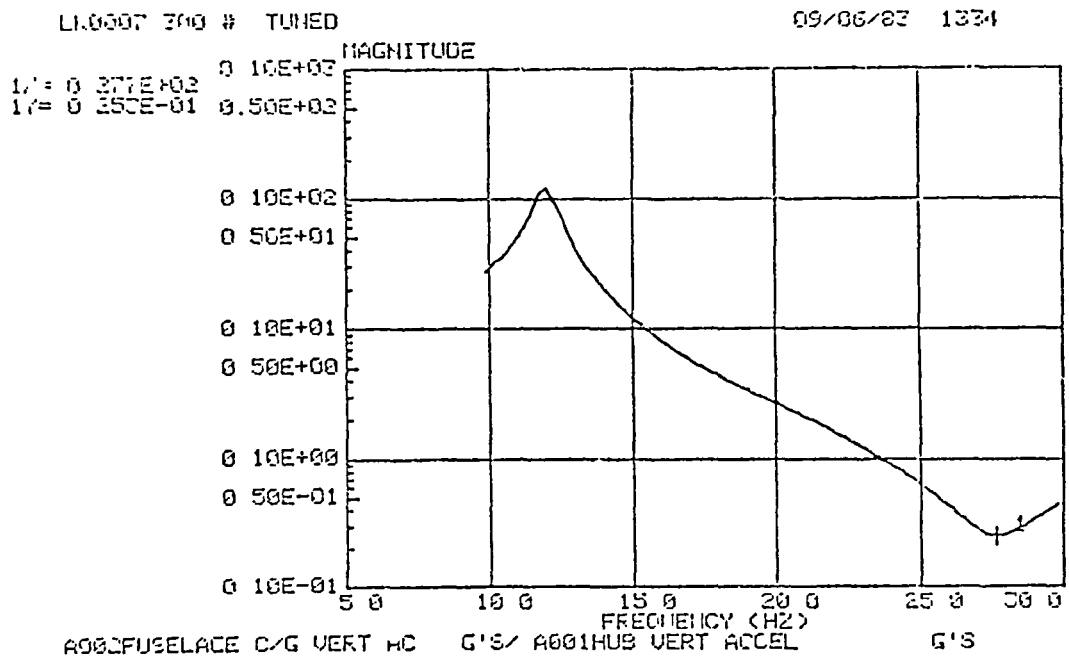

Figure 17c. Response of Isolator LK 0007--300 lb Force Input.

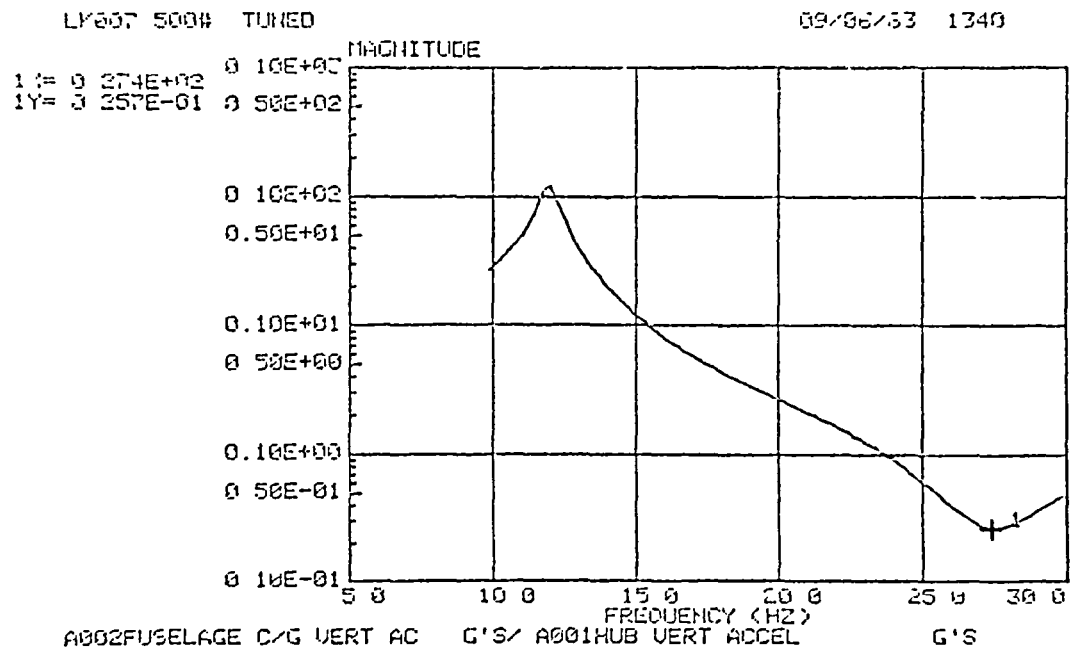

Figure 17d. Response of Isolator LK 0007--500 lb Force Input.

Figure 17. Responses of Individual LIVE Isolators.

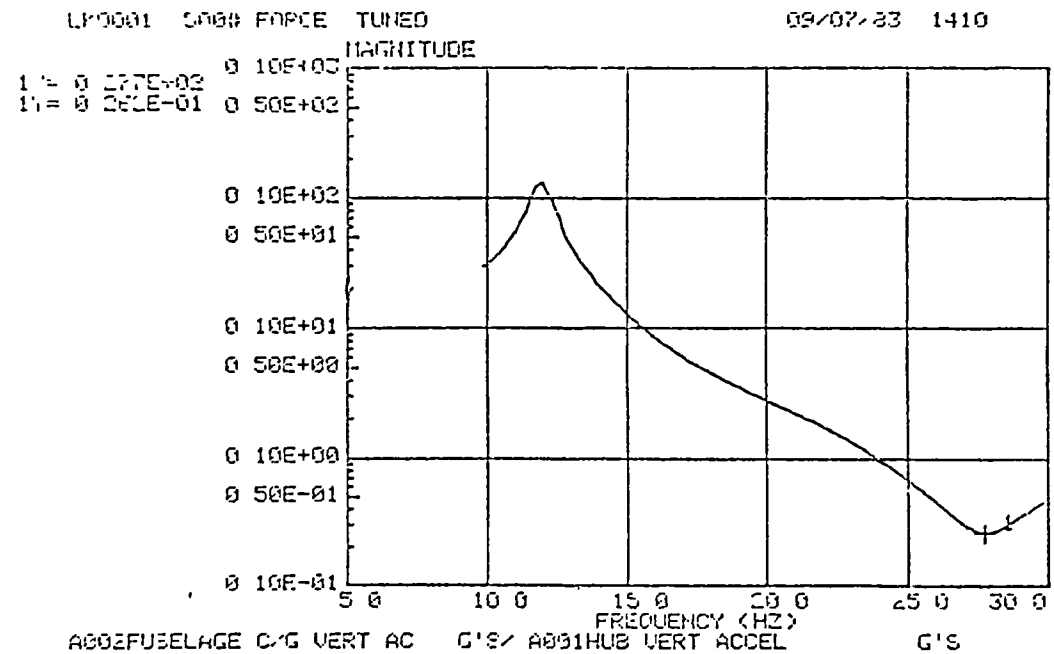

S/N LK0001

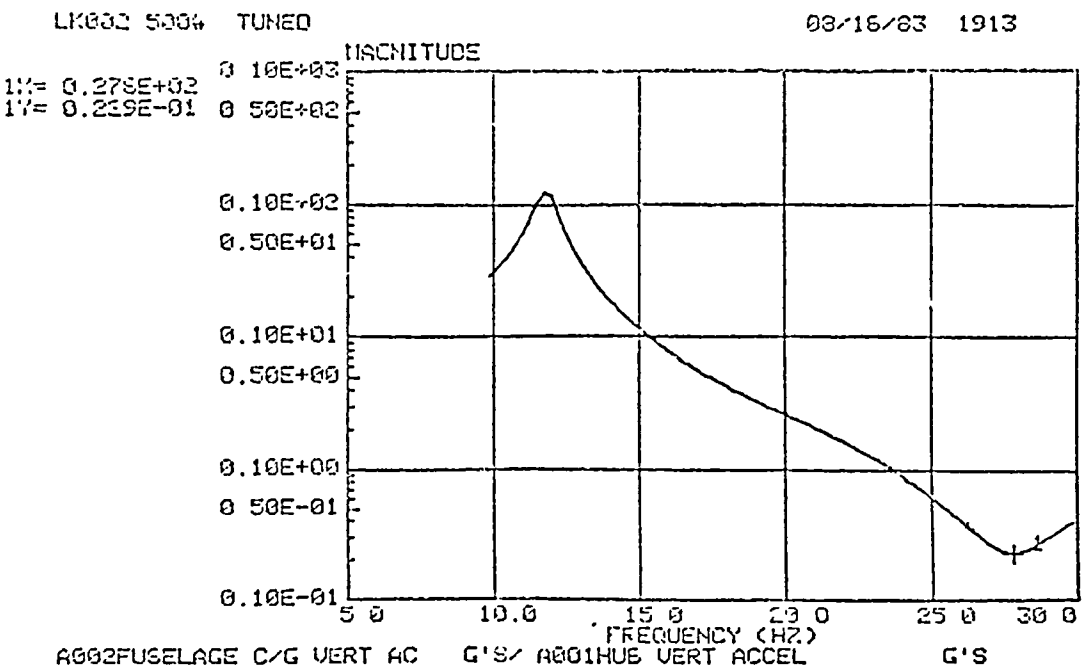

S/N LK0002

Figure 18. Responses of Individual LIVE Isolators After Tuning.

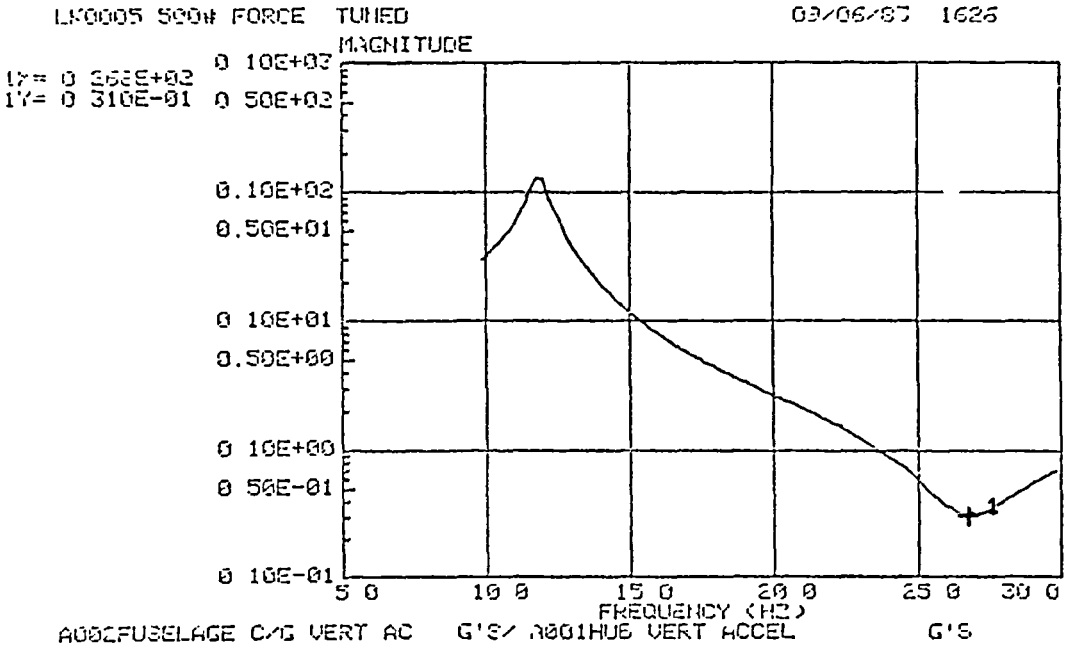

S/N LK0005

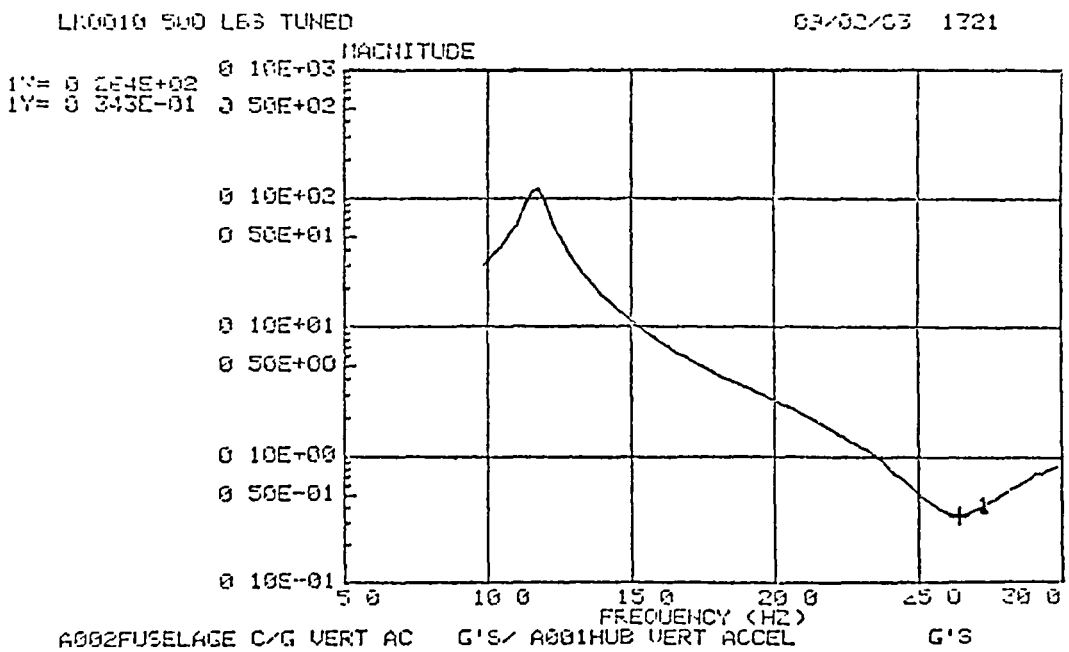

S/N LK0010

Figure 19. Responses of Individual LIVE Isolators After Tuning.

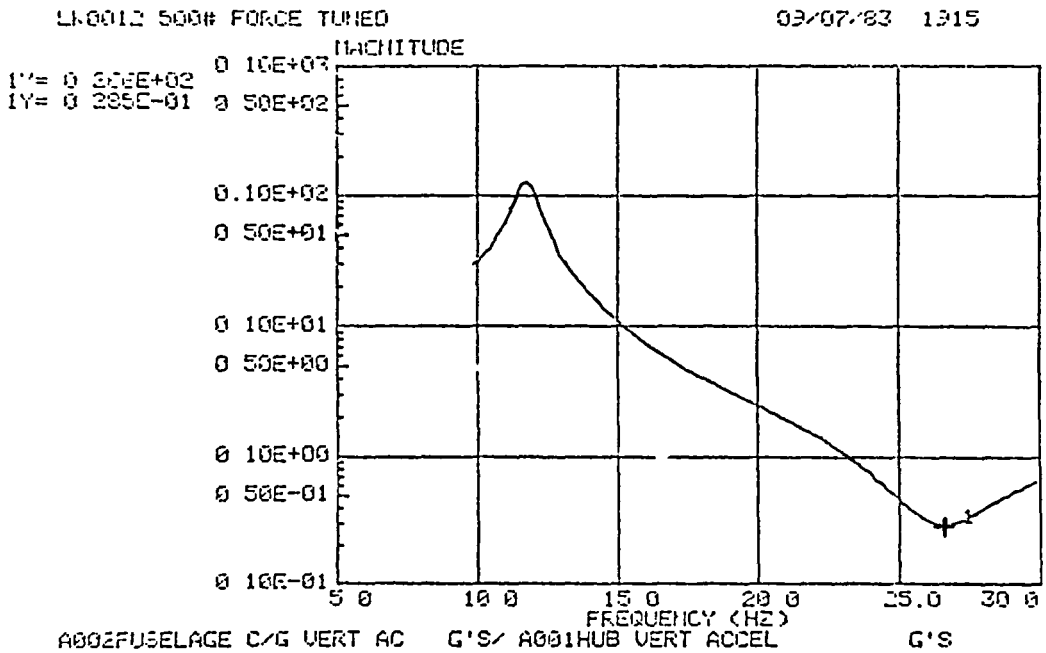

S/N LK0012

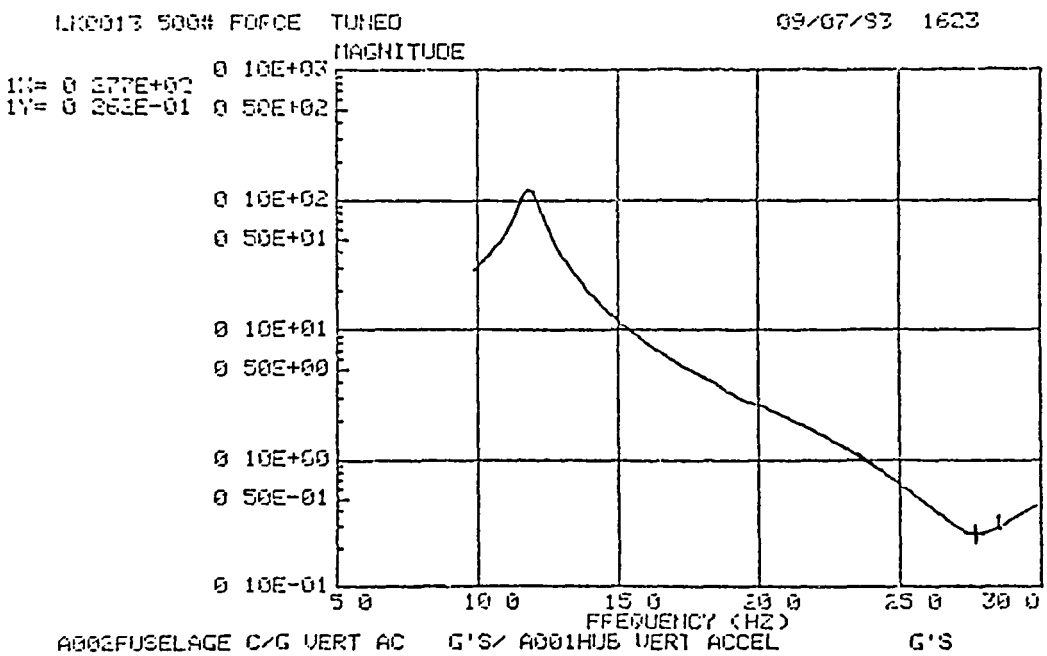

S/N LK0013

Figure 20. Responses of Individual LIVE Isolators After Tuning.

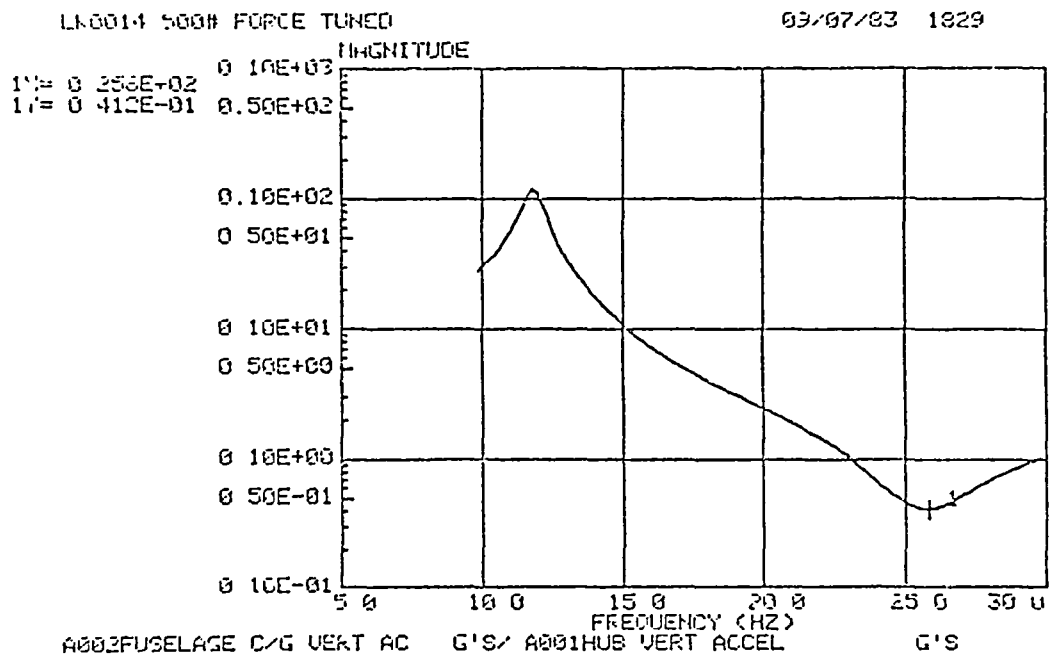

S/N LK0014

Figure 21. Responses of Individual LIVE Isolators After Tuning.

TABLE 2. ISOLATOR PERFORMANCE AT 500 LB INPUT FORCE

Isolator Serial No.	Figure No.	Tuned Isolation Frequency - Hz	% of Desired Isolation Frequency	Transmissibility Ratio @ 26.3 Hz
LK0001	18	27.7	105%	.040
LK0002	18	27.8	106%	.035
LK0005	19	26.8	102%	.032
LK0007	17d	27.4	104%	.033
LK0010	19	26.4	100%	.034
LK0012	20	26.6	101%	.030
LK0013	20	27.7	105%	.035
LK0014	21	25.8	98%	.040

Figure 22a is included to illustrate some characteristics of the isolators. The figure shows the measured response of a single isolator system to an oscillatory input force of 100 lb. The plot demonstrates that as pylon weight is reduced, the resonant frequency of the system increases, while the isolation frequency remains unchanged. Recalling equations 7 and 8, the resonant frequency f_n is dependent upon isolator stiffness, area ratio, and the pylon, tuning weight, and fuselage masses. The isolation frequency, however, is dependent only on isolator parameters; stiffness, area ratio, and tuning weight.

Damping affects the magnitude of response both at resonance and anti-resonance (isolation). Its presence is desirable to limit the peak response at resonance, but damping also limits the degree of isolation that can be achieved. Zero damping would provide optimum isolation performance. For this reason, the isolators use low viscosity fluid and low-damped elastomer.

Figure 22b shows the measured response of a double isolator system to an oscillatory input force of 100 lb. To generate this plot, two isolators were mounted side by side (in parallel), while supporting the same pylon and fuselage weight used previously. Therefore, isolator stiffness and tuning weight were doubled with respect to the single isolator setup. Doubling the system spring rate yields the same resonant frequency that the system would have with the original single isolator spring rate and half the pylon weight. The response of the double isolator system shows a distinct similarity to the response of the single isolator setup with 43% pylon weight. As noted before, the resonant frequency shifted upward due to increased stiffness, while the isolation frequency was unchanged. The actual isolation valley magnitude also compares closely to the 43% pylon weight case.

Figure 22a points out an important correlation between the placement of the resonant and isolation frequencies and the transmissibility at the isolation valley frequency. As the frequency separation between resonance and anti-resonance decreases, whether due to increased stiffness or decreased pylon mass, the isolation performance suffers dramatically. Therefore, in addition to minimizing damping, it is desirable to obtain as much frequency separation between isolation and any resonance as possible. The importance of this separation is discussed in the Results section of this report.

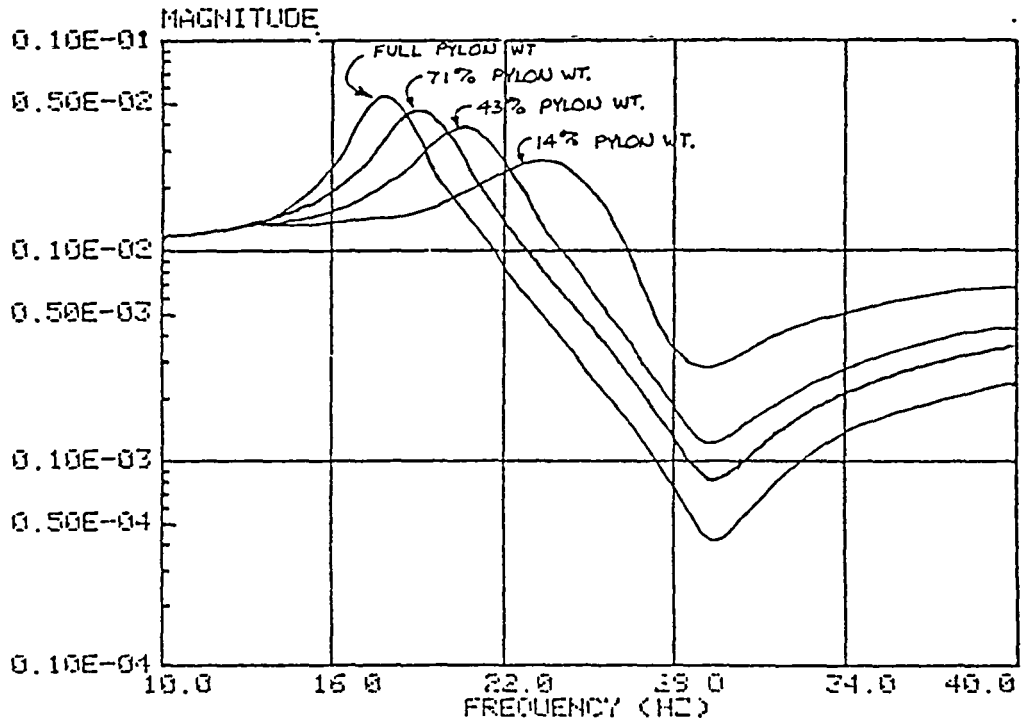

Figure 22a. Effect of Pylon Weight on Isolator Response.

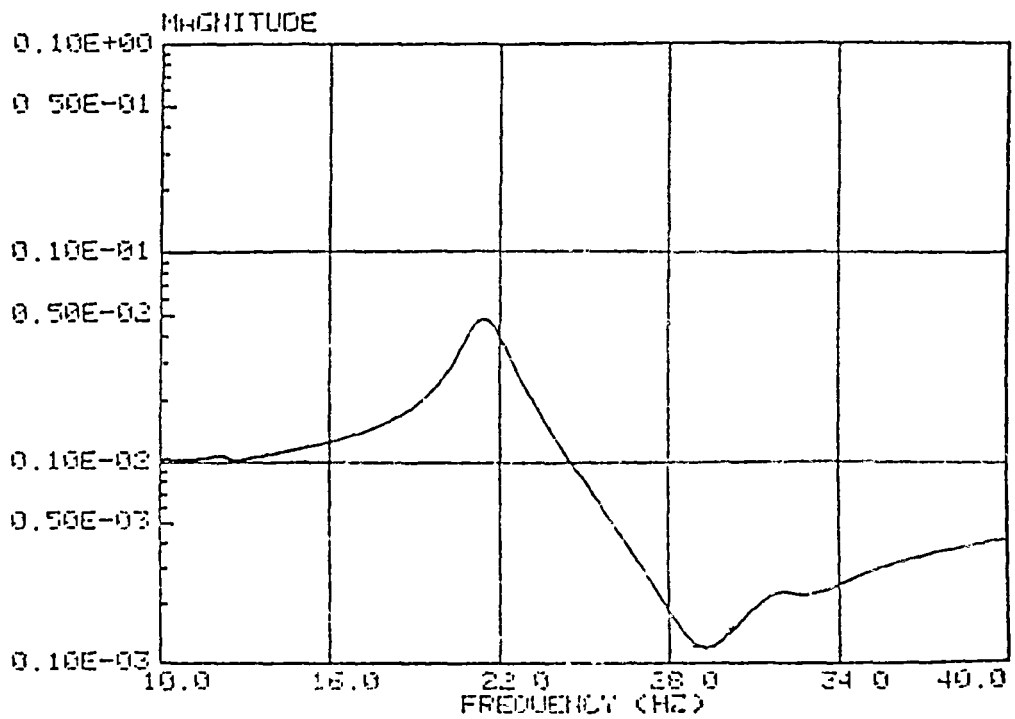

Figure 22b. Response of Two Isolators in Parallel.

Figure 22. Response Characteristics of LIVE Isolators.

4. ENDURANCE TEST OF AN ISOLATOR UNIT

In order to assure safety of flight, and to establish some baseline data for service-life projections, a representative "LIVE" isolator was subjected to an endurance test. The apparatus used in the test is shown in Figure 23.

The subject isolator was mounted horizontally, and was retained between a stationary clevis and a clevis mounted on the oscillating output shaft of a hydraulic shaker. Forces on the input (shaker) and output (isolated) sides of the isolator were monitored with strain gages, and relative motion between the inner and outer cylinders was measured with an LVDT.

Isolator S/N LK0002 was used in this test. The test was run with a mean isolator tension displacement of 0.10 inch and an oscillatory displacement of $\pm$0.02 inch, corresponding to expected V_H levels. The subject isolator was tested without failure for 10^6 cycles at 26.3 Hz, for a total time of 108.5 hours. During the test, a mercury vapor detector was used to monitor the isolator for leaks, of which none were detected.

The photographs of Figures 24 - 25 show the internal condition of the subject isolator after the endurance test. As illustrated in Figure 24, some slight erosion of the elastomer surface has occurred. This is believed to have been caused by cavitation of the mercury, as evidenced by the flow lines of microscopic elastomer particles left on the surface. These elastomer particles are also evident on the metal surface of the isolator end cap (Figure 25). This minor erosion had no effect on the performance of the isolator, and after cleaning off the residue, the surfaces appeared as smooth as when molded.

This endurance test demonstrated that these "LIVE" isolators can withstand static and dynamic loadings equivalent to those expected in flight. Furthermore, these tests indicate that the isolators are not affected by continuous cyclic loadings.

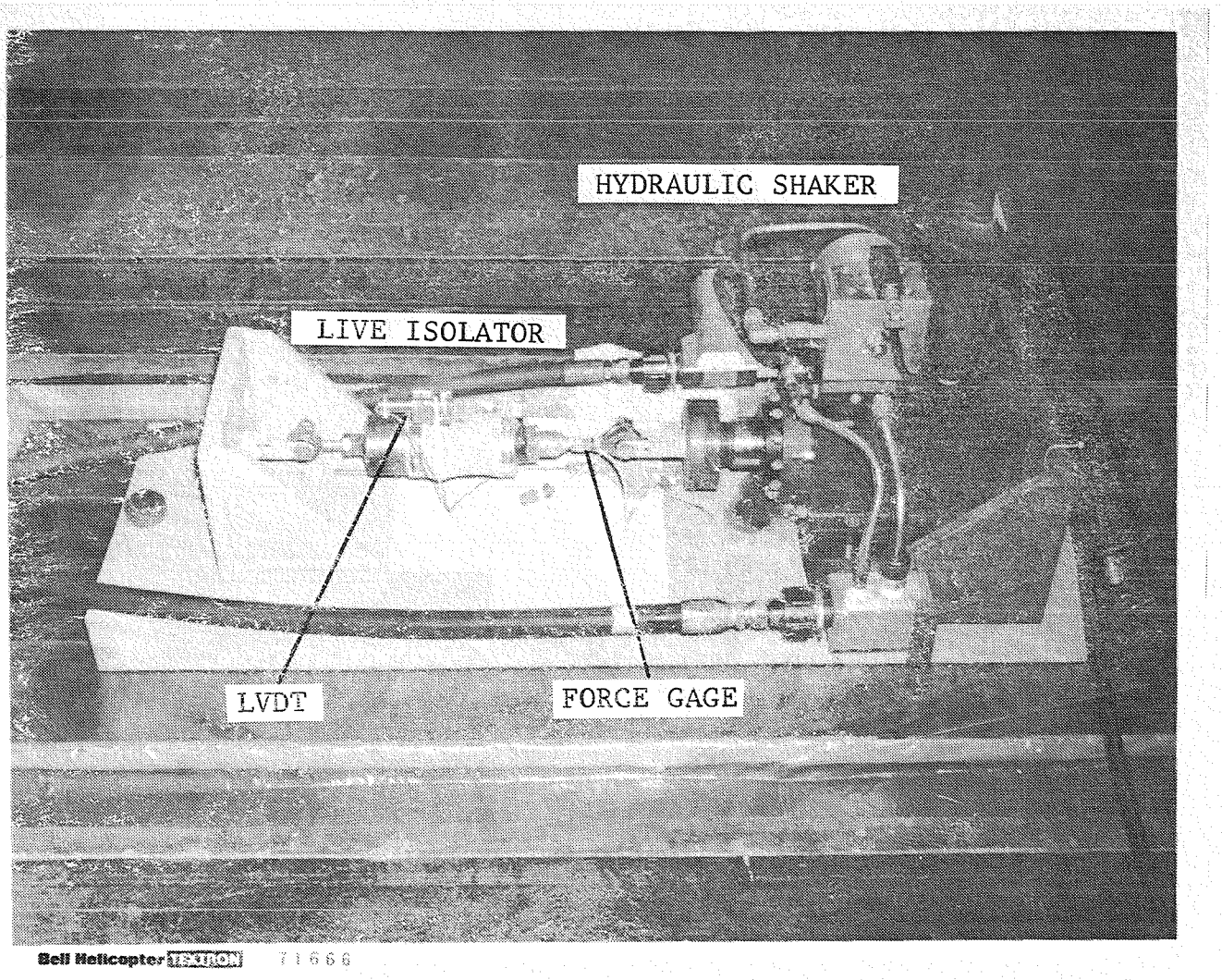

Figure 23. Apparatus Used for LIVE Isolator Endurance Test.

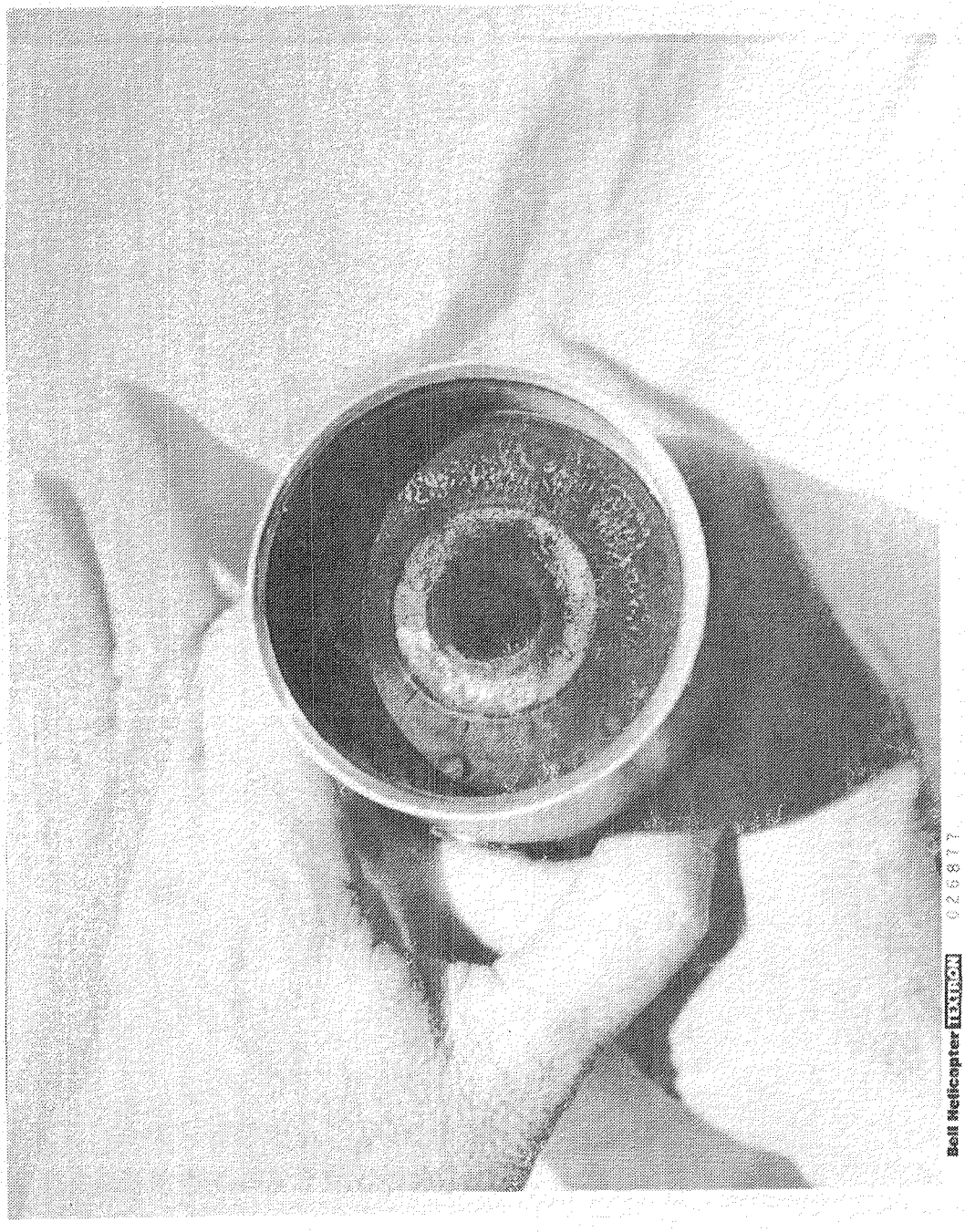

Figure 24. Internal Condition of LIVE Isolator Body After Testing.

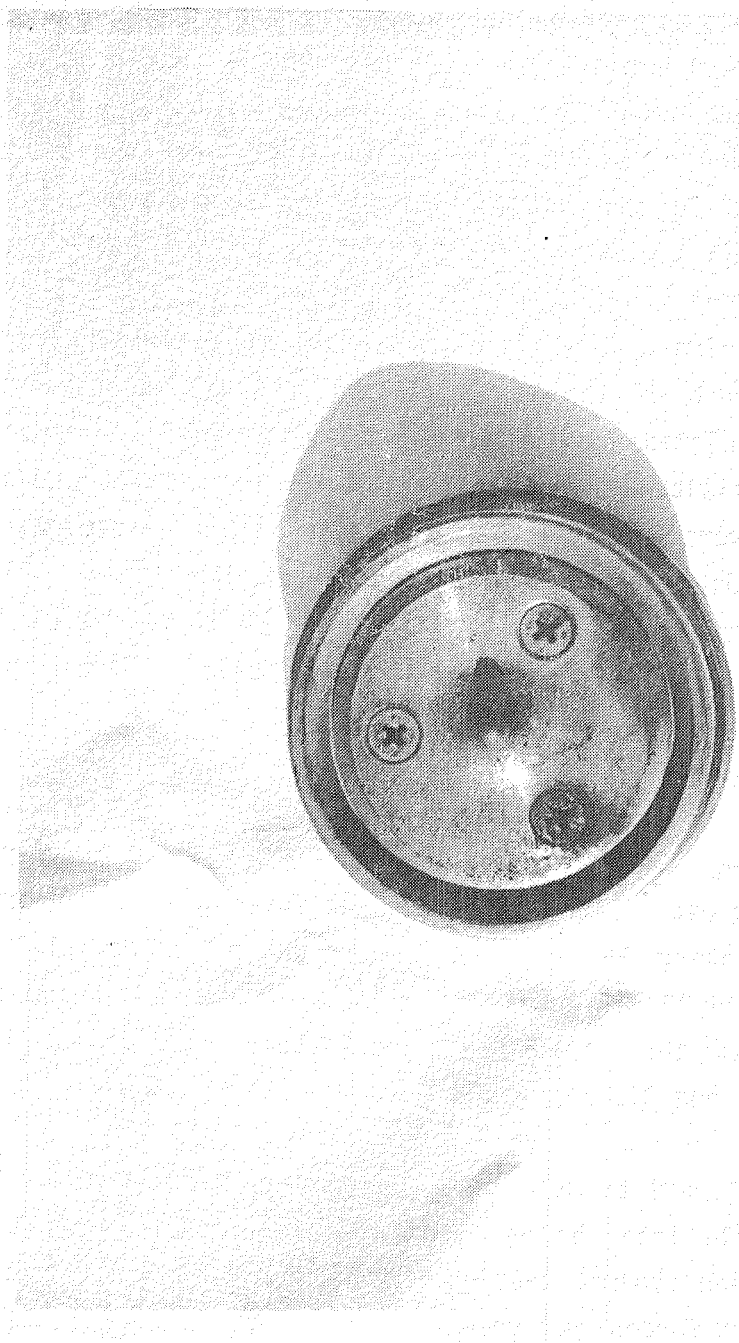

Figure 25. Internal Condition of LIVE Isolator End Cap After Testing.

5. SIX D.O.F. TEST METHODS AND PROCEDURES

The six degree-of-freedom isolation test setup is shown in the photographs of Figures 26 - 33. A 206LM transmission was used in the test program, and six "LIVE" isolators provided for the pylon's static mounting and constraint requirements, in addition to providing vibration isolation capabilities. The isolators were attached to mounting brackets which were bolted to a 1-inch thick aluminum plate. This plate was bolted solidly to the floor.

Strain gages for measuring axial forces were affixed to the isolated (roof-mounted) rod end of each of the six isolators. Also, accelerometers were mounted on the non-isolated (pylon-mounted) side of each isolator. These accelerometers were oriented axially with respect to the isolators. Additional accelerometers were attached to the pylon assembly in various locations and orientations according to the input force/moment direction. Pylon accelerometer orientation for each input is listed in Table 3. Input hub shear magnitudes were measured with piezoelectric load cells. Strain gages were used to measure input moments.

As the figures illustrate, static and oscillatory forces and moments corresponding to the six degrees-of-freedom can be input to the main rotor hub. Figures 26 and 27 show oscillatory lateral shear force and roll moment inputs, respectively. Oscillatory longitudinal shear and pitch moment inputs are shown in Figures 28 and 29. Figures 30 and 31 show the test setup for vertical shear inputs, and the static and oscillatory yaw moment inputs are depicted in Figures 32 and 33, respectively.

Static tests were performed to determine the coefficients of a 6 x 6 calibration matrix which would later be used to determine transmissibilities of the six D.O.F. system during dynamic testing. The calibration matrix relates measured orthogonal input forces and moments at the hub to reaction forces measured at the isolator roof mounts.

For the matrix determination, static loads (3 shears, 3 moments) corresponding to the six degrees-of-freedom were applied to the hub individually. Referring

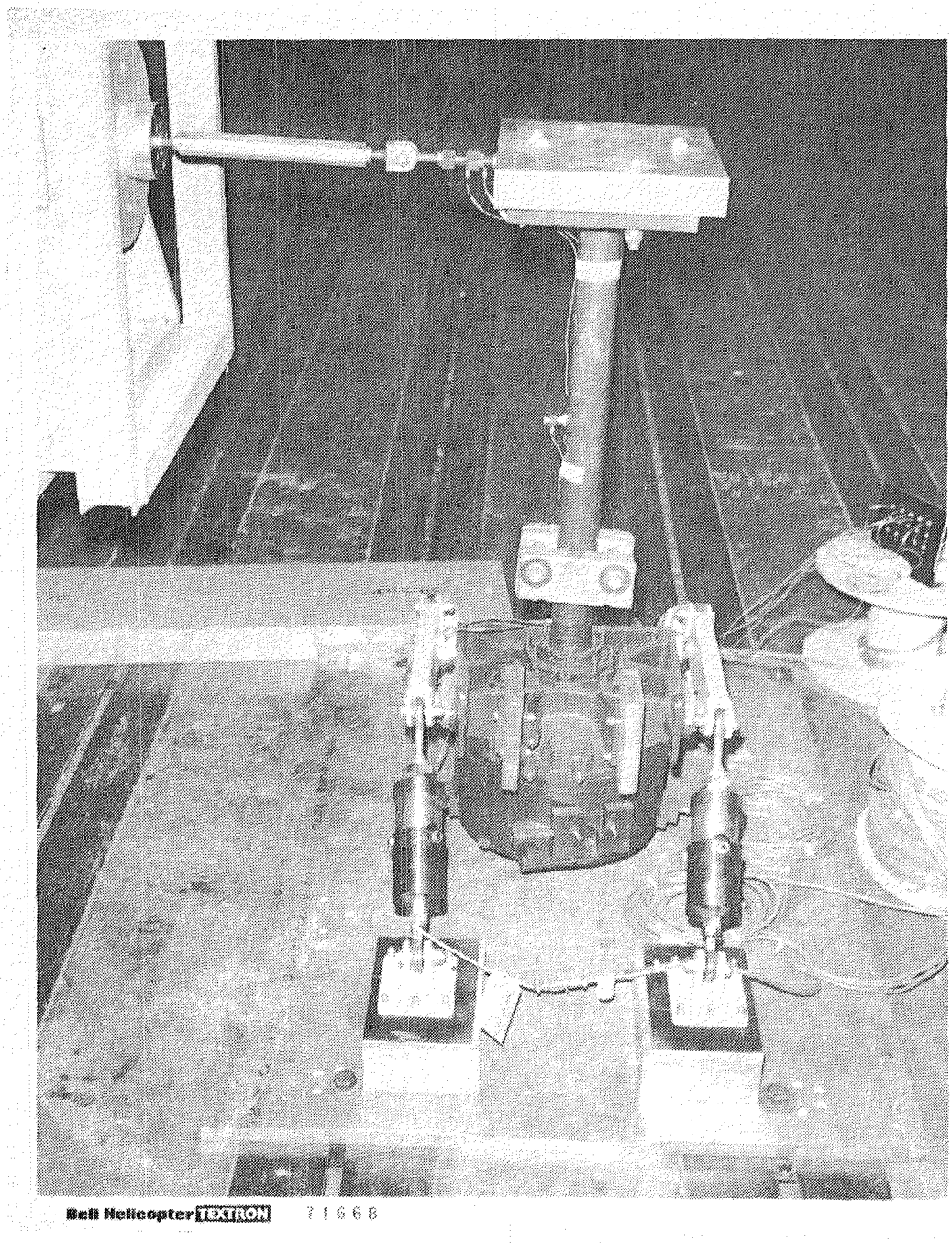

Figure 26. Six D.O.F. System with Lateral Hub Force Input.

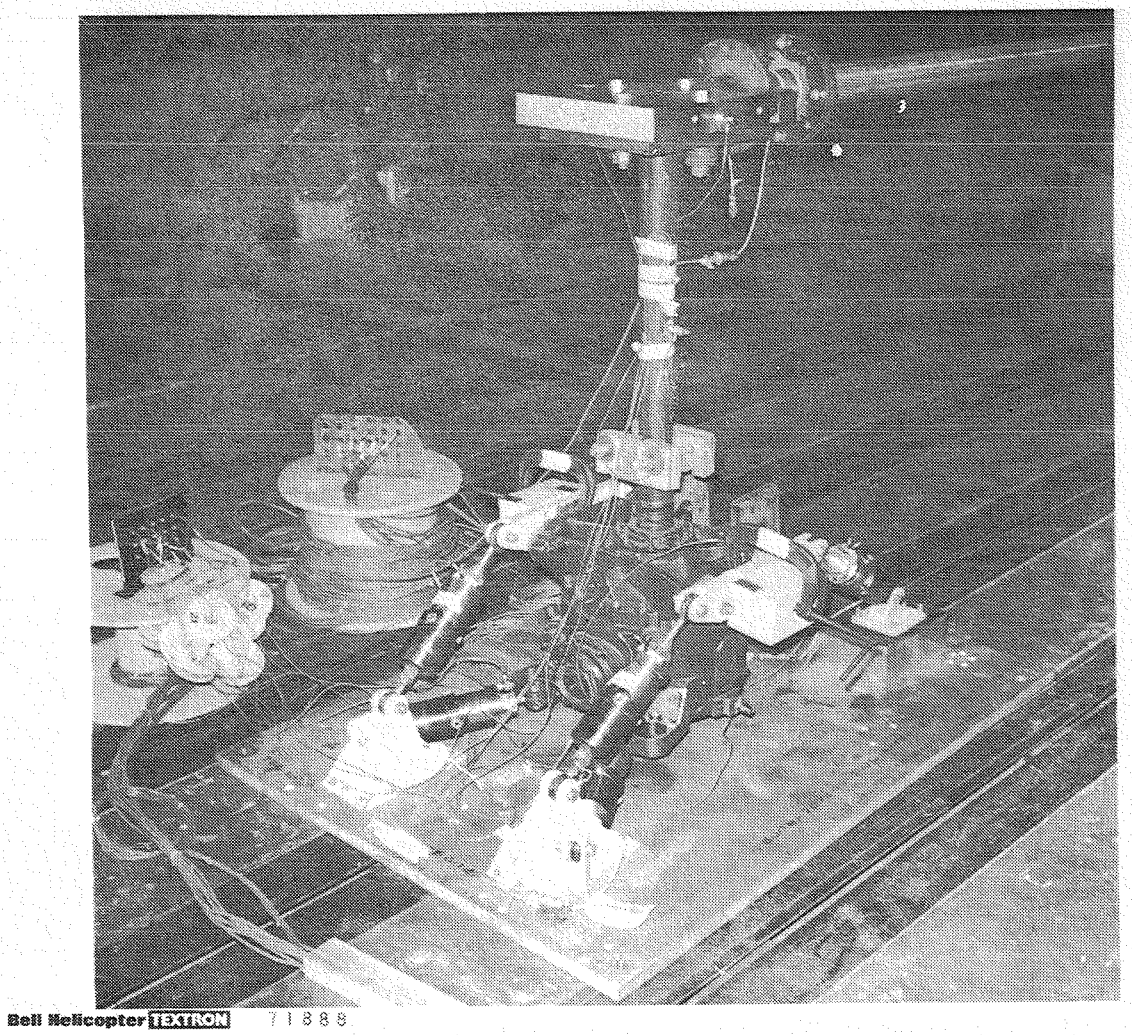

Figure 27. Six D.O.F. System with Roll Hub Moment Input.

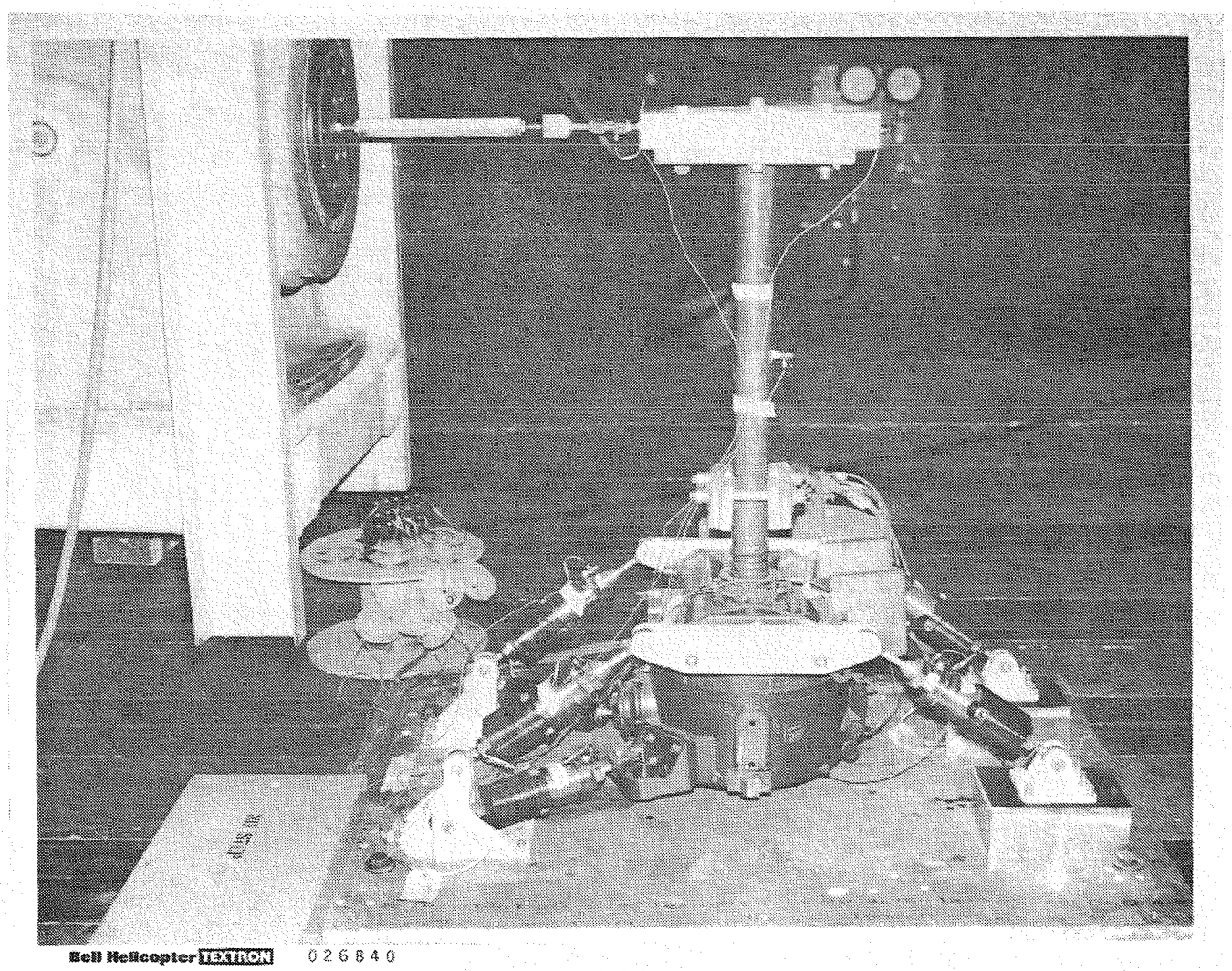

Figure 28. Six D.O.F. System with Longitudinal Hub Force Input.

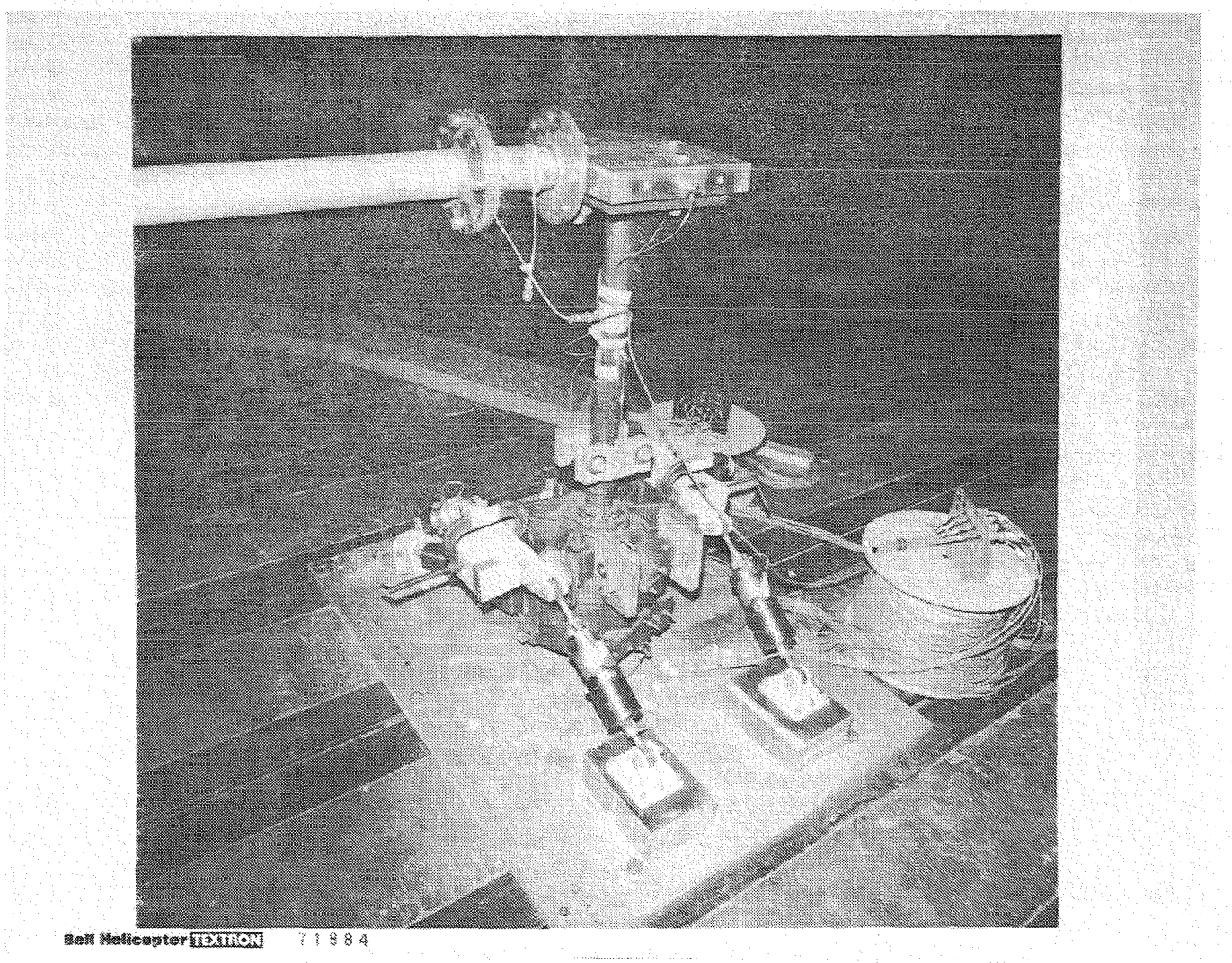

Figure 29. Six D.O.F. System with Pitch Hub Moment Input.

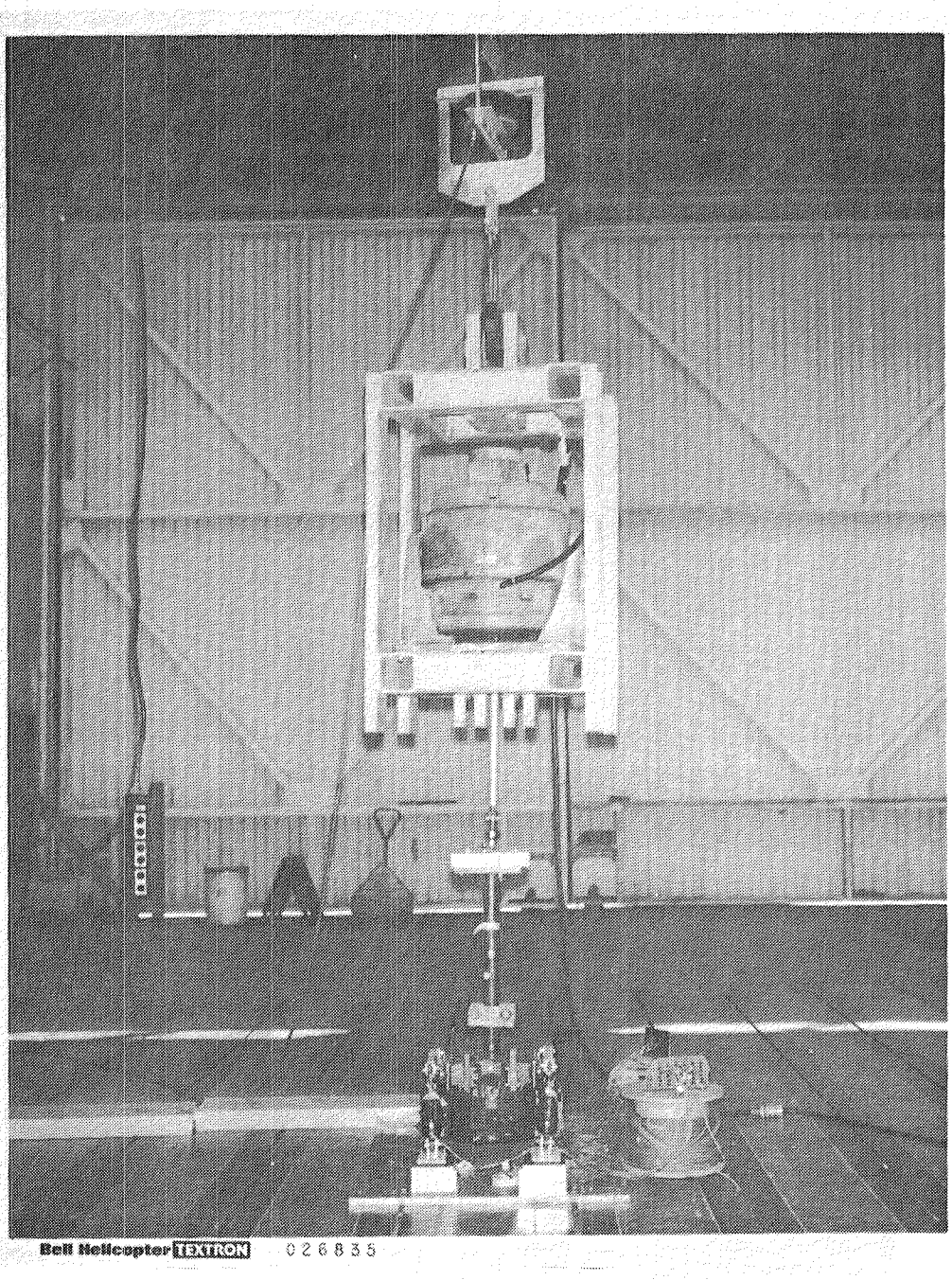

Figure 30. Six D.O.F. System with Vertical Hub Force Input (Front View).

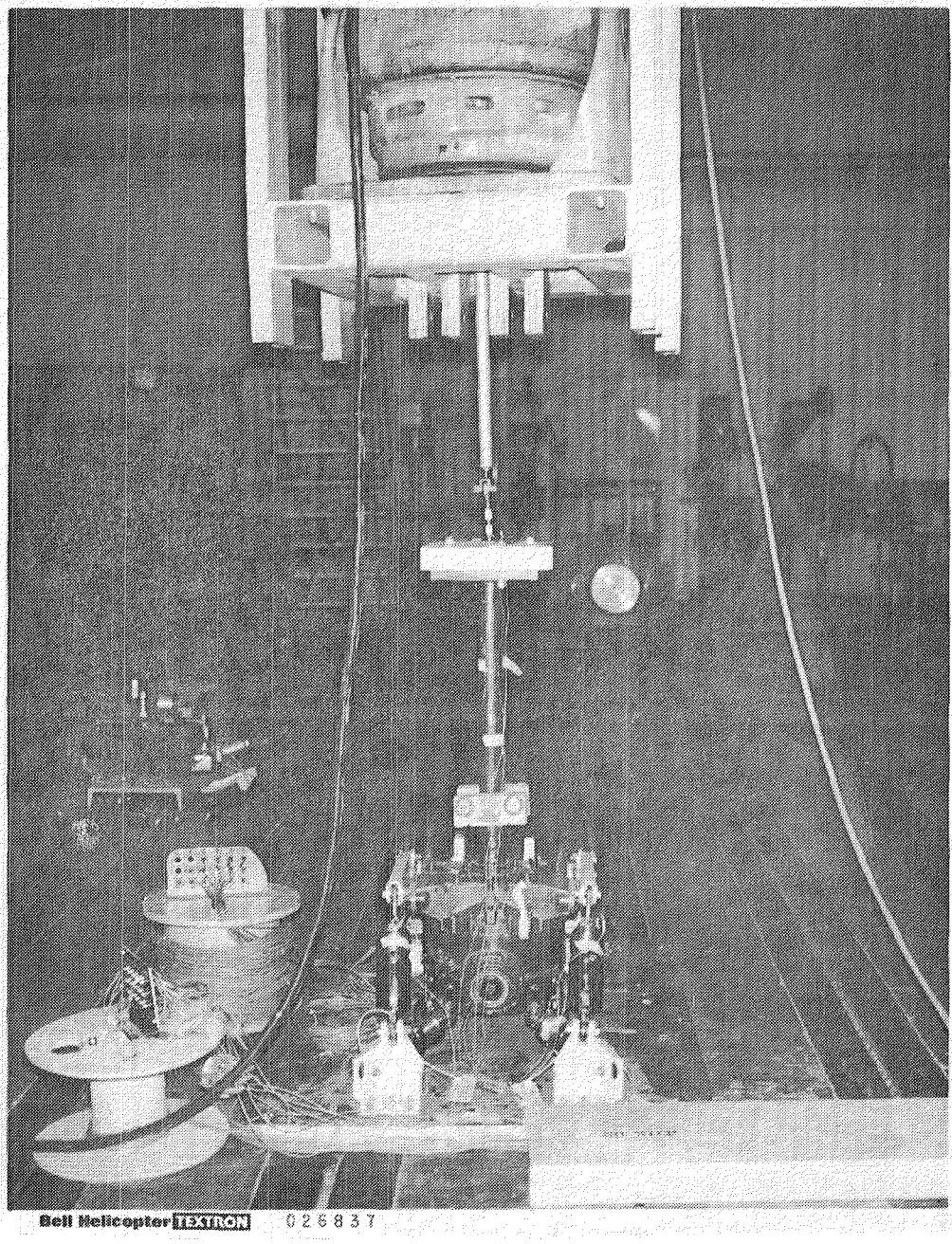

Figure 31. Six D.O.F. System with Vertical Hub Force Input (Rear View).

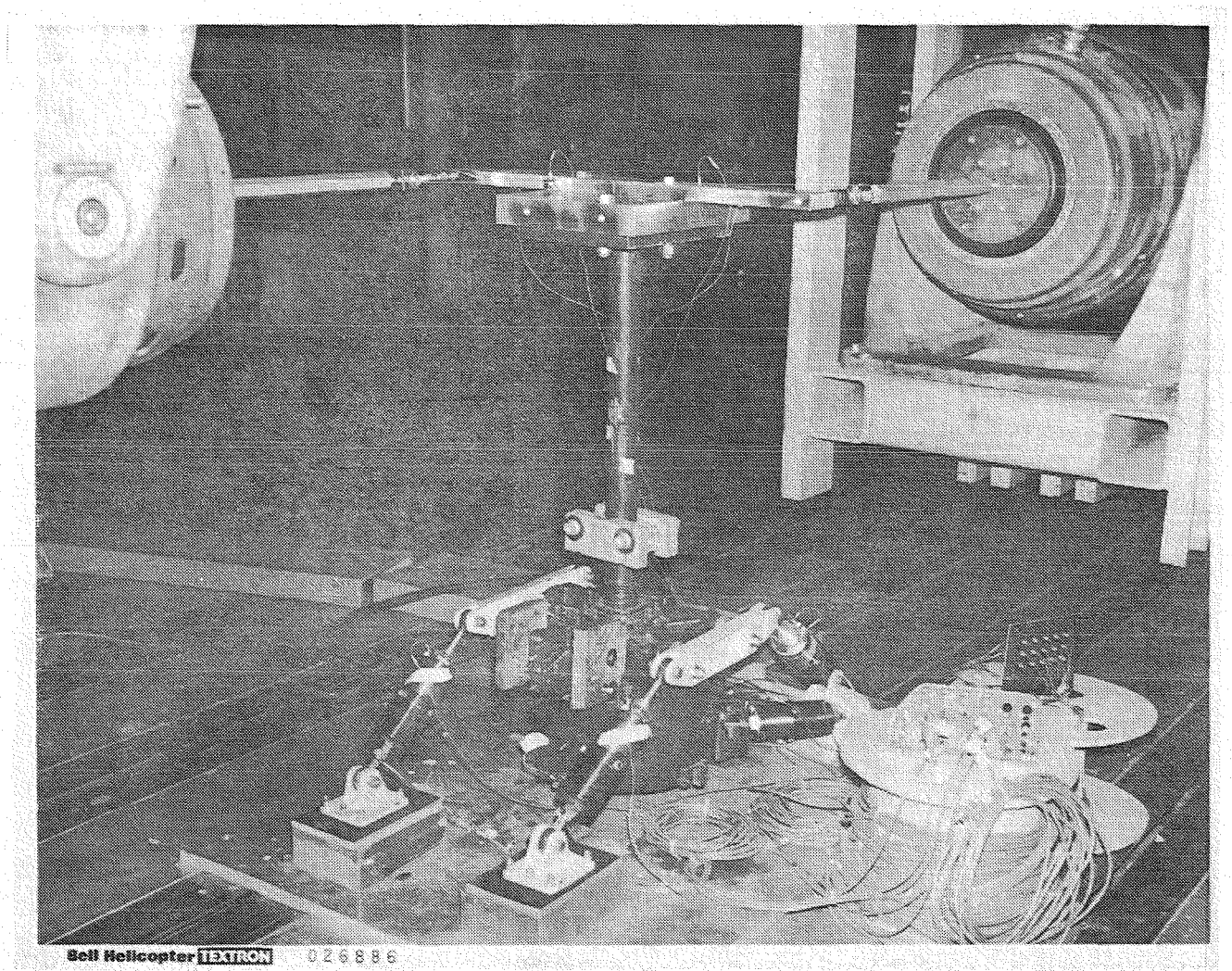

Figure 32. Six D.O.F. System with Yaw Hub Moment Input.

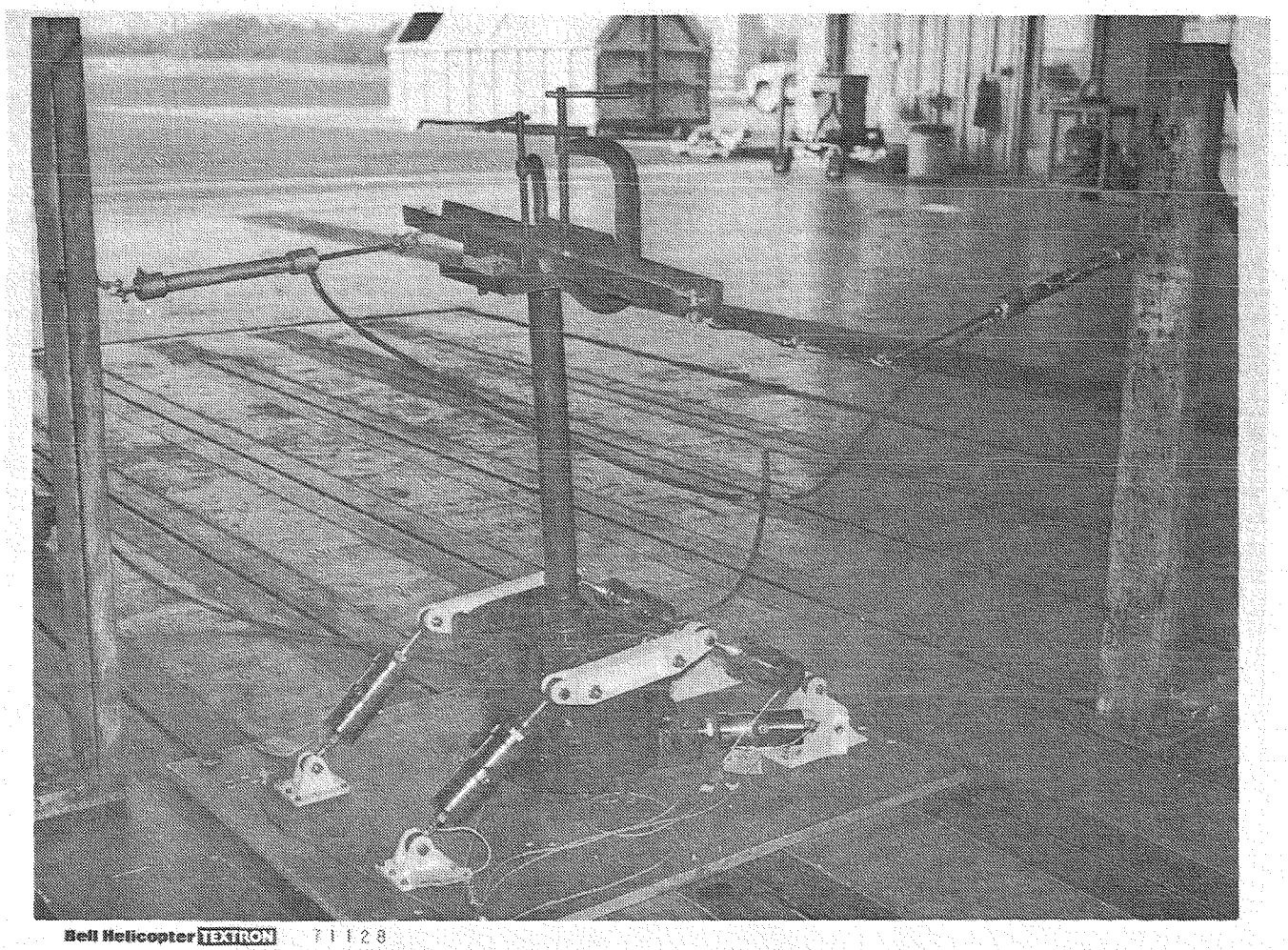

Figure 33. Six D.O.F. System with Static Yaw Hub Moment Input.

TABLE 3. PYLON ACCELEROMETER ORIENTATION FOR 6 D.O.F. ISOLATION TEST

		HUB INPUT					
LOCATION ON PYLON		VERTICAL SHEAR	LATERAL SHEAR	LONGITUDINAL SHEAR	YAW MOMENT	ROLL MOMENT	PITCH MOMENT
	Main Rotor Hub (Input)	Vertical	Lateral	Fore/Aft	Fore/Aft (2)	Lateral	Fore/Aft
	Mast Center	Fore/Aft	Lateral	Fore/Aft	Fore/Aft	None	Fore/Aft
	Transmission (top)	Fore/Aft	Lateral	Fore/Aft	Fore/Aft	Lateral	Fore/Aft
	Transmission (bottom)	Fore/Aft	Lateral	Fore/Aft	Fore/Aft	Lateral	Fore/AFt

to Fig. 34, the loads were applied at the origin of the hub-fixed ($X_H Y_H Z_H$) coordinate system, and the reaction forces at the isolator mounts were measured. These input and reaction forces are then used to define the force determination (calibration) matrix.

$$\underset{(6 \times 1)}{\begin{Bmatrix}\text{MEASURED}\\ \text{ISOLATOR}\\ \text{REACTION}\\ \text{FORCE}\end{Bmatrix}} = \underset{(6 \times 6)}{\begin{bmatrix}\text{RIGID BODY}\\ \text{CALIBRATION}\\ \text{MATRIX}\end{bmatrix}} \times \underset{(6 \times 1)}{\begin{Bmatrix}\text{MEASURED}\\ \text{INPUT}\\ \text{LOAD}\\ @\ \text{HUB}\end{Bmatrix}}$$

$$\rightarrow \quad \begin{bmatrix}\text{RIGID BODY}\\ \text{CALIBRATION}\\ \text{MATRIX}\end{bmatrix} = \begin{Bmatrix}\text{MEASURED}\\ \text{ISOLATOR}\\ \text{REACTION}\\ \text{FORCE}\end{Bmatrix} \times \begin{Bmatrix}\text{MEASURED}\\ \text{INPUT}\\ \text{LOAD}\\ @\ \text{HUB}\end{Bmatrix}^{-1}$$

By inverting the calibration matrix and multiplying by the reactions at the six isolators, equivalent, orthogonal forces and moments in the isolator mounting coordinate system are determined.

$$\begin{Bmatrix}\text{EQUIVALENT}\\ \text{ISOLATOR}\\ \text{REACTIONS}\\ \text{IN X Y Z}\\ \text{SYSTEM}\end{Bmatrix} = \begin{bmatrix}\text{RIGID BODY}\\ \text{CALIBRATION}\\ \text{MATRIX}\end{bmatrix}^{-1} \times \begin{Bmatrix}\text{MEASURED}\\ \text{ISOLATOR}\\ \text{REACTION}\\ \text{FORCE}\end{Bmatrix}$$

Therefore, this coordinate system translation provides for the direct determination of transmissibilities for various dynamic force and moment inputs at the hub.

In the dynamic portion of the six D.O.F. system test, frequency sweeps and harmonic analyses were implemented to determine the degree of isolation and the system responses to varying input force and moment directions, magnitudes, and frequencies. Input force levels ranged from approximately 20% to 200% of expected maximum dynamic loads, and input moments ranged from approximately 33% to 100% of the maximum anticipated torques. The results from both the static and dynamic tests are included in the section that follows.

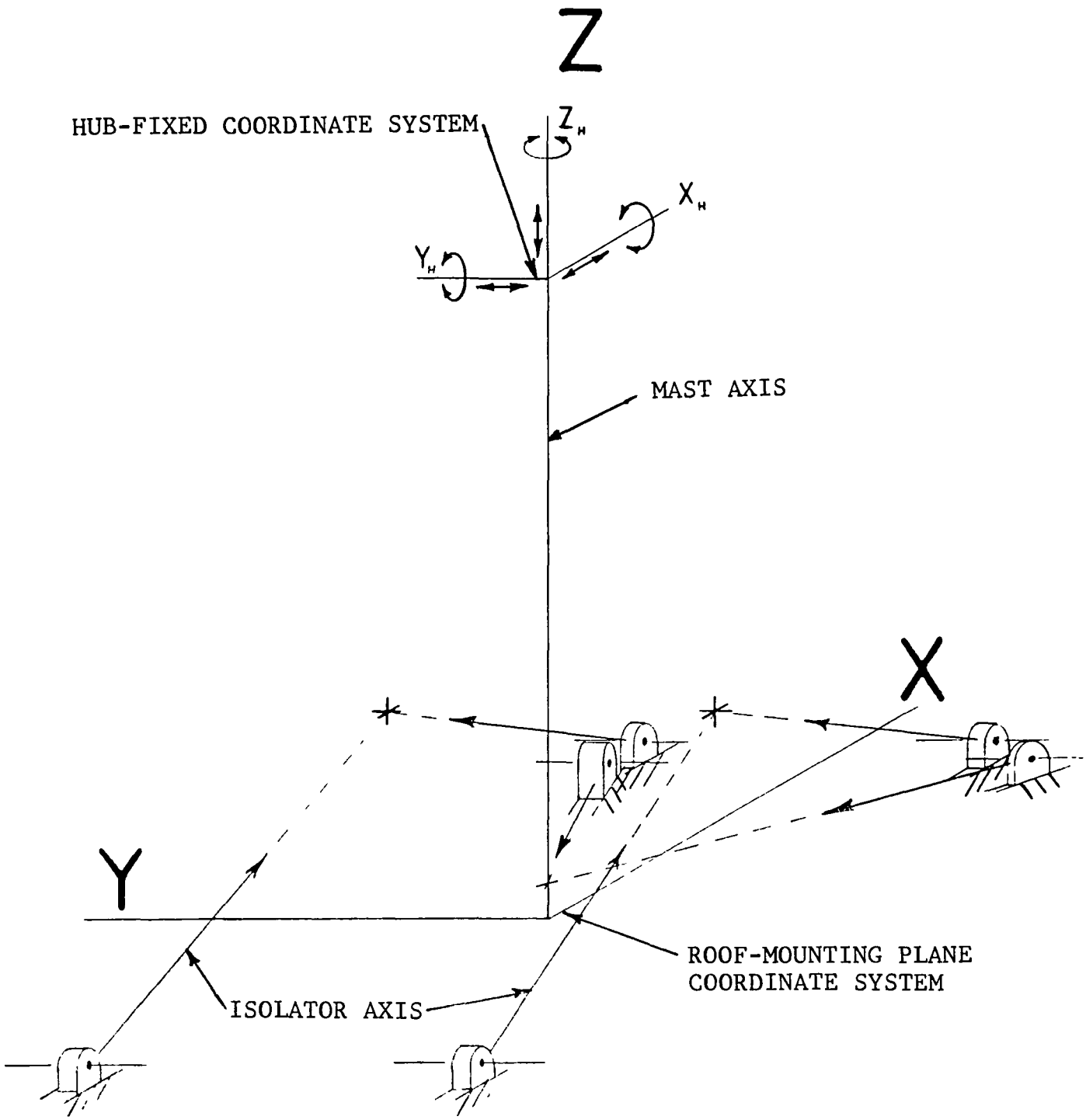

Figure 34. Coordinate Axes Used for Static Calibration Tests.

6. TEST RESULTS

As was discussed in the preceding section, the static tests yielded a rigid body calibration matrix. By inverting this matrix and multiplying by the measured reaction loads at the isolators, equivalent orthogonal reactions in the XYZ system were determined. The inverted rigid body calibration matrix is shown in Figure 35.

After the individual isolators were tuned and the static calibration was complete, dynamic testing of the six D.O.F. apparatus commenced. Responses of the system to oscillatory hub loads of varying magnitude and direction were determined.

Figures 36 - 38 show the isolation system's measured responses to hub inputs corresponding to the six degrees-of-freedom of the system. The predominant pylon resonances are noted for each case. The pylon pitch and roll modes (Figures 36 and 37) are resonances of the rigid pylon mass rotating about the roof on the isolator spring system. In the vertical mode, Figure 38, the pylon translates vertically above the roof. The yaw mode, Figure 38, is characterized by rotation of the transmission case on the isolator springs about the mast axis. The shuffle modes are longitudinal and lateral motions of the transmission case on the isolator springs as it pivots about a point near the hub. The mast-bending modes are dominated by bending of the mast as the primary spring in the system.

The resonant frequencies and response magnitudes are affected by hub mass. The addition of mass to the hub tends to lower the resonant frequencies and reduce the system's responses. In order to obtain response magnitudes which are representative of those expected in flight, no hub mass was used in the tests reported here.

Since the rotor hub mass is significant in these modes, the actual pylon pitch, roll, and vertical modes will occur at lower frequencies than these test results indicate when the pylon is installed on the 206LM. The fore/aft

$$\begin{Bmatrix} \text{EQUIVALENT} \\ \text{ISOLATOR} \\ \text{REACTIONS} \\ \text{IN XYZ} \\ \text{SYSTEM} \end{Bmatrix} = \begin{bmatrix} \text{INVERTED} \\ \text{RIGID BODY} \\ \text{CALIBRATION} \\ \text{MATRIX} \end{bmatrix} \times \begin{Bmatrix} \text{MEASURED} \\ \text{ISOLATOR} \\ \text{REACTION} \\ \text{FORCE} \end{Bmatrix}$$

$$\begin{Bmatrix} \text{FORCE X} \\ \text{FORCE Y} \\ \text{FORCE Z} \\ \text{MOMENT X} \\ \text{MOMENT Y} \\ \text{MOMENT Z} \end{Bmatrix} = \begin{bmatrix} -0.836 & 0.815 & -0.814 & -0.902 & 0.814 & -0.993 \\ -0.087 & -0.011 & -0.517 & 0.020 & 0.086 & 0.436 \\ 0.477 & 0.649 & -0.101 & 0.532 & 0.651 & 0.051 \\ -0.644 & -0.464 & -1.867 & 0.581 & 0.683 & 1.691 \\ 1.798 & -1.820 & 2.917 & 1.956 & -1.844 & 3.239 \\ -0.701 & 0.690 & -0.062 & 0.698 & -0.726 & 0.089 \end{bmatrix} \times \begin{Bmatrix} \text{ISOLATOR \#1 AXIAL FORCE} \\ \text{ISOLATOR \#2 AXIAL FORCE} \\ \text{ISOLATOR \#3 AXIAL FORCE} \\ \text{ISOLATOR \#4 AXIAL FORCE} \\ \text{ISOLATOR \#5 AXIAL FORCE} \\ \text{ISOLATOR \#6 AXIAL FORCE} \end{Bmatrix}$$

Figure 35. Matrix Transformation Used to Determine Reaction Forces in Roof Mounting Plane.

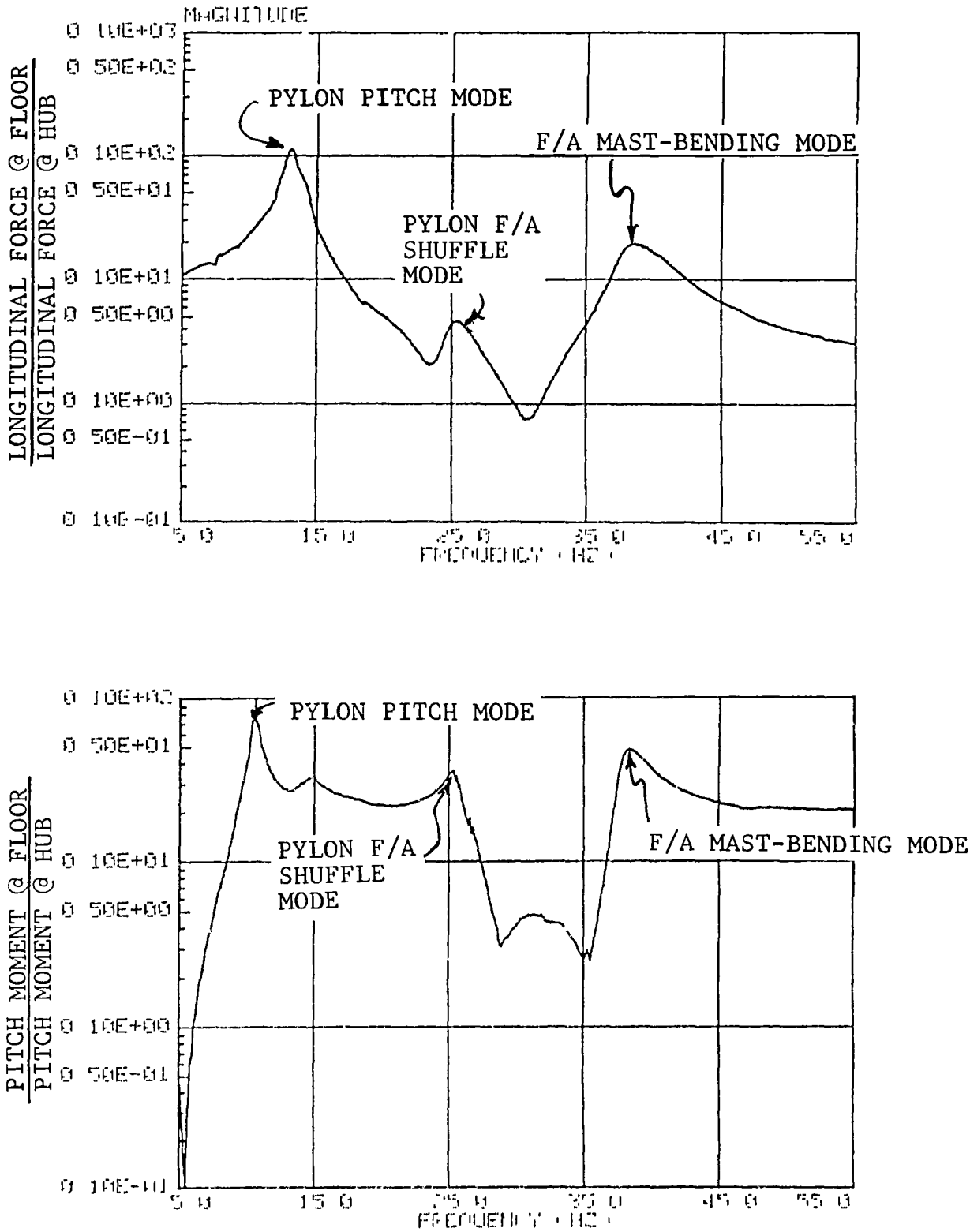

Figure 36. Six D.O.F. System Responses to Longitudinal Hub Force and Pitch Hub Moment.

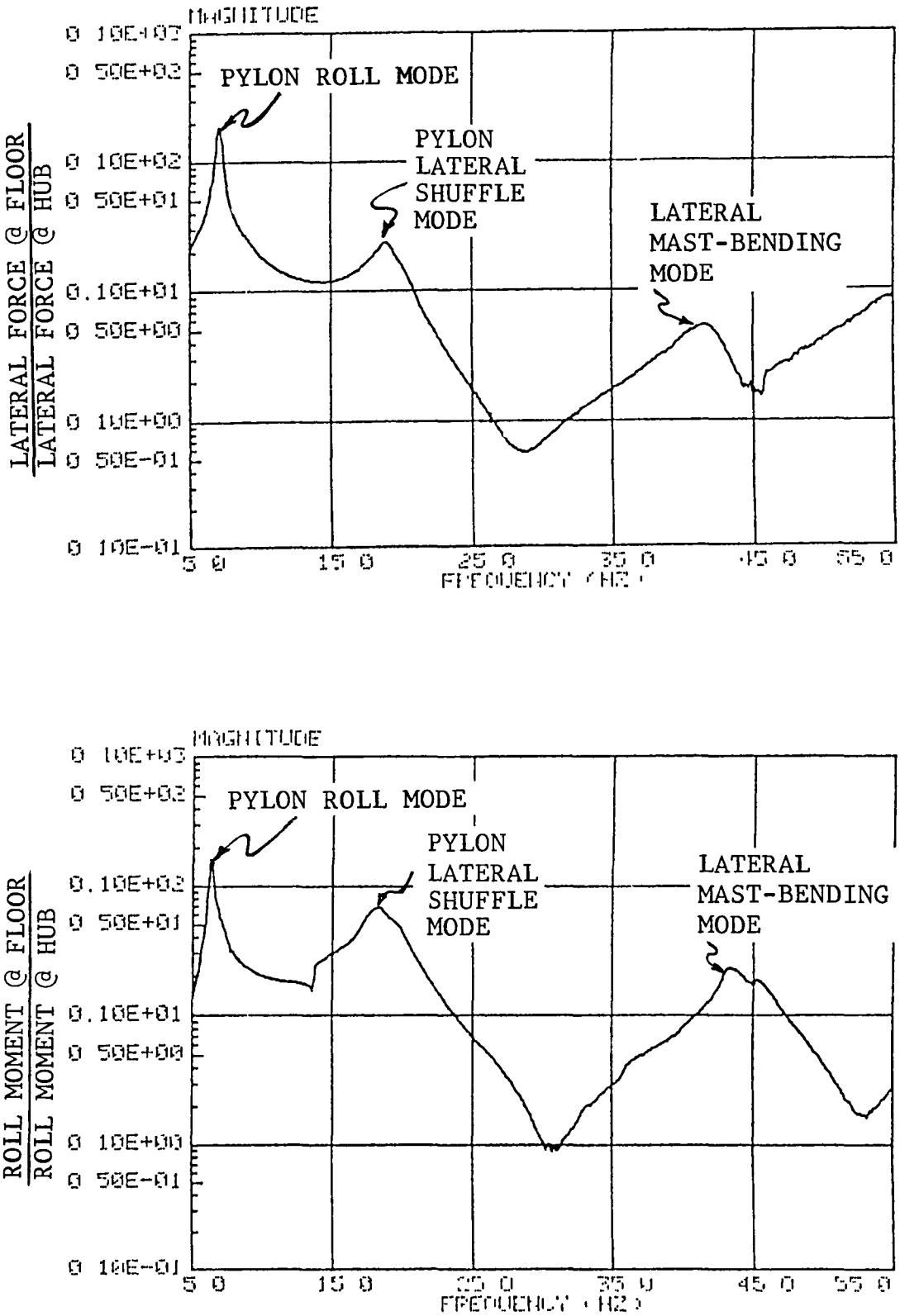

Figure 37. Six D.O.F. System Responses to Lateral Hub Force and Roll Hub Moment.

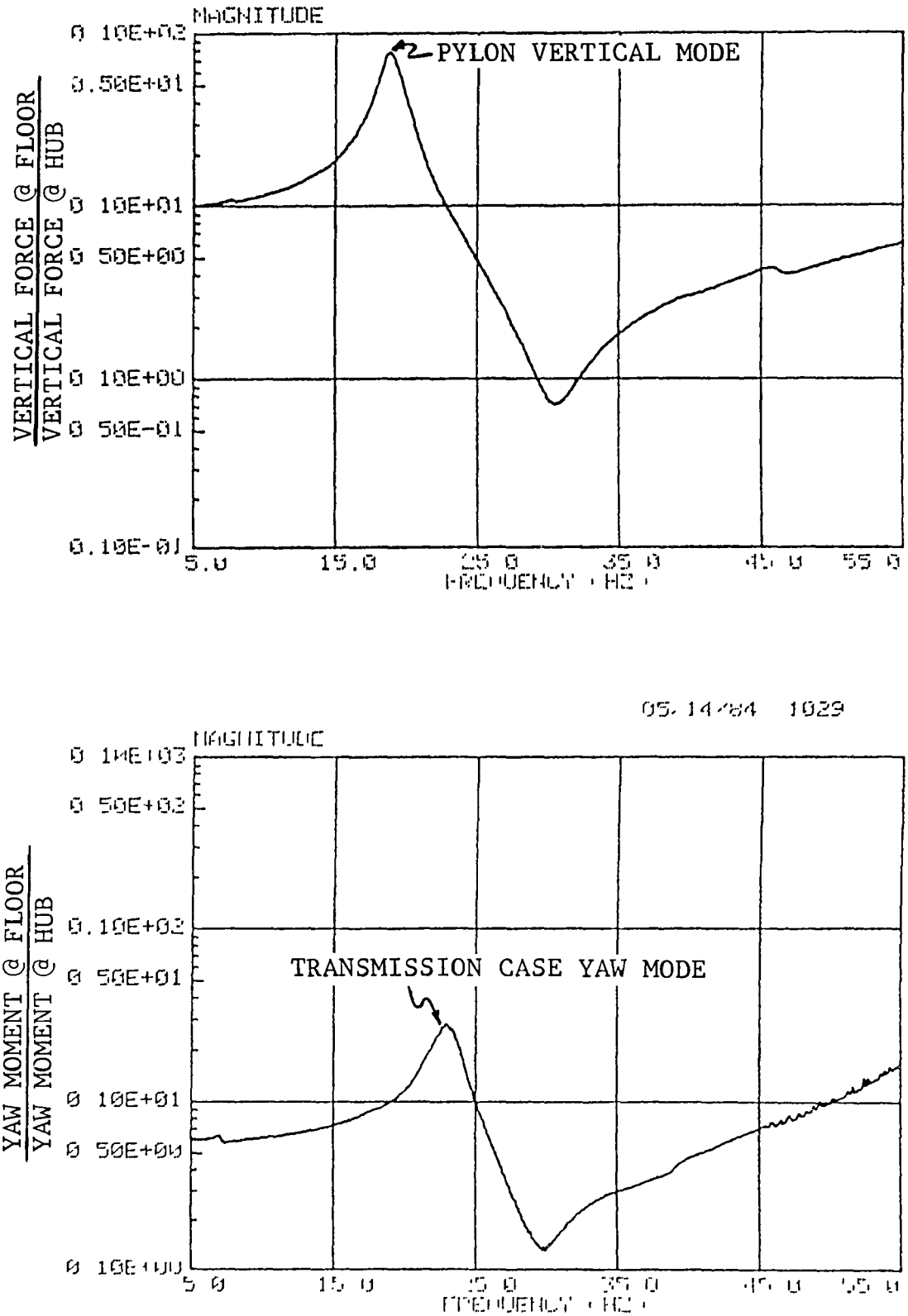

Figure 38. Six D.O.F. System Responses to Vertical Hub Force and Yaw Hub Moment.

and lateral mast-bending mode, the shuffle mode, and the yaw mode freqencies will be essentially unchanged since the hub mass is relatively ineffective in these modes.

Figure 39 shows the responses of Figures 36 - 38 transposed to a single plot. The composite plot illustrates that the system's actual isolation frequency is shifted upward from the desired 26.3 Hz (4/rev) frequency. Although the isolators had been individually tuned to isolate 26.3 Hz (4/rev) vibration, the system's isolation frequency was determined to be approximately 30.5 Hz.

The shift in isolation frequency was determined to be caused by a change in spring rate in the isolators. After their manufacture, the isolators were immediately shipped to BHT, and individual tuning commenced. All of the isolators were tuned within one month of their cure date, and due to program delays, the six D.O.F. tests were not performed until nine months later. Over this time, the elastomer in the isolators apparently continued to cure, and the spring rate increased. Since the isolators were tuned at a different stage of elastomer cure (and, therefore, spring rate), their tuned frequency was no longer 26.3 Hz when the six D.O.F. system was finally assembled and tested. Due to the shift in tuned frequency, the system's isolation performance at 4/rev is substantially worse than optimum. Figure 40 reiterates this reduced performance level by comparing the system transmissibilities at 4/rev to the best performance (minimum transmissibility) over the frequency range tested.

In order to verify that the tuning of the isolators had actually changed, they were re-tested individually after the six D.O.F. tests were completed. The results of the re-test are discussed in the section that follows.

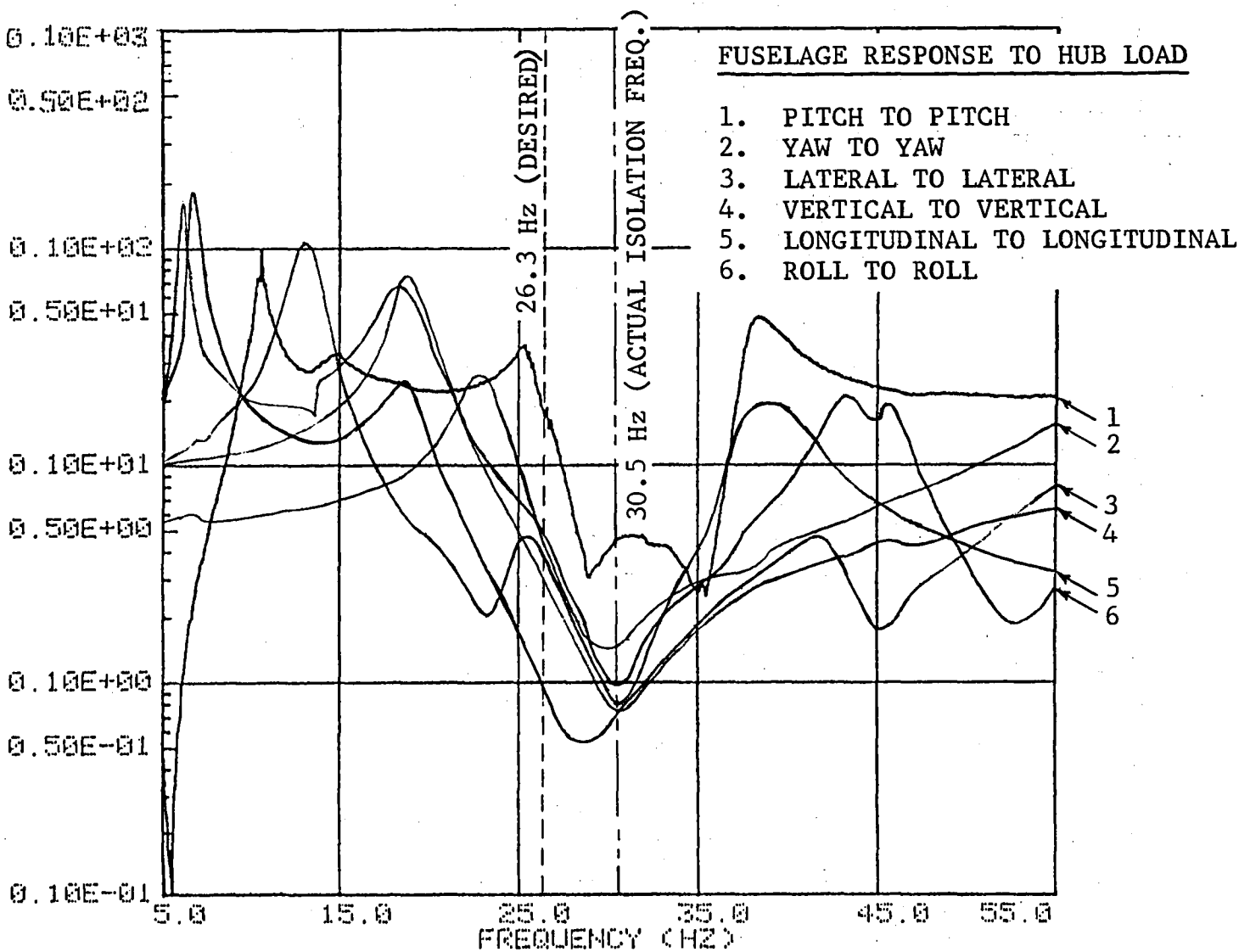

Figure 39. Six D.O.F. System Responses.

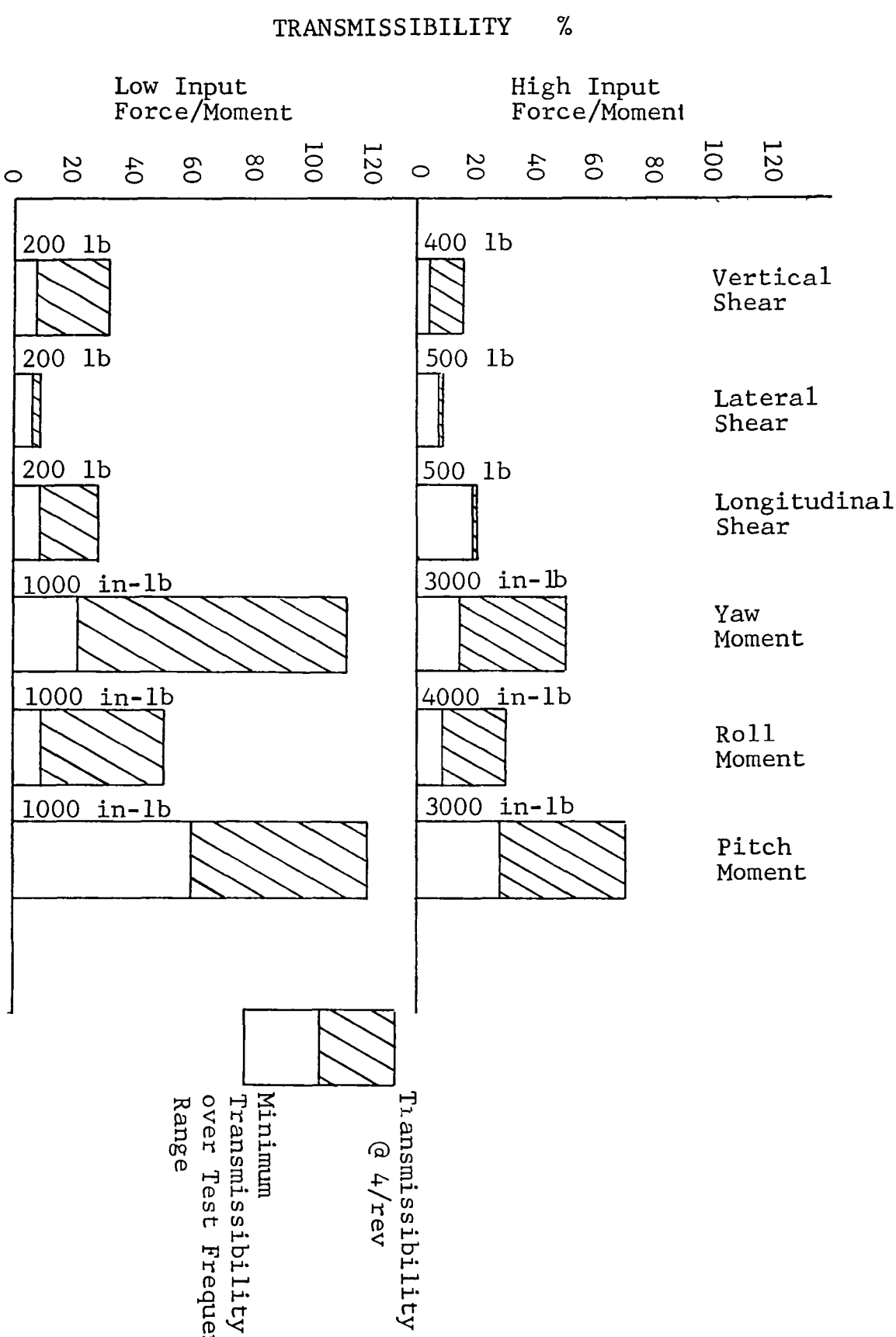

Figure 40. Transmissibility Ratio at 4/Rev versus Minimum Transmissibility for Six D.O.F. Isolation System.

7. TIME EFFECTS ON ISOLATOR PERFORMANCE

In order to examine why the isolation performance of the complete six D.O.F. system was not on par with that of the individual isolators, the original individual isolator tuning and test apparatus was again set up. This was done to provide vertification that the isolators' spring rates (and, therefore, tuned frequency) had changed as suggested in the Test Results section of this report.

Figures 41 - 44 show the responses of the individual isolators measured after the six D.O.F. system bench tests were completed. The plots show the acceleration of the fuselage weight divided by the input force as the frequency of the input force varied. Table 4 and a comparison of these plots with those made after the initial isolator tuning indicate a shift of the response for each isolator to a slightly higher frequency. The largest upward shift in isolation frequency is 6.3 Hz; the smallest is 0.8 Hz. The resonant frequencies of the isolators have shifted upward accordingly.

This overall upward shift in responses indicates that the spring rates of the isolators increased somewhat as time passed between their initial tuning and completion of six D.O.F. system testing. The stiffer isolators are now tuned to provide isolation at a frequency above the desired 26.3 Hz and, therefore, transmissibility at 4P (26.3 Hz) increases. The relatively small transmissibility increase in each of the individual isolators results in a more significant degradation in isolation performance for the complete six D.O.F. system.

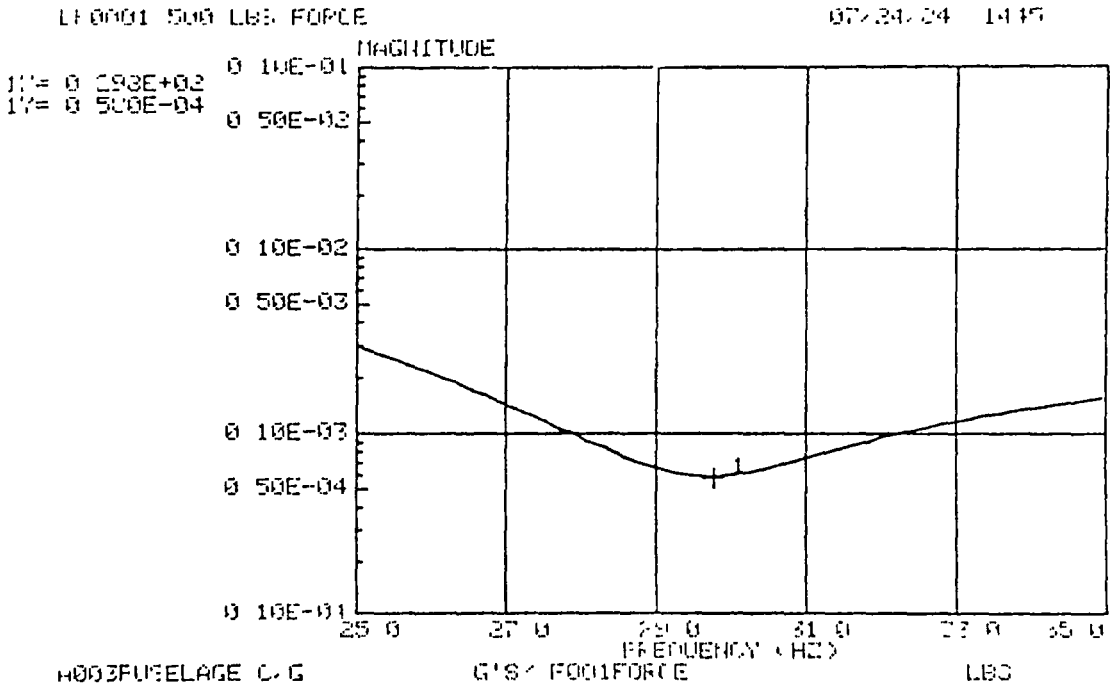

S/N LK0001

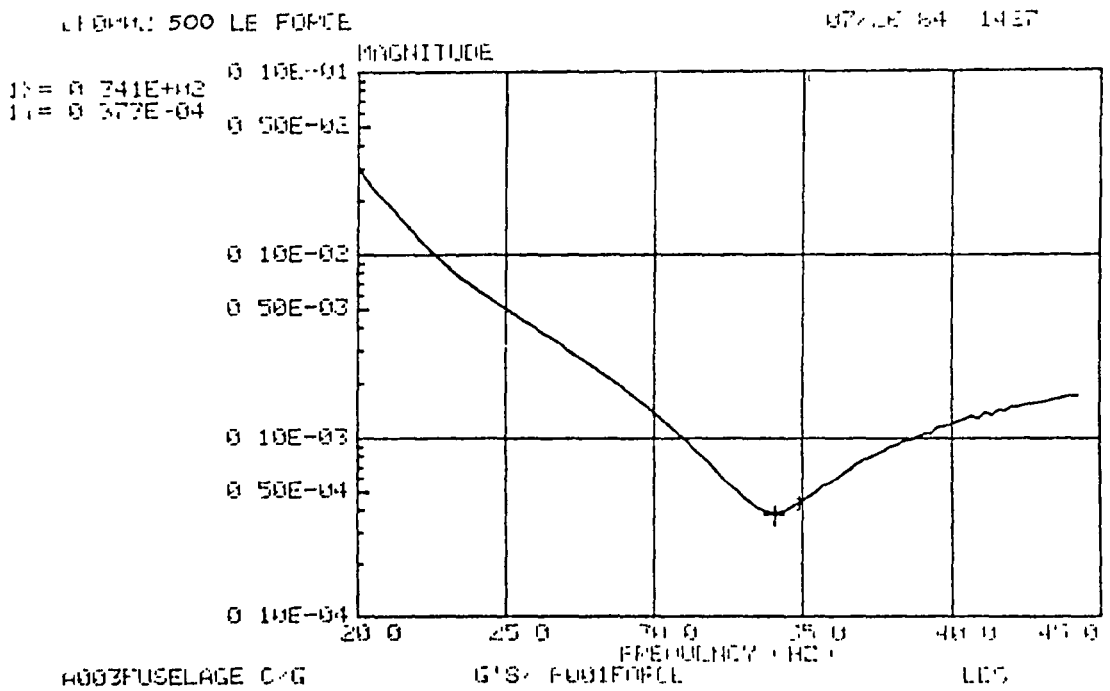

S/N LK0002

Figure 41. Responses of Individual LIVE Units After Six D.O.F. Testing.

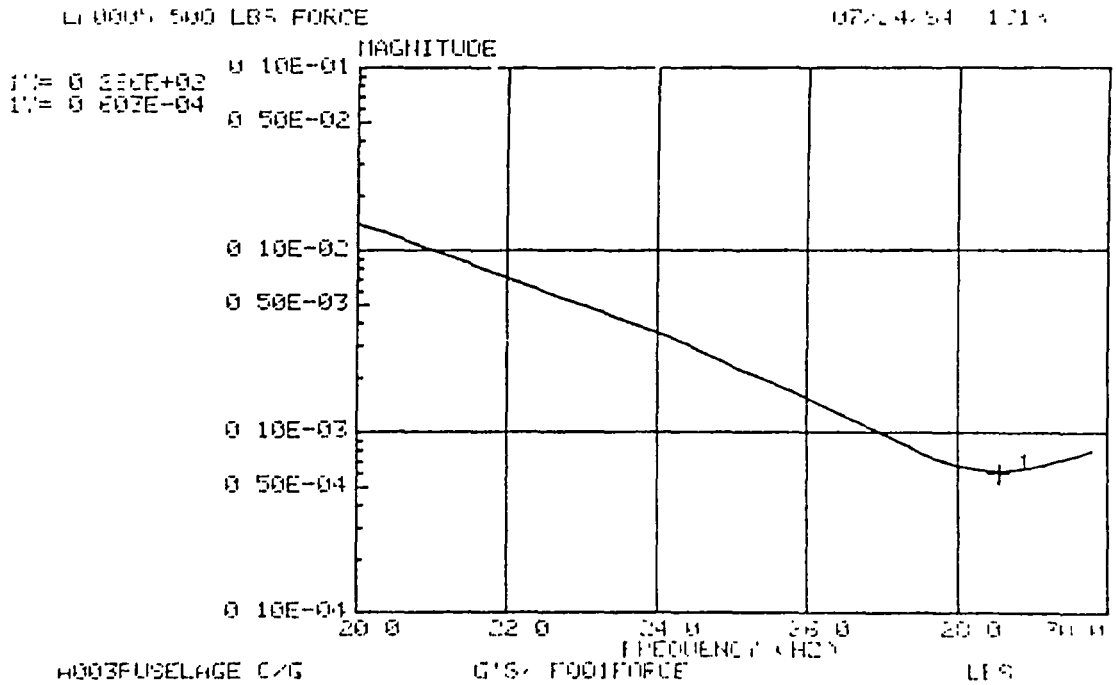

S/N LK0005

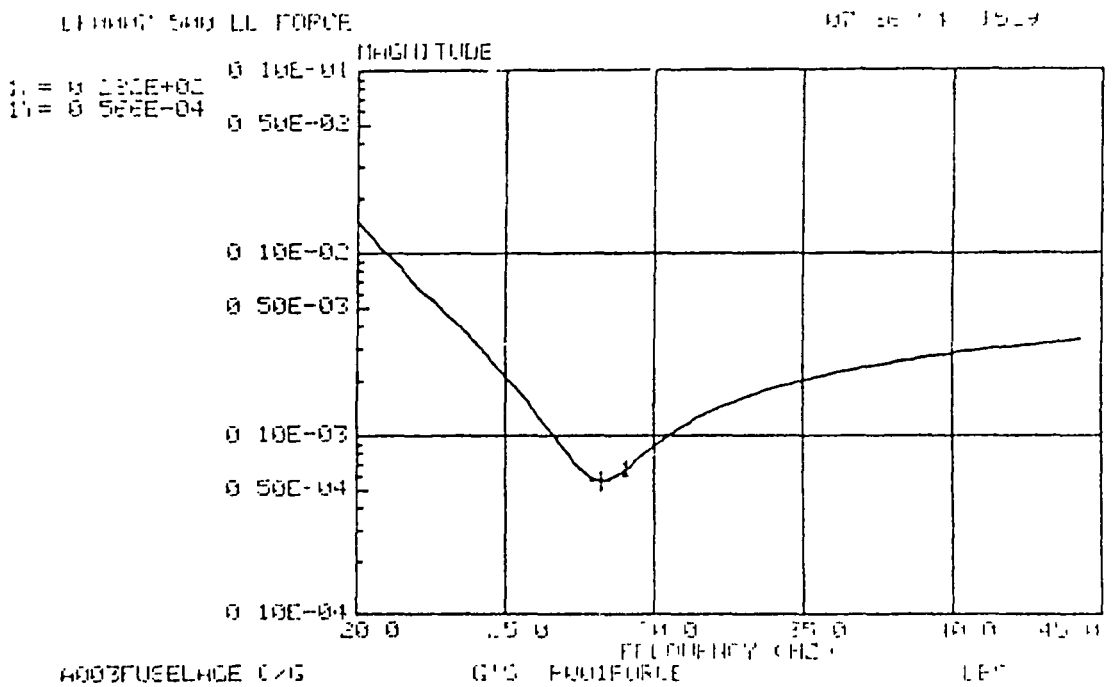

S/N LK0007

Figure 42. Responses of Individual LIVE Units After Six D.O.F. Testing.

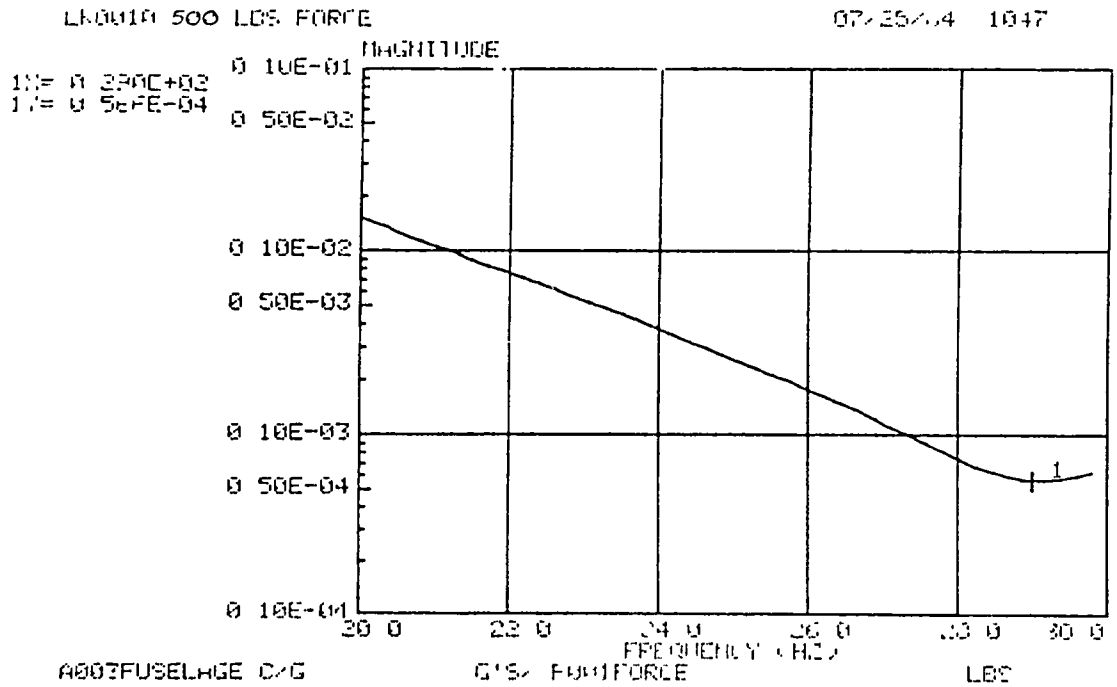

S/N LK0010

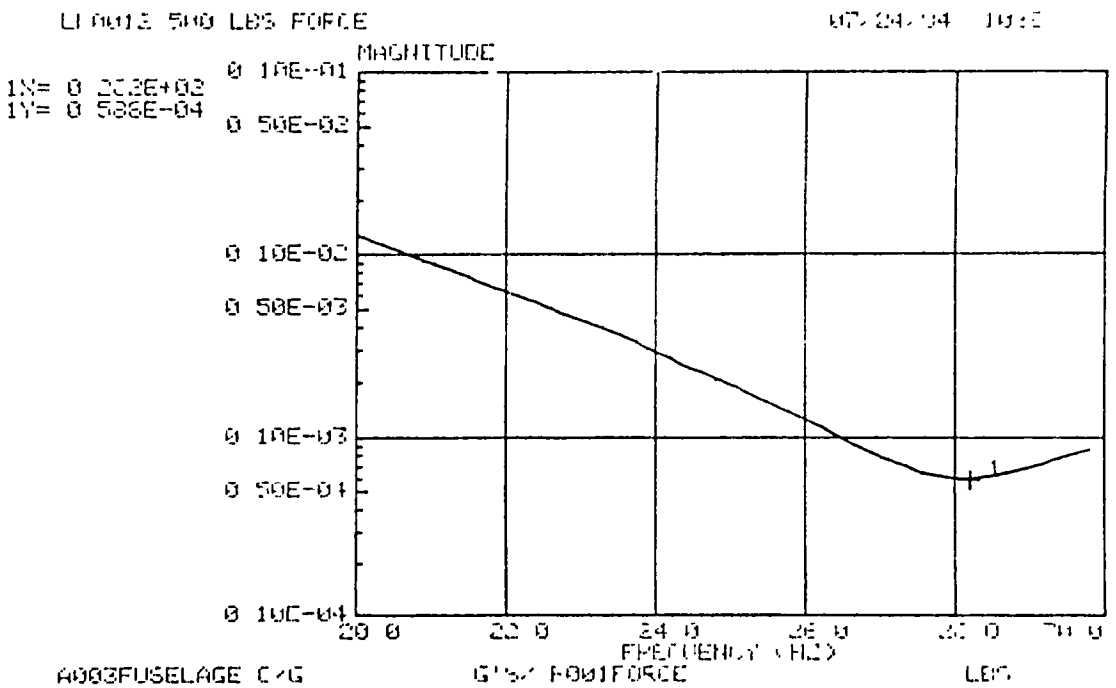

S/N LK0012

Figure 43. Responses of Individual LIVE Units After Six D.O.F. Testing.

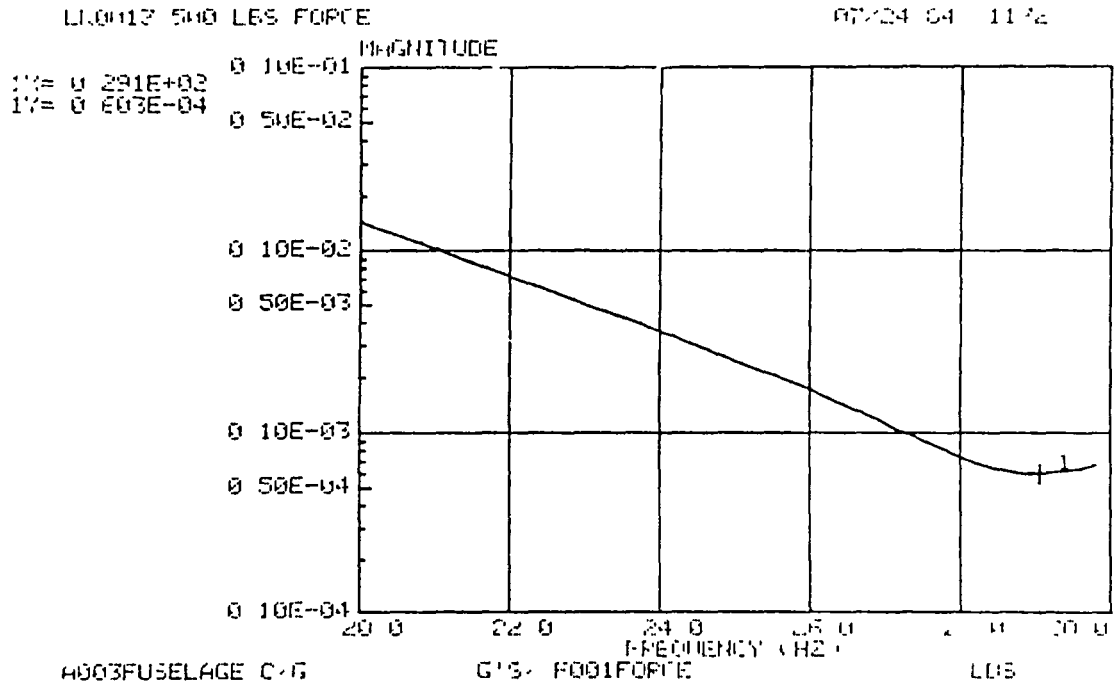

S/N LK0013

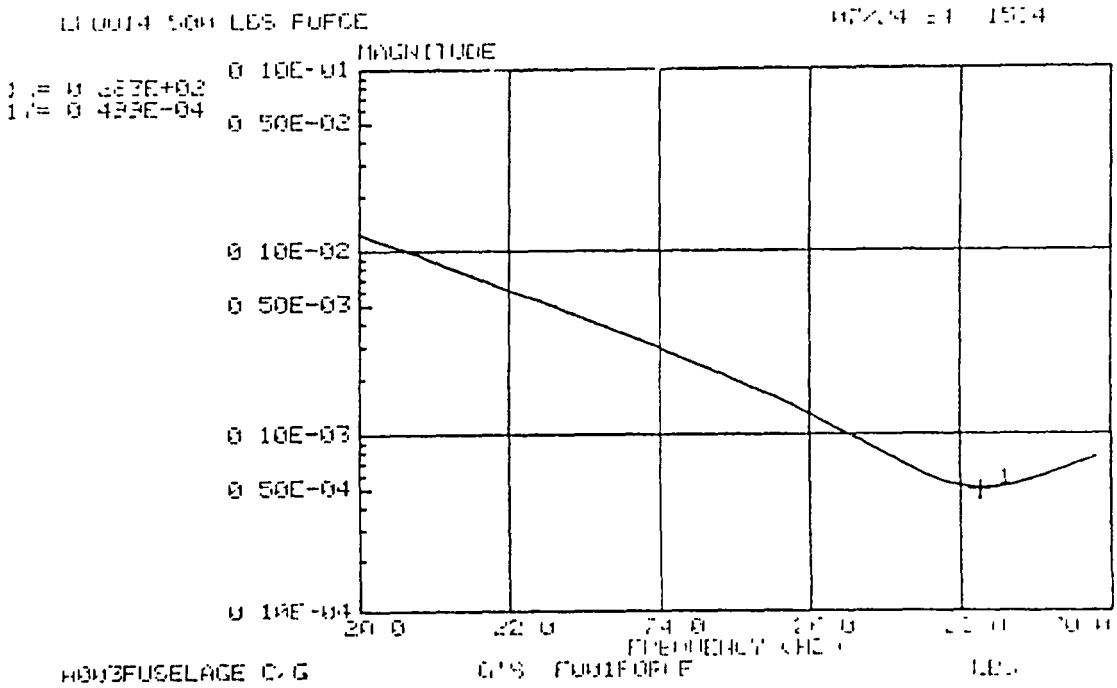

S/N LK0014

Figure 44. Responses of Individual LIVE Units After Six D.O.F. Testing.

TABLE 4. ISOLATOR PERFORMANCE AT 500-LB INPUT FORCE BEFORE AND AFTER 6 D.O.F. TESTING

ISOLATOR SERIAL NUMBER	TUNED ISOLATION FREQUENCY - Hz		TRANSMISSIBILITY RATIO @ 26.3 Hz	
	BEFORE	AFTER	BEFORE	AFTER
LK0001	27.7	29.8	0.040	0.182
LK0002	27.8	34.1	0.035	0.381
LK0005	26.8	28.6	0.032	0.145
LK0007	27.4	28.2	0.033	0.130
LK0010	26.4	29.0	0.034	0.150
LK0012	26.6	28.2	0.030	0.095
LK0013	27.7	29.1	0.035	0.163
LK0014	25.8	28.3	0.040	0.104

8. CONCLUSIONS

The test results reported herein support the following conclusions:

1) All six D.O.F. of pylon motion can be isolated using pinned-pinned "LIVE" links which have been tuned independently. The isolators can be tuned to isolate a desired frequency, the transmission/isolator system can be assembled, and the isolation frequency of the system will be the same as that of the individual isolators. Therefore, no "on-ship" or "post-assembly" system tuning is required after the individual isolators are tuned.

2) The six D.O.F. system with fully adjustable, steel-bodied isolators has a weight penalty of 69.6 lbs, which represents approximately 1.7% of design gross weight for the 206LM. This weight penalty is greater than the 1.0% GW design goal. By limiting isolator adjustability and replacing some steel components with aluminum ones, the 1.0% GW weight penalty goal can be met.

3) Results from the endurance test of an isolator unit indicate that the LIVE isolators can withstand static and dynamic loadings equivalent to those expected in flight. Furthermore, these tests indicate that the isolators are not affected by continuous cyclic loadings.

4) During the six D.O.F. system bench test, the system was not properly tuned to isolate the desired (4/rev) frequency. Due to incomplete curing of the isolators' elastomer at the time of tuning, their spring rates increased over time, and therefore the tuning of the individual isolators changed (according to their spring rate and degree of cure at the time of tuning). The stiffer spring rates produced a higher isolation frequency than desired for the individual isolators, and therefore for the complete six D.O.F. system.

5) The isolators can be retuned to provide 6 D.O.F. isolation at 4/rev. This tuning can be achieved by either softening the spring rates or reducing the tuning port diameter. For the next flight test phase of this program, spring rate reduction, attained by removing some elastomer length from the isolators, is the more desirable alternative. Reducing the isolator spring

rates will have the effect of lowering the system's resonant frequencies, in addition to shifting the isolation frequency to 4/rev. Placing the pylon modes farther away from 4/rev will result in improved isolation at the 4/rev isolation valley.

At this time, the isolators' spring rates have been reduced by machining an appropriate amount of elastomer to provide 4/rev isolation tuning. Also, a Bell Model 206L-1 is being modified to the 206LM configuration. After a tuning check of the individual isolators, the six D.O.F. isolation system will be installed on the subject helicopter, and the flight testing phase of the program will be initiated.

REFERENCES

1. Flannelly, W. G., THE DYNAMIC ANTI-RESONANT VIBRATION ISOLATOR, Presented at the 22nd Annual AHS National Forum, Washington, D.C., May 1966.

2. Desjardins, R. A., and Hooper, W. E., ROTOR ISOLATION OF THE HINGELESS ROTOR BO-105 AMD YUH-61 HELICOPTERS, Presented at the Second European Rotorcraft and Powered Lift Aircraft Forum, September 1976.

3. Shipman, D. P., White, J. A., and Cronkhite, J. D., FUSELAGE NODALIZATION, Presented at the 28th Annual AHS National Forum, Washington, D.C., May 1972.

4. Halwes, D. R., LIVE-LIQUID INERTIA VIBRATION ELIMINATOR, Presented at the 36th Annual AHS National Forum, Washington, D.C., May 1980.

1 Report No	2 Government Accession No	3 Recipient's Catalog No
NASA CR-177928		

4 Title and Subtitle	5 Report Date
Six Degree-of-Freedom "LIVE" Isolation System Tests - Part 1: Interim Report	April 1986
	6 Performing Organization Code
7 Author(s)	8 Performing Organization Report No
Dennis R. Halwes and Colby O. Nicks	
9 Performing Organization Name and Address	10 Work Unit No
Bell Helicopter Textron P.O. Box 482 Fort Worth, TX 76101	11 Contract or Grant No NAS1-16969
	13 Type of Report and Period Covered Contractor Report
12 Sponsoring Agency Name and Address U.S. Army Aviation System Command St. Louis, MO 63120-1798 National Aeronautics and Space Administration Washington, DC 20546-0001	14 Sponsoring Agency Code 505-42-39-03

15 Supplementary Notes

Technical Monitor, John H. Cline, U.S. Army Aerostructures Directorate, USAARTA (AVSCOM)
Interim Report

16 Abstract

A Total Main Rotor Isolation System (TRIS) has been analyzed, designed, fabricated, and bench tested for the reduction of main rotor vibration levels transmitted to the helicopter fuselage. The TRIS consists of a six degree-of-freedom passive system using six Liquid Inertia Vibration Eliminators (LIVE) units developed by Bell Helicopter Textron. The objective of the program is to develop a helicopter isolation system that will achieve 90% (or greater) isolation at minimum weight with no degradation in vehicle stability, handling qualities, alignment tolerance, and reliability or maintainability.

17 Key Words (Suggested by Author(s))	18 Distribution Statement
Isolation Total Rotor Isolation System Vibration Helicopter	Unclassified - Unlimited Subject Category 05

19 Security Classif (of this report)	20 Security Classif (of this page)	21 No of Pages	22 Price*
Unclassified	Unclassified	80	A05

*For sale by the National Technical Information Service, Springfield, Virginia 22161

End of Document